

Supplementary information

Discovery of di- and trihaloacetamides as covalent SARS-CoV-2 main protease inhibitors with high target specificity

Chunlong Ma,^{1,#} Zilei Xia,^{1,#} Michael Dominic Sacco,² Yanmei Hu,¹ Julia Alma Townsend,³ Xiangzhi Meng,⁴ Juliana Choza,¹ Haozhou Tan,¹ Janice Jang,¹ Maura V Gongora,² Xiujun Zhang,² Fushun Zhang,⁴ Yan Xiang,⁴ Michael Thomas Marty,³ Yu Chen,^{2,*} Jun Wang^{1,*}

¹Department of Pharmacology and Toxicology, College of Pharmacy, The University of Arizona, Tucson, AZ, 85721, United States

²Department of Molecular Medicine, Morsani College of Medicine, University of South Florida, Tampa, FL, 33612, United States

³Department of Chemistry and Biochemistry, The University of Arizona, Tucson, AZ, 85721, United States

⁴Department of Microbiology, Immunology and Molecular Genetics, University of Texas Health Science Center at San Antonio, San Antonio, TX, 78229, United States

*Corresponding authors:

Jun Wang, Tel: 520-626-1366, Fax: 520-626-0749, email:
junwang@pharmacy.arizona.edu

Yu Chen, Tel: 813-974-7809, email: ychen1@usf.edu

Table of Contents

Materials and Methods

Figure S1

Table S1

Synthesis procedure, HNMR, and CNMR characterization of the final products

MATERIALS AND METHODS

Protein Expression and Purification. SARS-CoV-2 main protease (M^{pro}) gene from strain BetaCoV/Wuhan/WIV04/2019 (GenBank: MN996528.1) was purchased from GenScript (Piscataway, NJ) with *E. coli* codon optimization and inserted into pET29a(+) plasmid. The M^{pro} genes were then subcloned into the pE-SUMO plasmid as previously described.¹ The expression and purification procedures were previously described.¹ SARS-CoV main protease (M_{pro}) (accession no.: 6W79_A) was expressed and purified and previously described.² Cathepsin K (catalog no. 219461) and cathepsin L (catalog no. 219402) were purchased from EMD Millipore. Human cathepsin B (catalog no. CTB-H5222) was purchased from Acro Biosystems (Newark, DE), Calpain I (catalog no. C6108) and trypsin (catalog no. T6763) were purchased from Sigma-Aldrich, and caspas-3 (catalog no. 1083–25) was purchased from BioVision (Milpitas, CA)

Differential Scanning Fluorimetry (DSF). Direct binding of testing compounds to SARS CoV-2 M^{pro} was detected by differential scanning fluorimetry (DSF) using a Thermal Fisher QuantStudio 5 Real-Time PCR System as previously described.³ M^{pro} protein was diluted in enzymatic reaction buffer containing 20 mM HEPES, pH 6.5, 120 mM NaCl, 0.4 mM EDTA, 4 mM DTT, and 20% glycerol to a final concentration of 3 μ M and incubated with 6 μ M testing compounds at 30 °C for 30 min. DMSO was included as a reference. Fluorescence signal was recorded from 20 to 95 °C (incremental step of 0.05 °C/s) after adding 1X SYPRO orange (Thermal Fisher, catalog no.: S6650). The melting temperature (T_m) was calculated as the mid log of the transition phase from the native to the denatured protein using a Boltzmann model in Protein Thermal Shift Software v1.3.

Enzymatic Assays. IC₅₀ values for the testing compounds against SARS-CoV-2 M^{pro} was determined as previously described.³ Briefly, 100 nM M^{pro} was incubated with serial concentrations of the compounds at 30 °C for 30 min in 100 µl enzymatic reaction buffer (20 mM HEPES, pH 6.5, 120 mM NaCl, 0.4 mM EDTA, 4 mM DTT, and 20% glycerol). The proteolytic reactions were monitored in Cytaion 5 imaging reader (Thermo Fisher Scientific) with filters for excitation at 360/40 nm and emission at 460/40 nm for 1 h after adding 1 µl of 1 mM of FRET substrate. The initial velocity of the proteolytic reaction was calculated by linear regression for the first 15 min of the kinetic progress curves. IC₅₀ values were calculated in dose-response-variable slope (4 parameters) function in Prism 8. Compound **Jun9-62-2R** was pre-incubated with M^{pro} for 0 min to 2 hrs before the addition of substrate to test the time dependency of IC₅₀ values.

Proteolytic reaction progress curve kinetics measurements with Jun9-66-2R, Jun9-90-3R, Jun9-90-4R and Jun9-88-6R were carried out as previously described with minor modification: 5 nM SARS-CoV-2 M^{pro} was added into 20 µM FRET-substrate premixed with serial concentrations of the compounds in 200 µl of reaction buffer at 30 °C to initiate the proteolytic reaction; the reaction was monitored for 4 h. The first two hours of kinetic curves were utilized in the curve fitting. The progression curves fittings were detailed described in previous publication.³ The k₂/K_i value is commonly used to evaluate the efficacy for covalent inhibitor. For compound Jun9-90-4R, we could not get accurate individual k₂ and K_i values, The calculated slope of K_{obs} over Jun9-90-4R concentration was deemed as k₂/K_i.⁴

To test the inhibition reversibility, 1 µl of DMSO or testing compounds was added to 50 µl of 10 µM SARS CoV-2 M^{pro} protein to final concentration of 10 µM, and incubated at 30 °C for 2 hrs. 1 µl of compound and M^{pro} enzyme mixture was added to 100 µl enzymatic reaction buffer (100-fold dilution), then was incubated for 5 min at room temperature before the addition of 1 µl

of 1 mM FRET substrate to initiate the enzymatic reaction. The initial velocity was measured as described in above paragraph.

Enzymatic reactions against host proteases (Calpain I, Cathepsin K, Cathepsin L, Caspase-3 and Trypsin) were carried out as previously described. Cathepsin B assay reaction was carried out as follows: Cathepsin B (catalog no. CTB-H5222) was diluted into 100 nM final concentration in a buffer containing 20 mM sodium acetate pH5.5, 1 mM EDTA and 2 mM DTT and the mixture was incubated for 30 min at 30 °C. Activated Cathepsin B was further diluted to 500 pm in the reaction buffer (100 mM MES pH6.0, 1 mM EDTA, 2 mM DTT and 0.01% TWEEN 20). Then 1 µl of serial concentrations of testing compounds were added and incubated for 30 min at 30 °C, and the enzymatic reaction was initiated by adding 1 µl of 500 µM of FRET substrate Z-Phe-Arg-AMC (BACHEM, catalog #. 4003379.0050); the IC₅₀ value was calculated same as cathepsin K and L.

Cellular-Based FlipGFP M^{pro} Assay. Plasmid pcDNA3-SARS2-M^{pro}-flipGFP-T2A-mCherry was construct as previously described. SARS-CoV-2 M^{pro} expression plasmid pcDNA3.1 SARS-CoV-2 M^{pro} were ordered from Genscript (Piscataway NJ) with codon optimization. The FlipGFP M^{pro} assay was carried out exact as previously described. Briefly, 50 ng of pcDNA3-SARS2-M^{pro} -flipGFP-T2A-mCherry plasmid and 50 ng of protease expression plasmid pcDNA3.1 SARSCoV-2 M^{pro} were transfected into 293T cells with transfection reagent TransIT-293 (Mirus catalog no. MIR 2700) according to the manufacturer's protocol. Three hours after transfection, testing compound was added to each well at 100-fold dilution. Two days after transfection, GFP and mCherry signals were taken with Cyvation 5 imaging reader (Biotek) using GFP and mCherry channels via 10× objective lens and were analyzed with Gen5 3.10 software (Biotek). SARS-CoV-2 M^{pro} protease activity was evaluated as the ratio of GFP signal

over mCherry signal, the mCherry signal alone in the presence of testing compounds was used to evaluate the compound cytotoxicity.

Native mass spectrometry assay. Prior to analysis, SARS-CoV-2 M^{pro} was buffer exchanged into 0.2 M ammonium acetate and diluted to a final protein concentration of 5 µM. Compounds were added to the protein at a 5:1 molar ratio and allowed to incubate at room temperature for 10 minutes. Native mass spectrometry (MS) was performed using a Q-Exactive HF quadrupole Orbitrap mass spectrometer with the Ultra-High Mass Range research modifications. Samples were ionized using nano-electrospray ionization in positive mode with 1.1 kV of spray voltage at 200 °C. The samples were analyzed with an m/z range of 2,000–10,000, the resolution set to 15,000, and with the trapping gas pressure set to 5. 50 V of source fragmentation were applied to all samples to aid in desolvation. All data were deconvolved and analyzed with UniDec.⁵

X-ray crystallization. Jun9-57-3R and Jun9-62-2R were added to 15 mg/mL SARS-CoV-2 M^{pro} to a final concentration of 2 mM and incubated overnight at 4°C. The protein-inhibitor slurry was spun down at 13,000g for 1 minute. The supernatant was removed and diluted to 5 mg/mL with protein stock buffer (20 mM Tris pH 7.5, 200 mM NaCl, 1 mM DTT). Crystals were grown by mixing protein with an equal volume of crystallization buffer (25 % PEG 3350, 0.2 M AmSO₄, 0.1 M HEPES 7.5) in a vapor diffusion, hanging drop apparatus. Crystals typically grew to full size in several days, at which time they were transferred to a cryoprotectant solution of 30 % PEG 3350, 0.2 M AmSO₄, 0.1 M HEPES 7.5, and 15% glycerol for 5 seconds and flash-frozen in liquid nitrogen.

X-ray diffraction data for SARS-CoV-2 M^{pro} with **Jun9-57-3R** and **Jun9-62-2R** were collected on the SBC 19-ID and SER-CAT 22ID beamlines at the Advanced Photon Source (APS) in Argonne, IL. Diffraction data was indexed and processed with the CCP4 versions of iMosflm.⁶

Diffraction data was then scaled with AIMLESS and molecular replacement performed with MOLREP.⁷ Structural refinement was performed with REFMAC5 and COOT.⁸⁻⁹ SARS-CoV-2 M^{pro} complex structures are deposited in the protein data bank under the accession numbers 7RN0 (**Jun9-57-3R**) and 7RN1 (**Jun9-62-2R**). Crystallographic statistics are presented in Table S1.

Data Availability. The drug-bound complex structures for SARS-CoV-2 M^{pro} with **Jun9-57-3R** and **Jun9-62-2R** were deposited in the Protein Data Bank with accession numbers of 7RN0 and 7RN1, respectively.

Table S1. Crystallographic statistics.

<u>Data Collection</u>	<u>PDB ID_7RN0</u>	<u>PDB ID_7RN1</u>
Inhibitor	Jun9-57-3R	Jun9-62-2R
Space Group	I 1 2 1	C 1 2 1
Cell Dimension		
a, b, c (Å)	45.42, 53.43, 112.03	114.27, 53.26, 45.46
α, β, γ (°)	90.00, 101.37, 90.00	90, 102.82, 90
Resolution (Å)	48.05 - 2.25 (2.33 – 2.25)	48.05 – 2.30 (2.38 – 2.30)
R _{merge}	0.071 (0.709)	0.088 (0.423)
<I>/σ<I>	7.6 (2.2)	7.2 (2.4)
Completeness (%)	92.4 (95.4)	76.7 (82.2)
Multiplicity	2.7 (2.8)	2.9 (2.9)
<hr/>		
<u>Refinement</u>		
Resolution (Å)	38.70 – 2.25 (2.33 – 2.25)	48.05 – 2.30 (2.38 – 2.30)
No. reflections/free	11607 / 597	9032 / 434
R _{work} /R _{free}	0.219 / 0.248	0.204 / 0.230
No. Atoms		
Protein	2335	2361
Ligand/Ion	45	52
Water	22	7
B-Factors (Å ²)		
Overall	58.26	44.70
Protein	58.52	44.83
Ligand/Ion	49.15	39.72
Solvent	49.34	37.61
RMS Deviations		
Bond Lengths (Å)	0.015	0.014
Bond Angles (°)	1.92	1.91
Ramachandran Favored (%)	95.00	96.04
Ramachandran Allowed (%)	5.00	3.96
Ramachandran Outliers (%)	0.00	0.00
Rotameric Outliers (%)	2.32	1.91
Clashscore	8.76	5.71

* Values in parentheses refer to the last resolution shell.

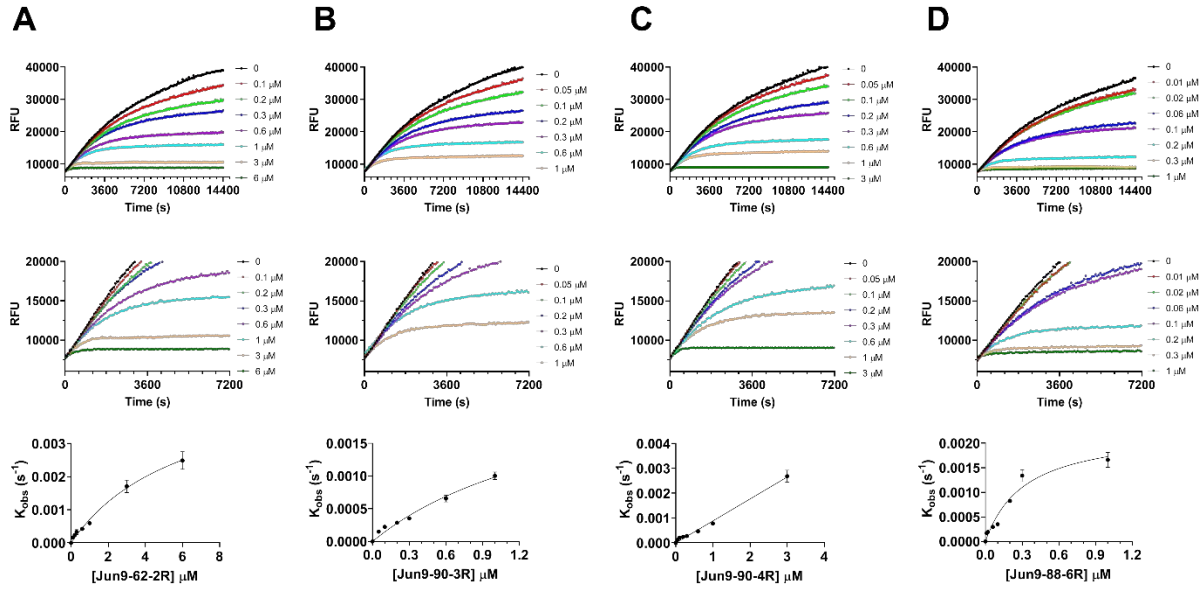


Figure S1. Enzymatic kinetic studies of Jun9-62-2R (A), Jun9-90-3R (B), Jun9-90-4R (C), and Jun9-88-6R (D) in inhibiting SARS-CoV-2 M^{pro}.

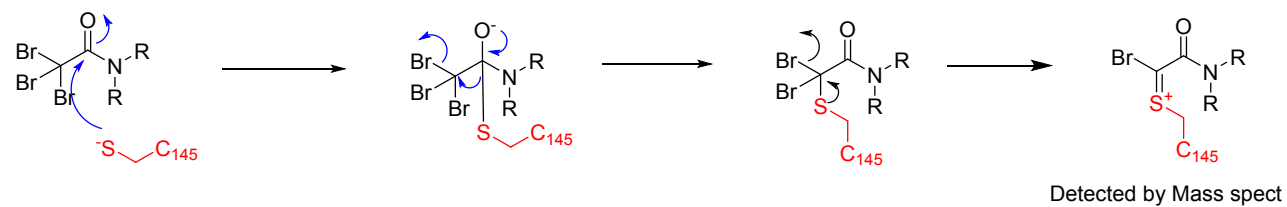
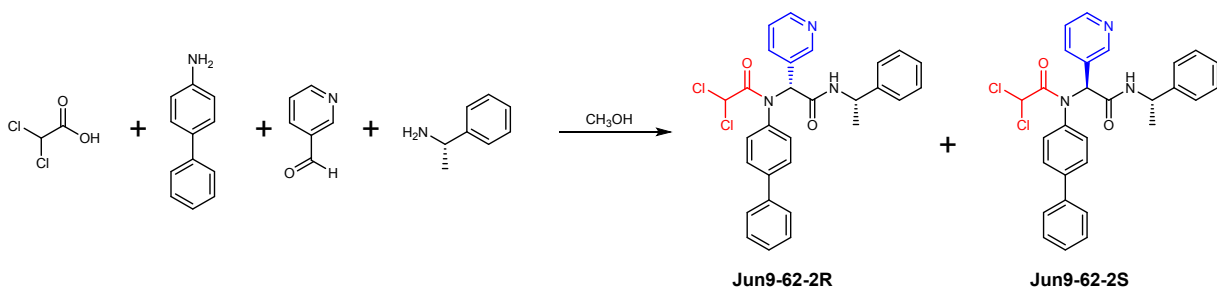


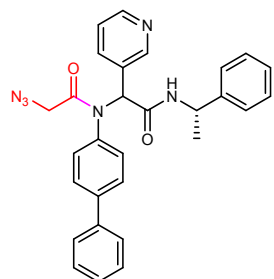
Figure S2. Putative drug conjugation mechanism for the tribromide compound **Jun9-88-6.**

Chemistry. Chemicals were ordered from commercial sources and were used without further purification. All final compounds were purified by flash column chromatography. ^1H and ^{13}C NMR spectra were recorded on a Bruker-400 NMR spectrometer. Chemical shifts are reported in parts per million referenced with respect to residual solvent DMSO-d6) 2.50 ppm and from internal standard tetramethylsilane (TMS) 0.00 ppm. The following abbreviations were used in reporting spectra: s, singlet; d, doublet; t, triplet; q, quartet; m, multiplet; dd, doublet of doublets. All reactions were carried out under N_2 atmosphere unless otherwise stated. HPLC-grade solvents were used for all reactions. Flash column chromatography was performed using silica gel (230-400 mesh, Merck). Low-resolution mass spectra were obtained using an ESI technique on a 3200 Q Trap LC/MS/MS system (Applied Biosystems). The purity was assessed by using Shimadzu LC-MS with Waters Xterra MS C-18 column (part #186000538), 50 \times 2.1 mm, at a flow rate of 0.3 mL/min; λ = 250 and 220 nm; mobile phase A, 0.1% formic acid in H_2O , and mobile phase B', 0.1% formic in 60% isopropanol, 30% CH_3CN and 9.9% H_2O . The diastereomers were separated using the ACCQPrep HP150 HPLC system equipped with the Chiral HPLC Lux®5 μM i-Amylose-3 chiral HPLC column.

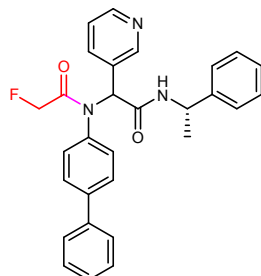


General Synthesis Procedure. The M^{pro} inhibitors were synthesized using the Ugi four-component reaction methodology as described previously.¹⁰ Briefly, aldehyde (1

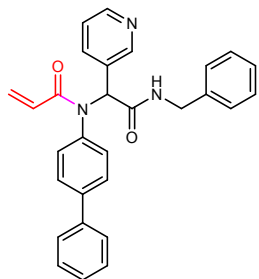
mmol) and amine (1 mmol) were mixed in methanol (10 ml) and stirred at room temperature for 30 minutes. Then acid (1 mmol) and isocyanide (1 mmol) were added sequentially. The resulting mixture was stirred at room temperature overnight. Solvent was removed under reduced pressure and the residue was purified by silica gel flash column chromatography (CH_2Cl_2 to $\text{CH}_2\text{Cl}_2/\text{MeOH} = 10:1$) to afford the target product.



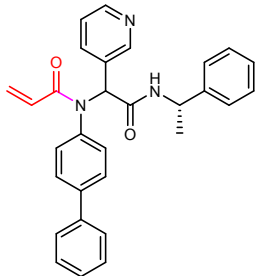
N-([1,1'-biphenyl]-4-yl)-2-azido-N-(2-oxo-2-((S)-1-phenylethyl)amino)-1-(pyridin-3-yl)ethylacetamide (Jun9-61-1). White solid, 50% yield, dr = 1:1. ^1H NMR (500 MHz, DMSO-d6) δ 8.78-8.72 (m, 1H), 8.50-8.19 (m, 2H), 7.64-7.03 (m, 16H), 6.25 (s, 0.5H), 6.22 (s, 0.5H), 5.14-4.85 (m, 1H), 3.84-3.75 (m, 1H), 3.68-3.61 (m, 1H), 1.40 (d, $J = 7.0$ Hz, 1.5H), 1.28 (d, $J = 7.0$ Hz, 1.5H). ^{13}C NMR (125 MHz, DMSO-d6) δ 168.0, 167.8, 167.4, 167.3, 151.2, 151.1, 148.9, 148.8, 144.2, 143.9, 139.7, 138.6, 137.4, 137.3, 136.8, 131.2, 130.6, 130.2, 128.9, 128.9, 128.2, 128.1, 127.8, 126.8, 126.7, 126.6, 126.6, 126.2, 125.8, 123.0, 122.7, 61.7, 50.6, 48.4, 48.3, 22.3, 22.1. $\text{C}_{29}\text{H}_{26}\text{N}_6\text{O}_2$, HRMS calculated for m/z [M+H] $^+$: 491.219549 (calculated), 491.21900 (found).



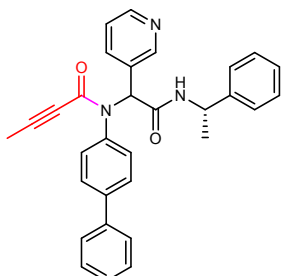
N-([1,1'-biphenyl]-4-yl)-2-fluoro-N-(2-oxo-2-((S)-1-phenylethyl)amino)-1-(pyridin-3-yl)ethylacetamide (**Jun9-61-4**). White solid, 79% yield, dr = 1:1. ¹H NMR (500 MHz, DMSO-d6) δ 8.90-8.61 (m, 1H), 8.47-8.22 (m, 2H), 7.66-7.08 (m, 16H), 6.25 (s, 0.5H), 6.23 (s, 0.5H), 5.04-4.93 (m, 1H), 4.80-4.51 (m, 2H), 1.40 (d, *J* = 7.0 Hz, 1.5H), 1.28 (d, *J* = 7.0 Hz, 1.5H). ¹³C NMR (125 MHz, DMSO-d6) δ 167.9, 167.7, 166.5, 166.5, 166.4, 166.3, 151.2, 151.1, 148.9, 148.9, 144.2, 143.9, 139.8, 138.6, 137.4, 137.4, 135.9, 135.8, 131.2, 130.5, 130.0, 129.0, 128.9, 128.2, 128.1, 127.9, 126.8, 126.7, 126.7, 126.6, 126.2, 125.8, 123.0, 122.8, 79.3, 78.0, 61.3, 61.2, 48.4, 48.3, 22.3, 22.1. C₂₉H₂₆FN₃O₂, HRMS calculated for m/z [M+H]⁺: 468.208730 (calculated), 468.20818 (found).



N-([1,1'-biphenyl]-4-yl)-N-(2-(benzylamino)-2-oxo-1-(pyridin-3-yl)ethyl)acrylamide (**Jun10-15-2**). White solid, 75% yield. ¹H NMR (500 MHz, DMSO-d6) δ 8.78 (t, *J* = 6.0 Hz, 1H), 8.40-8.28 (m, 2H), 7.66-7.12 (m, 16H), 6.33-6.20 (m, 2H), 6.00-5.93 (m, 1H), 5.61 (dd, *J* = 10.5, 2.0 Hz, 1H), 4.47-4.33 (m, 2H). ¹³C NMR (125 MHz, DMSO-d6) δ 168.9, 164.7, 151.1, 148.8, 139.3, 139.1, 138.7, 138.2, 137.5, 131.3, 130.9, 128.9, 128.2, 127.9, 127.7, 127.2, 126.7, 126.5, 122.9, 61.8, 42.4. C₂₉H₂₅N₃O₂, HRMS calculated for m/z [M+H]⁺: 448.202502, (calculated), 448.20195 (found).

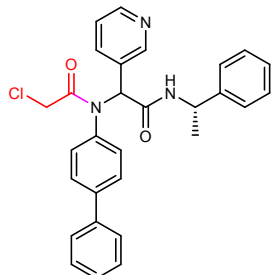


N-([1,1'-biphenyl]-4-yl)-N-(2-oxo-2-((S)-1-phenylethyl)amino)-1-(pyridin-3-yl)ethyl)acrylamide (Jun9-51-3), dr = 1.4:1. White solid, 84% yield. ^1H NMR (500 MHz, DMSO-d6) δ 8.76-.70 (m, 1H), 8.41-8.24 (m, 2H), 7.62-7.07 (m, 15H), 6.33-6.17 (m, 2H), 5.98-5.88 (m, 1H), 5.62-5.55 (m, 1H), 5.07-4.96 (m, 1H), 1.38 (d, J = 7.0 Hz, 1.75H), 1.27 (d, J = 7.0 Hz, 1.25H). ^{13}C NMR (125 MHz, DMSO-d6) 168.2, 168.0, 164.6, 164.6, 151.2, 151.1, 148.8, 144.3, 140.0, 139.3, 139.3, 138.7, 138.1, 138.1, 137.4, 137.4, 131.4, 131.1, 130.7, 128.9, 128.9, 128.2, 128.1, 128.0, 127.7, 126.7, 126.6, 126.5, 126.2, 125.8, 123.0, 122.7, 61.5, 48.4, 48.3, 22.3, 22.2. $\text{C}_{30}\text{H}_{27}\text{N}_3\text{O}_2$, HRMS calculated for m/z [M+H] $^+$: 462.218152 (calculated), 462.21760 (found).

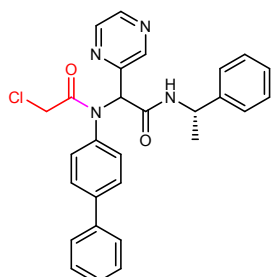


N-([1,1'-biphenyl]-4-yl)-N-(2-oxo-2-((S)-1-phenylethyl)amino)-1-(pyridin-3-yl)ethyl)but-2-ynamide (Jun9-62-1), dr = 1:1. White solid, 50% yield. ^1H NMR (500 MHz, DMSO-d6) δ 8.74 (d, J = 7.5 Hz, 1H), 8.42-8.25 (m, 2H), 7.56-7.09 (m, 16H), 6.18 (d, J = 13.0 Hz, 1H), 5.05-4.95 (m, 1H), 1.69 (d, J = 6.5 Hz, 3H), 1.37 (d, J = 7.0 Hz, 1.5H), 1.27 (d, J = 7.0 Hz, 1.5H). ^{13}C NMR (125 MHz, DMSO-d6) 167.7, 167.5, 153.5, 153.5, 151.1, 151.0, 148.9,

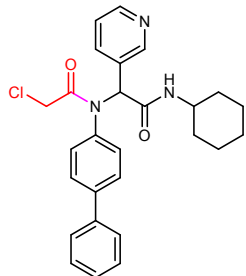
148.9, 144.2, 143.9, 139.1, 139.1, 138.7, 138.2, 138.2, 137.4, 137.3, 131.4, 130.5, 130.2, 128.9, 128.2, 128.1, 127.7, 126.7, 126.7, 126.5, 126.1, 126.1, 125.8, 123.1, 122.8, 90.8, 90.7, 74.3, 74.3, 61.3, 61.3, 48.5, 48.3, 22.3, 22.1, 3.2, 3.2. $C_{31}H_{27}N_3O_2$, HRMS calculated for m/z [M+H]⁺: 474.218152 (calculated), 474.21760 (found).



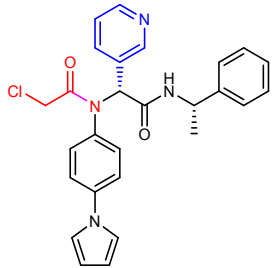
2-(N-{{[1,1'-biphenyl]-4-yl}-2-chloroacetamido)-N-[(1S)-1-phenylethyl]-2-(pyridin-3-yl)acetamide (**Jun9-54-1**). dr = 1:1. White solid, 88% yield. ¹H NMR (400 MHz, DMSO-*d*₆) δ 8.73 (dd, *J* = 10.4, 7.8 Hz, 1H), 8.52 – 8.20 (m, 2H), 7.69 – 7.29 (m, 10H), 7.29 – 7.03 (m, 5H), 6.20 (d, *J* = 6.8 Hz, 1H), 5.00 (h, *J* = 7.3 Hz, 1H), 4.19 – 3.90 (m, 2H), 1.39 (d, *J* = 7.0 Hz, 1.5H), 1.26 (d, *J* = 7.0 Hz, 1.5H). ¹³C NMR (101 MHz, DMSO-*d*₆) δ 167.74, 167.59, 165.47, 165.41, 151.05, 150.97, 148.81, 144.15, 143.80, 139.63, 138.52, 137.31, 137.21, 137.15, 131.20, 130.57, 130.18, 128.86, 128.85, 128.21, 128.15, 128.01, 127.75, 126.70, 126.63, 126.55, 126.49, 126.48, 126.10, 125.68, 122.96, 122.67, 61.84, 48.32, 48.20, 42.99, 22.20, 22.01. $C_{29}H_{26}ClN_3O_2$, HRMS calculated for m/z [M+H]⁺: 484.179180 (calculated), 484.17863 (found).



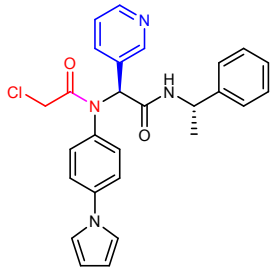
2-(N-{{[1,1'-biphenyl]-4-yl}-2-chloroacetamido)-N-[(1S)-1-phenylethyl]-2-(pyrazin-2-yl)acetamide (**Jun9-59-1**). White solid, 82% yield, dr = 1:1. ^1H NMR (500 MHz, DMSO- d_6) δ 8.76 (dd, J = 28.6, 7.8 Hz, 1H), 8.62 – 8.33 (m, 3H), 7.73 – 7.12 (m, 14H), 6.33 (d, J = 3.9 Hz, 1H), 4.99 (dp, J = 21.6, 7.1 Hz, 1H), 4.24 – 3.91 (m, 2H), 1.34 (d, J = 7.1 Hz, 2H), 1.30 (d, J = 7.0 Hz, 1H). ^{13}C NMR (126 MHz, DMSO- d_6) δ 166.16, 166.03, 165.74, 160.02, 150.97, 150.82, 145.92, 145.81, 144.05, 143.90, 143.74, 143.68, 143.47, 139.87, 139.82, 138.66, 130.79, 130.71, 128.94, 128.28, 128.21, 128.11, 127.84, 126.88, 126.85, 126.73, 126.68, 126.63, 126.60, 126.13, 125.95, 125.93, 64.41, 64.34, 48.43, 48.37, 42.89, 22.17, 22.14. $\text{C}_{28}\text{H}_{25}\text{ClN}_4\text{O}_2$, HRMS calculated for m/z [M+H] $^+$: 485.174429 (calculated), 485.17388 (found).



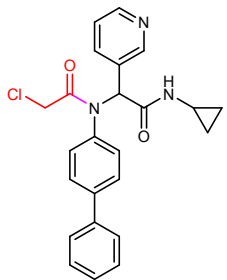
N-({[1,1'-biphenyl]-4-yl)-2-chloro-N-(2-(cyclohexylamino)-2-oxo-1-(pyridin-3-yl)ethyl)acetamide (**Jun9-55-2**). White solid, 85% yield. ^1H NMR (500 MHz, DMSO-d6) δ 8.45-8.40 (m, 1H), 7.55-7.30 (m, 8H), 7.08 (dd, J = 8.0, 5.0 Hz, 1H), 6.65 (d, J = 7.5 Hz, 1H), 6.12 (s, 1H), 3.98-3.87 (m, 2H), 3.84-3.72 (m, 1H), 2.06-1.56 (m, 5H), 1.44-0.98 (m, 5H). ^{13}C NMR (125 MHz, DMSO-d6) δ 167.7, 167.3, 151.2, 149.6, 142.1, 139.4, 138.1, 136.8, 130.9, 130.4, 128.9, 128.0, 127.1, 123.4, 62.6, 49.1, 42.5, 32.7, 32.7, 25.5, 24.9, 24.8. $\text{C}_{27}\text{H}_{28}\text{ClN}_3\text{O}_2$, HRMS calculated for m/z [M+H] $^+$: 462.194830 (calculated), 462.19428 (found).



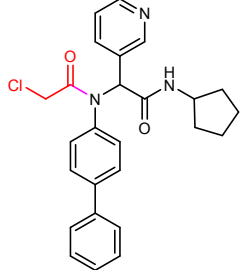
N-(4-(1H-pyrrol-1-yl)phenyl)-2-chloro-N-((R)-2-oxo-2-((S)-1-phenylethyl)amino)-1-(pyridin-3-yl)ethylacetamide (**Jun9-57-3R**). White solid, 30% yield. ^1H NMR (500 MHz, DMSO-d6) δ 8.64 (d, J = 8.0 Hz, 1H), 8.34-8.22 (m, 2H), 7.51-7.02 (m, 13H), 6.18-6.10 (m, 3H), 5.06-4.85 (m, 1H), 4.00-3.85 (m, 2H), 1.18 (d, J = 7.0 Hz, 3H). ^{13}C NMR (125 MHz, DMSO-d6) δ 167.9, 165.6, 151.1, 149.0, 143.9, 139.2, 137.3, 134.5, 132.1, 130.6, 128.2, 126.7, 126.2, 123.1, 118.7, 118.5, 110.9, 61.8, 48.3, 43.1, 22.1. $\text{C}_{27}\text{H}_{25}\text{ClN}_4\text{O}_2$, HRMS calculated for m/z [M+H] $^+$: 473.174429 (calculated), 473.17388 (found).



N-(4-(1H-pyrrol-1-yl)phenyl)-2-chloro-N-((S)-2-oxo-2-((S)-1-phenylethyl)amino)-1-(pyridin-3-yl)ethylacetamide (**Jun9-57-3S**). White solid, 31% yield. ^1H NMR (500 MHz, DMSO-d6) δ 8.67 (d, J = 7.5 Hz, 1H), 8.24 (dd, J = 4.5, 1.5 Hz, 1H), 8.17 (d, J = 2.0 Hz, 1H), 7.52-6.91 (m, 13H), 6.24-6.04 (m, 3H), 5.05-4.81 (m, 1H), 3.95 (dd, J = 39.0, 14.0 Hz, 2H), 1.31 (d, J = 7.0 Hz, 3H). ^{13}C NMR (125 MHz, DMSO-d6) δ 167.7, 165.7, 151.2, 149.0, 144.2, 139.2, 137.4, 134.5, 132.1, 130.2, 128.1, 126.6, 125.7, 122.8, 118.7, 118.6, 110.9, 61.8, 48.4, 43.1, 22.3. $\text{C}_{27}\text{H}_{25}\text{ClN}_4\text{O}_2$, HRMS calculated for m/z [M+H] $^+$: 473.174429 (calculated), 473.17388 (found).

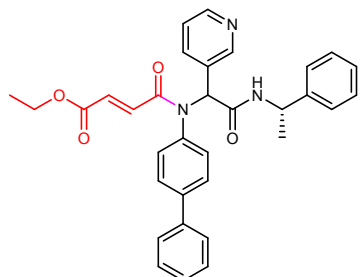


N-([1,1'-biphenyl]-4-yl)-2-chloro-N-(2-(cyclopropylamino)-2-oxo-1-(pyridin-3-yl)ethyl)acetamide (Jun9-57-2). White solid, 75% yield. ¹H NMR (500 MHz, DMSO-d₆) δ 8.36 (d, *J* = 4.0 Hz, 1H), 8.32 (d, *J* = 2.5 Hz, 2H), 7.63-7.32 (m, 11H), 7.15 (dd, *J* = 8.0, 4.5 Hz, 1H), 6.02 (s, 1H), 4.03 (dd, *J* = 35.5, 14.0 Hz, 2H), 2.74-2.61 (m, 1H), 0.70-0.55 (m, 2H), 0.43-0.26 (m, 2H). ¹³C NMR (125 MHz, DMSO-d₆) δ 170.1, 166.0, 151.4, 149.4, 131.7, 131.0, 129.4, 128.3, 127.3, 127.1, 123.5, 62.4, 43.6, 23.0, 6.1. C₂₄H₂₂CIN₃O₂, HRMS calculated for m/z [M+H]⁺: 420.147880 (calculated), 420.14733 (found).

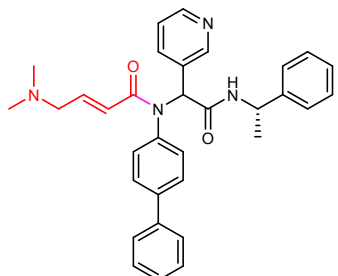


2-(N-([1,1'-biphenyl]-4-yl)-2-chloroacetamido)-N-cyclopentyl-2-(pyridin-3-yl)acetamide (Jun9-55-1). White solid, 72% yield. ¹H NMR (500 MHz, DMSO-d₆) δ 8.46 – 8.28 (m, 2H), 8.23 (d, *J* = 7.0 Hz, 1H), 7.78 – 7.49 (m, 4H), 7.49 – 7.25 (m, 5H), 7.15 (dd, *J* = 7.9, 4.7 Hz, 1H), 6.09 (s, 1H), 4.17 – 4.02 (m, 2H), 4.02 – 3.88 (m, 1H), 1.94 – 1.67 (m, 2H), 1.67 – 1.32 (m, 5H), 1.32 – 1.14 (m, 1H). ¹³C NMR (126 MHz, DMSO-d₆) δ 168.58, 167.88, 165.47, 150.94, 148.79, 139.70, 138.62, 137.33, 137.29, 131.26, 130.78, 129.00, 128.94, 127.83, 126.77, 126.57, 122.99, 61.92, 50.71, 43.11, 32.13, 31.85,

23.48, 23.43. $C_{26}H_{26}ClN_3O_2$, HRMS calculated for m/z [M+H]⁺: 448.179180 (calculated), 448.17863 (found).

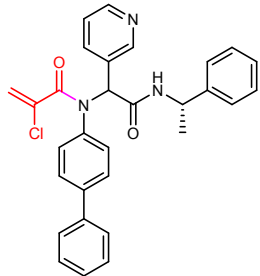


Ethyl (E)-4-([1,1'-biphenyl]-4-yl)(2-oxo-2-((S)-1-phenylethyl)amino)-1-(pyridin-3-yl)ethylamino-4-oxobut-2-enoate (**Jun9-72-3**), dr = 1:1. White solid, 69% yield. ¹H NMR (500 MHz, DMSO-d6) δ 8.78 (t, J = 7.6 Hz, 1H), 8.57-8.16 (m, 2H), 7.79-7.00 (m, 16H), 6.82-6.53 (m, 2H), 6.31 (d, J = 11.2 Hz, 1H), 5.17-4.85 (m, 1H), 4.27-3.90 (m, 2H), 1.40 (d, J = 7.2 Hz, 1.5H), 1.29 (d, J = 7.2 Hz, 1.5H), 1.17-1.11 (m, 3H). ¹³C NMR (125 MHz, DMSO-d6) δ 167.7, 167.6, 164.7, 164.7, 163.0, 163.0, 151.2, 151.1, 148.9, 144.2, 143.9, 139.6, 138.5, 137.4, 137.4, 134.3, 131.3, 130.7, 130.3, 130.3, 129.0, 128.9, 128.2, 128.1, 127.9, 126.8, 126.7, 126.6, 126.6, 126.2, 125.8, 123.1, 122.8, 61.9, 60.8, 60.8, 48.4, 48.4, 22.3, 22.1, 13.9. $C_{33}H_{31}N_3O_4$, HRMS calculated for m/z [M+H]⁺: 534.239282 (calculated), 534.23873 (found).



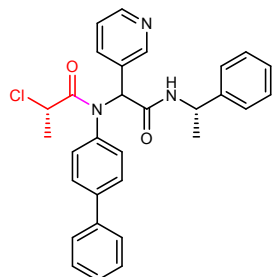
(2E)-N-([1,1'-biphenyl]-4-yl)-4-(dimethylamino)-N-([(1S)-1phenylethyl]carbamoyl)-(pyridine-3-yl)methylbut-2-enamide (**Jun10-31-4**). dr = 1:1. White solid, 75% yield. ¹H

¹H NMR (500 MHz, DMSO-*d*₆) δ 8.79 – 8.65 (m, 1H), 8.44 – 8.21 (m, 2H), 7.68 – 7.02 (m, 15H), 6.84 – 6.53 (m, 1H), 6.31 (s, 0.5H), 6.28 (s, 0.5H), 5.81 – 5.56 (m, 1H), 5.13 – 4.89 (m, 1H), 2.94 – 2.74 (m, 2H), 2.01 (s, 3H), 2.00 (s, 3H), 1.37 (d, *J* = 7.0 Hz, 1.5H), 1.26 (d, *J* = 7.0 Hz, 1.5H). ¹³C NMR (126 MHz, DMSO-*d*₆) δ 168.23, 168.10, 164.66, 164.63, 151.14, 151.07, 148.73, 144.35, 143.96, 142.37, 139.03, 139.01, 138.63, 138.32, 138.25, 137.36, 137.33, 131.43, 131.41, 131.21, 130.80, 128.93, 128.91, 128.27, 128.19, 128.05, 127.73, 126.66, 126.57, 126.52, 126.48, 126.19, 125.92, 125.74, 123.08, 122.97, 122.68, 61.42, 59.62, 59.61, 48.35, 48.24, 44.85, 22.31, 22.17. C₃₃H₃₄N₄O₂, HRMS calculated for m/z [M+H]⁺: 519.276001 (calculated), 519.27545 (found).

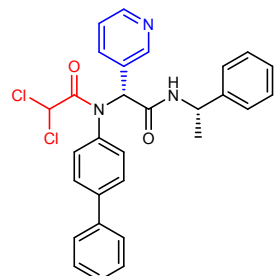


N-[(1,1'-biphenyl)-4-yl]-2-chloro-N-[(1S)-1-phenylethyl]carbamoyl(pyridin-3-yl)methyl)prop-2-enamide (**Jun10-38-2**). dr = 1:1. White solid, 72% yield. ¹H NMR (500 MHz, DMSO-*d*₆) δ 8.82 – 8.67 (m, 1H), 8.47 – 8.23 (m, 2H), 7.75 – 7.54 (m, 2H), 7.54 – 7.14 (m, 12H), 7.12 – 7.00 (m, 1H), 6.22 (s, 0.5H), 6.19 (s, 0.5H), 5.64 – 5.43 (m, 2H), 5.13 – 4.86 (m, 1H), 1.36 (d, *J* = 7.0 Hz, 1.5H), 1.27 (d, *J* = 7.0 Hz, 1.5H). ¹³C NMR (126 MHz, DMSO-*d*₆) δ 167.46, 167.33, 164.30, 164.25, 151.16, 151.11, 149.00, 144.20, 143.77, 139.12, 138.54, 138.09, 138.05, 137.42, 131.53, 131.49, 131.23, 131.19, 130.51, 130.13, 128.90, 128.89, 128.22, 128.09, 127.74, 126.72, 126.64, 126.47, 126.15, 125.76, 123.06, 122.76, 119.96, 119.94, 61.89, 61.86, 48.45, 48.26, 22.22, 22.12.

$C_{30}H_{26}ClN_3O_2$, HRMS calculated for m/z [M+H]⁺: 496.179180 (calculated), 496.17863 (found).

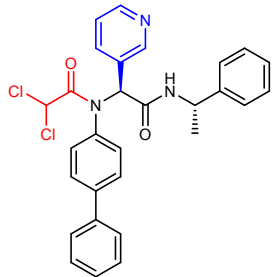


(2S)-N-([1,1'-biphenyl]-4-yl)-2-chloro-N-(2-oxo-2-((S)-1-phenylethyl)amino)-1-(pyridin-3-yl)ethylpropanamide (**Jun9-77-1**), dr = 1:1. White solid, 74% yield. ¹H NMR (500 MHz, DMSO-d6) δ 8.70 (d, *J* = 7.5 Hz, 1H), 8.51-8.39 (m, 2H), 7.62-7.45 (m, 5H), 7.39-7.33 (m, 3H), 7.31-7.26 (m, 1H), 7.17-7.07 (m, 3H), 7.05-6.99 (m, 2H), 6.16 (s, 1H), 4.9-4.83 (m, 1H), 4.25 (q, *J* = 6.5 Hz, 1H), 1.43 (d, *J* = 7.0 Hz, 3H), 1.27 (d, *J* = 7.0 Hz, 3H). ¹³C NMR (125 MHz, DMSO-d6) δ 168.7, 166.7, 147.7, 145.9, 144.1, 141.3, 140.1, 138.6, 137.2, 132.2, 131.1, 129.0, 128.2, 127.9, 127.1, 126.7, 126.6, 125.8, 124.3, 61.8, 51.0, 48.6, 22.2, 21.2. $C_{30}H_{28}ClN_3O_2$, HRMS calculated for m/z [M+H]⁺: 498.194830 (calculated), 498.19428 (found).

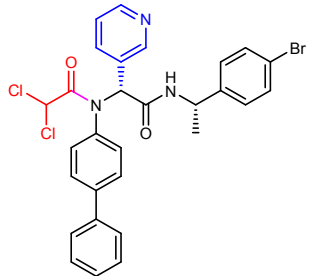


N-([1,1'-biphenyl]-4-yl)-2,2-dichloro-N-((R)-2-oxo-2-((S)-1-phenylethyl)amino)-1-(pyridin-3-yl)ethylacetamide (**Jun9-62-2R**). White solid, 41% yield. ¹H NMR (500 MHz,

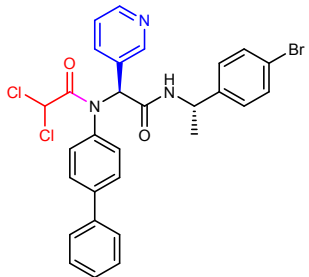
DMSO-d6) δ 8.65 (d, J = 8.0 Hz, 1H), 8.33 (d, J = 2.0 Hz, 1H), 8.28 (dd, J = 4.5, 1.5 Hz, 1H), 7.83-6.73 (m, 16H), 6.07 (d, J = 20.0 Hz, 2H), 4.95 (p, J = 7.0 Hz, 1H), 1.18 (d, J = 7.0 Hz, 3H). ^{13}C NMR (125 MHz, DMSO-d6) δ 167.2, 163.1, 151.2, 149.2, 143.7, 140.2, 138.5, 137.4, 136.1, 131.2, 130.0, 129.0, 128.2, 127.9, 127.0, 126.8, 126.6, 126.2, 123.1, 65.1, 62.5, 48.3, 22.1. $\text{C}_{29}\text{H}_{25}\text{Cl}_2\text{N}_3\text{O}_2$, HRMS calculated for m/z [M+H] $^+$: 518.140208 (calculated), 518.13966 (found).



N-([1,1'-biphenyl]-4-yl)-2,2-dichloro-N-((S)-2-oxo-2-((S)-1-phenylethyl)amino)-1-(pyridin-3-yl)ethylacetamide (**Jun9-62-2S**). White solid, 40% yield. ^1H NMR (500 MHz, DMSO-d6) δ 8.69 (d, J = 7.5 Hz, 1H), 8.24 (dd, J = 4.5, 1.5 Hz, 1H), 8.20 (d, J = 2.0 Hz, 1H), 7.80-6.71 (m, 16H), 6.07 (s, 2H), 4.92 (p, J = 7.0 Hz, 1H), 1.31 (d, J = 7.0 Hz, 3H). ^{13}C NMR (125 MHz, DMSO-d6) δ 167.1, 163.1, 151.3, 149.1, 144.2, 140.2, 138.5, 137.4, 136.1, 131.2, 129.5, 128.9, 128.1, 127.9, 127.0, 126.6, 126.6, 125.7, 122.7, 65.1, 62.5, 48.5, 22.3. $\text{C}_{29}\text{H}_{25}\text{Cl}_2\text{N}_3\text{O}_2$, HRMS calculated for m/z [M+H] $^+$: 518.140208 (calculated), 518.13966 (found).

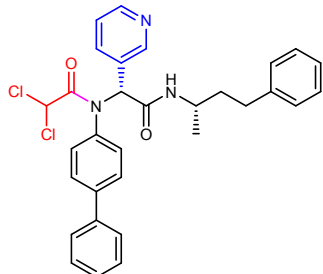


N-([1,1'-biphenyl]-4-yl)-N-((R)-2-(((S)-1-(4-bromophenyl)ethyl)amino)-2-oxo-1-(pyridin-3-yl)ethyl)-2,2-dichloroacetamide (Jun9-90-3R). White solid, 35% yield. ^1H NMR (500 MHz, DMSO-d6) δ 8.70 (d, J = 7.5 Hz, 1H), 8.33 (s, 1H), 8.28 (d, J = 4.5 Hz, 1H), 7.80-6.72 (m, 16H), 6.06 (d, J = 5.5 Hz, 2H), 4.91 (p, J = 7.0 Hz, 1H), 1.17 (d, J = 7.0 Hz, 3H). ^{13}C NMR (125 MHz, DMSO-d6) δ 167.3, 163.1, 151.2, 149.2, 143.3, 140.2, 138.5, 137.4, 136.1, 131.1, 129.9, 129.0, 128.4, 128.0, 127.0, 126.6, 123.1, 119.8, 65.1, 62.6, 47.9, 22.0. $\text{C}_{29}\text{H}_{24}\text{BrCl}_2\text{N}_3\text{O}_2$, HRMS calculated for m/z [M+H] $^+$: 596.050719 (calculated), 596.05017 (found).

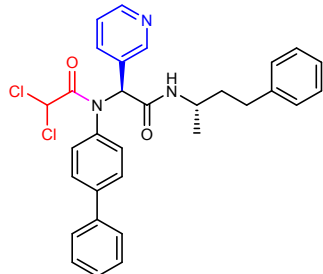


N-([1,1'-biphenyl]-4-yl)-N-((S)-2-(((S)-1-(4-bromophenyl)ethyl)amino)-2-oxo-1-(pyridin-3-yl)ethyl)-2,2-dichloroacetamide (Jun9-90-3S). White solid, 34% yield. ^1H NMR (500 MHz, DMSO-d6) δ 8.73 (d, J = 7.5 Hz, 1H), 8.25 (d, J = 4.5 Hz, 1H), 8.19 (s, 1H), 7.83-6.71 (m, 16H), 6.06 (d, J = 9.0 Hz, 2H), 4.89 (p, J = 7.0 Hz, 1H), 1.28 (d, J = 7.0 Hz, 3H). ^{13}C NMR (125 MHz, DMSO-d6) δ 167.2, 163.1, 151.2, 149.2, 143.8, 140.2, 138.5, 137.4, 136.0, 131.1, 131.0, 129.4, 128.9, 128.0, 127.9, 127.0, 126.6, 122.8, 119.6, 65.1, 62.5, 48.1,

22.1. $C_{29}H_{24}BrCl_2N_3O_2$, HRMS calculated for m/z [M+H]⁺: 596.050719 (calculated), 596.05017 (found).

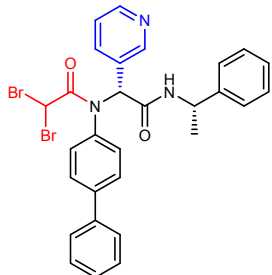


N-([1,1'-biphenyl]-4-yl)-2,2-dichloro-N-((R)-2-oxo-2-(((S)-4-phenylbutan-2-yl)amino)-1-(pyridin-3-yl)ethyl)acetamide (**Jun9-90-4R**). White solid, 32% yield. ¹H NMR (500 MHz, DMSO-d₆) δ 8.33 (s, 1H), 8.26 (d, *J* = 4.0 Hz, 1H), 8.16 (d, *J* = 8.0 Hz, 1H), 7.88-6.77 (m, 16H), 6.08 (s, 1H), 6.01 (s, 1H), 3.83-3.71 (m, 1H), 2.66-2.52 (m, 2H), 1.62 (dd, *J* = 14.5, 7.5 Hz, 2H), 0.89 (d, *J* = 6.5 Hz, 3H). ¹³C NMR (125 MHz, DMSO-d₆) δ 167.2, 163.1, 151.2, 149.1, 142.0, 140.2, 138.5, 137.4, 136.2, 131.2, 130.0, 128.9, 128.5, 128.2, 127.9, 127.0, 126.6, 125.6, 123.0, 65.2, 62.7, 44.3, 37.8, 31.7, 20.5. $C_{31}H_{29}Cl_2N_3O_2$, HRMS calculated for m/z [M+H]⁺: 546.171508 (calculated), 546.17096 (found).

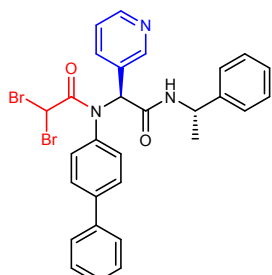


N-([1,1'-biphenyl]-4-yl)-2,2-dichloro-N-((S)-2-oxo-2-(((S)-4-phenylbutan-2-yl)amino)-1-(pyridin-3-yl)ethyl)acetamide (**Jun9-90-4S**). White solid, 33% yield. ¹H NMR (500 MHz, DMSO-d₆) δ 8.34 (s, 1H), 8.27 (d, *J* = 4.5 Hz, 1H), 8.15 (d, *J* = 8.0 Hz, 1H), 7.92-6.70 (m, 16H), 6.07 (s, 1H), 5.99 (s, 1H), 3.84-3.72 (m, 1H), 2.28-2.20 (m, 2H), 1.59-1.43 (m, 2H), 1.05 (d, *J* = 6.5 Hz, 3H). ¹³C NMR (125 MHz, DMSO-d₆) δ 167.2, 163.1, 151.2, 149.2,

141.7, 140.2, 138.5, 137.5, 136.2, 131.2, 130.1, 128.9, 128.2, 128.1, 127.9, 127.0, 126.6, 125.6, 122.9, 65.2, 62.8, 44.5, 31.5, 20.6. $C_{31}H_{29}Cl_2N_3O_2$, HRMS calculated for m/z [M+H]⁺: 546.171508 (calculated), 546.17096 (found).

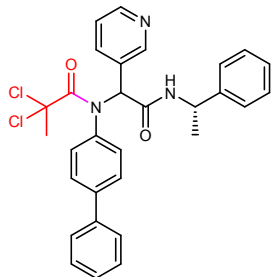


N-([1,1'-biphenyl]-4-yl)-2,2-dibromo-N-((R)-2-oxo-2-(((S)-1-phenylethyl)amino)-1-(pyridin-3-yl)ethyl)acetamide (Jun9-89-2R). White solid, 37% yield. 1H NMR (500 MHz, DMSO-d₆) δ 8.63 (d, J = 8.0 Hz, 1H), 8.33 (s, 1H), 8.28 (d, J = 4.5 Hz, 1H), 7.78-6.77 (m, 16H), 6.08 (s, 1H), 5.79 (s, 1H), 4.95 (p, J = 7.0 Hz, 1H), 1.18 (d, J = 7.0 Hz, 3H). ^{13}C NMR (125 MHz, DMSO-d₆) δ 167.2, 163.6, 151.1, 149.1, 143.6, 140.2, 138.5, 137.5, 136.7, 130.9, 130.1, 129.0, 128.3, 128.0, 127.0, 126.7, 126.6, 126.2, 123.1, 62.5, 48.2, 36.2, 22.1. $C_{29}H_{25}Br_2N_3O_2$, HRMS calculated for m/z [M+H]⁺: 606.039174 (calculated), 606.03863 (found).

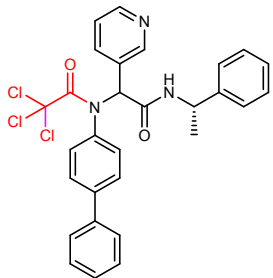


N-([1,1'-biphenyl]-4-yl)-2,2-dibromo-N-((S)-2-oxo-2-(((S)-1-phenylethyl)amino)-1-(pyridin-3-yl)ethyl)acetamide (Jun9-89-2S). White solid, 38% yield. 1H NMR (500 MHz,

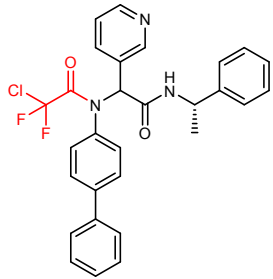
DMSO-d6) δ 8.67 (d, J = 7.5 Hz, 1H), 8.24 (d, J = 4.5 Hz, 1H), 8.19 (s, 1H), 7.82-6.66 (m, 16H), 6.04 (s, 1H), 5.80 (s, 1H), 4.97-4.84 (m, 1H), 1.30 (d, J = 7.0 Hz, 3H). ^{13}C NMR (125 MHz, DMSO-d6) δ 167.2, 163.6, 151.2, 149.1, 143.6, 140.2, 138.5, 137.5, 136.7, 130.8, 130.2, 129.0, 128.3, 128.0, 127.1, 126.7, 126.6, 126.2, 123.1, 62.5, 48.2, 36.2, 22.1. $\text{C}_{29}\text{H}_{25}\text{Br}_2\text{N}_3\text{O}_2$, HRMS calculated for m/z [M+H] $^+$: 606.039174 (calculated), 606.03863 (found).



N-([1,1'-biphenyl]-4-yl)-2,2-dichloro-N-(2-oxo-2-((S)-1-phenylethyl)amino)-1-(pyridin-3-yl)ethylpropanamide (**Jun9-76-4**), dr = 1:1. White solid, 79% yield. ^1H NMR (500 MHz, DMSO-d6) δ 8.77-8.35 (m, 3H), 7.99-6.75 (m, 15H), 6.11 (s, 1H), 4.98-4.6 (m, 1H), 2.15 (s, 1.5H), 2.12 (s, 1.5H), 1.29 (d, J = 7.0 Hz, 1.5H), 1.17 (d, J = 7.0 Hz, 1.5H). ^{13}C NMR (125 MHz, DMSO-d6) δ 166.9, 166.8, 164.0, 148.7, 148.2, 146.2, 144.2, 143.7, 139.7, 138.6, 133.6, 132.1, 131.5, 128.9, 128.9, 128.3, 128.1, 127.9, 127.9, 126.8, 126.7, 126.6, 126.6, 126.2, 125.7, 125.5, 124.4, 124.0, 81.4, 81.3, 64.3, 64.3, 48.5, 48.3, 36.9, 22.3, 22.0. $\text{C}_{30}\text{H}_{27}\text{Cl}_2\text{N}_3\text{O}_2$, HRMS calculated for m/z [M+H] $^+$: 532.155858 (calculated), 532.15531 (found).

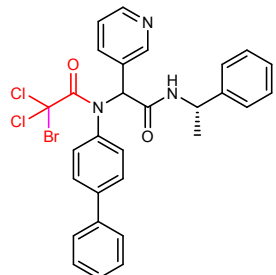


N-([1,1'-biphenyl]-4-yl)-2,2,2-trichloro-N-(2-oxo-2-((S)-1-phenylethyl)amino)-1-(pyridin-3-yl)ethylacetamide (**Jun9-72-4**), dr = 1:1. White solid, 74% yield. ^1H NMR (500 MHz, DMSO-d6) δ 8.73 (dd, J = 19.5, 7.5 Hz, 1H), 8.45-8.35 (m, 2H), 8.03-6.81 (m, 16H), 6.15 (s, 0.5H), 5.10-4.97 (m, 1H), 1.40 (d, J = 7.0 Hz, 1.5H), 1.25 (d, J = 7.0 Hz, 1.5H). ^{13}C NMR (125 MHz, DMSO-d6) δ 167.2, 167.1, 159.4, 159.4, 151.7, 151.6, 149.1, 144.2, 143.7, 139.7, 139.7, 138.5, 138.5, 137.0, 137.7, 136.4, 133.5, 133.5, 129.8, 129.3, 128.9, 128.9, 128.2, 128.1, 127.9, 127.8, 126.8, 126.6, 126.5, 126.5, 126.1, 125.7, 122.9, 122.5, 92.9, 92.9, 65.6, 65.6, 48.5, 48.3, 22.3, 22.1. C₂₉H₂₄Cl₃N₃O₂, HRMS calculated for m/z [M+H]⁺: 552.101236 (calculated), 552.10069 (found).

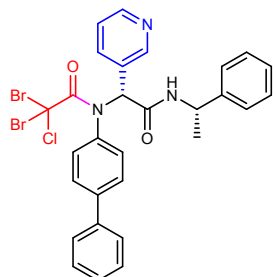


N-([1,1'-biphenyl]-4-yl)-2-chloro-2,2-difluoro-N-(2-oxo-2-((S)-1-phenylethyl)amino)-1-(pyridin-3-yl)ethylacetamide (**Jun9-77-2**), dr = 1:1. White solid, 60% yield. ^1H NMR (500 MHz, CDCl₃) δ 8.41-8.15 (m, 2H), 7.76-6.81 (m, 15H), 6.55-6.35 (m, 2H), 5.88 (d, J = 7.5 Hz, 1H), 5.11-5.03 (m, 1H), 1.42 (d, J = 7.0 Hz, 1.5H), 1.34 (d, J = 7.0 Hz, 1.5H). ^{13}C NMR (125 MHz, CDCl₃) δ 166.6, 166.4, 151.5, 151.5, 150.3, 150.3, 142.7, 142.4, 142.1, 141.9, 139.4, 138.2, 138.0, 135.0, 131.7, 131.4, 128.9, 128.9, 128.8, 128.6, 128.0, 127.9, 127.6,

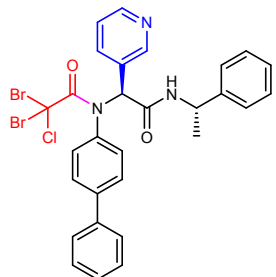
127.4, 127.3, 127.1, 127.1, 126.7, 126.2, 125.9, 123.3, 123.2, 64.5, 64.2, 49.7, 49.6, 21.9, 21.5. $C_{29}H_{24}ClF_2N_3O_2$, HRMS calculated for m/z [M+H]⁺: 520.160336 (calculated), 520.15979 (found).



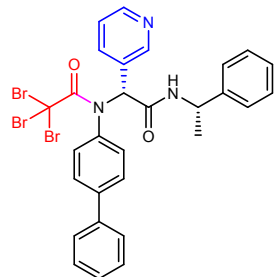
N-([1,1'-biphenyl]-4-yl)-2-bromo-2,2-dichloro-N-(2-oxo-2-((S)-1-phenylethyl)amino)-1-(pyridin-3-yl)ethylacetamide (Jun9-89-3). White solid, 35% yield, dr = 1:1. 1H NMR (500 MHz, DMSO-d6) δ 8.82 (d, J = 12.5 Hz, 1H), 8.69 (d, J = 4.5 Hz, 0.5H), 8.56 (d, J = 5.0 Hz, 0.5H), 8.08 (d, J = 8.2 Hz, 0.5H), 7.87 (d, J = 8.1 Hz, 0.5H), 7.53-7.10 (m, 16H), 6.30 (s, 0.5H), 6.22 (s, 0.5H), 5.15-5.07 (m, 1H), 1.53 (d, J = 7.0 Hz, 1.5H), 1.50 (d, J = 7.0 Hz, 1.5H). ^{13}C NMR (125 MHz, DMSO-d6) δ 165.6, 165.4, 161.9, 161.6, 145.6, 145.5, 145.1, 143.3, 143.0, 142.7, 142.7, 142.5, 142.3, 139.0, 136.3, 135.8, 133.2, 133.1, 132.7, 132.5, 129.1, 129.0, 128.8, 128.7, 128.3, 128.2, 127.7, 127.6, 127.1, 127.0, 126.8, 126.3, 126.0, 125.2, 125.2, 65.7, 65.0, 50.2, 50.0, 21.9, 21.5. $C_{29}H_{24}BrCl_2N_3O_2$, HRMS calculated for m/z [M+H]⁺: 596.050719 (calculated), 596.05017 (found).



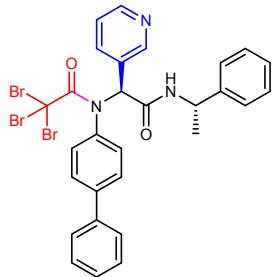
N-([1,1'-biphenyl]-4-yl)-2,2-dibromo-2-chloro-N-((R)-2-oxo-2-(((S)-1-phenylethyl)amino)-1-(pyridin-3-yl)ethyl)acetamide (**Jun9-89-4R**). White solid, 38% yield. ^1H NMR (500 MHz, CDCl_3) δ 8.35 (d, $J = 4.5$ Hz, 2H), 7.63-6.66 (m, 16H), 6.26 (d, $J = 7.5$ Hz, 1H), 5.89 (s, 1H), 5.07 (p, $J = 7.0$ Hz, 1H), 1.34 (d, $J = 7.0$ Hz, 2H). ^{13}C NMR (125 MHz, CDCl_3) δ 166.8, 161.1, 151.6, 150.2, 142.5, 141.9, 139.5, 138.2, 137.0, 132.8, 129.5, 128.9, 128.8, 127.9, 127.6, 127.1, 126.3, 123.2, 67.0, 55.2, 49.6, 21.5. $\text{C}_{29}\text{H}_{24}\text{Br}_2\text{ClN}_3\text{O}_2$, HRMS calculated for m/z [M+H] $^+$: 640.000202 (calculated), 639.99966 (found).



N-([1,1'-biphenyl]-4-yl)-2,2-dibromo-2-chloro-N-((S)-2-oxo-2-(((S)-1-phenylethyl)amino)-1-(pyridin-3-yl)ethyl)acetamide (**Jun9-89-4S**). White solid, 40% yield. ^1H NMR (500 MHz, CDCl_3) δ 8.31 (s, 1H), 8.25 (d, $J = 4.0$ Hz, 1H), 7.90-6.53 (m, 16H), 6.28 (d, $J = 7.5$ Hz, 1H), 5.92 (s, 1H), 5.03 (p, $J = 7.0$ Hz, 1H), 1.39 (d, $J = 7.0$ Hz, 3H). ^{13}C NMR (125 MHz, CDCl_3) δ 167.1, 161.1, 151.6, 150.1, 142.9, 141.7, 139.4, 137.9, 136.8, 133.1, 129.1, 128.8, 128.6, 127.9, 127.3, 127.0, 125.9, 123.0, 67.2, 55.2, 49.7, 22.1. $\text{C}_{29}\text{H}_{24}\text{Br}_2\text{ClN}_3\text{O}_2$, HRMS calculated for m/z [M+H] $^+$: 640.000202 (calculated), 639.99966 (found).

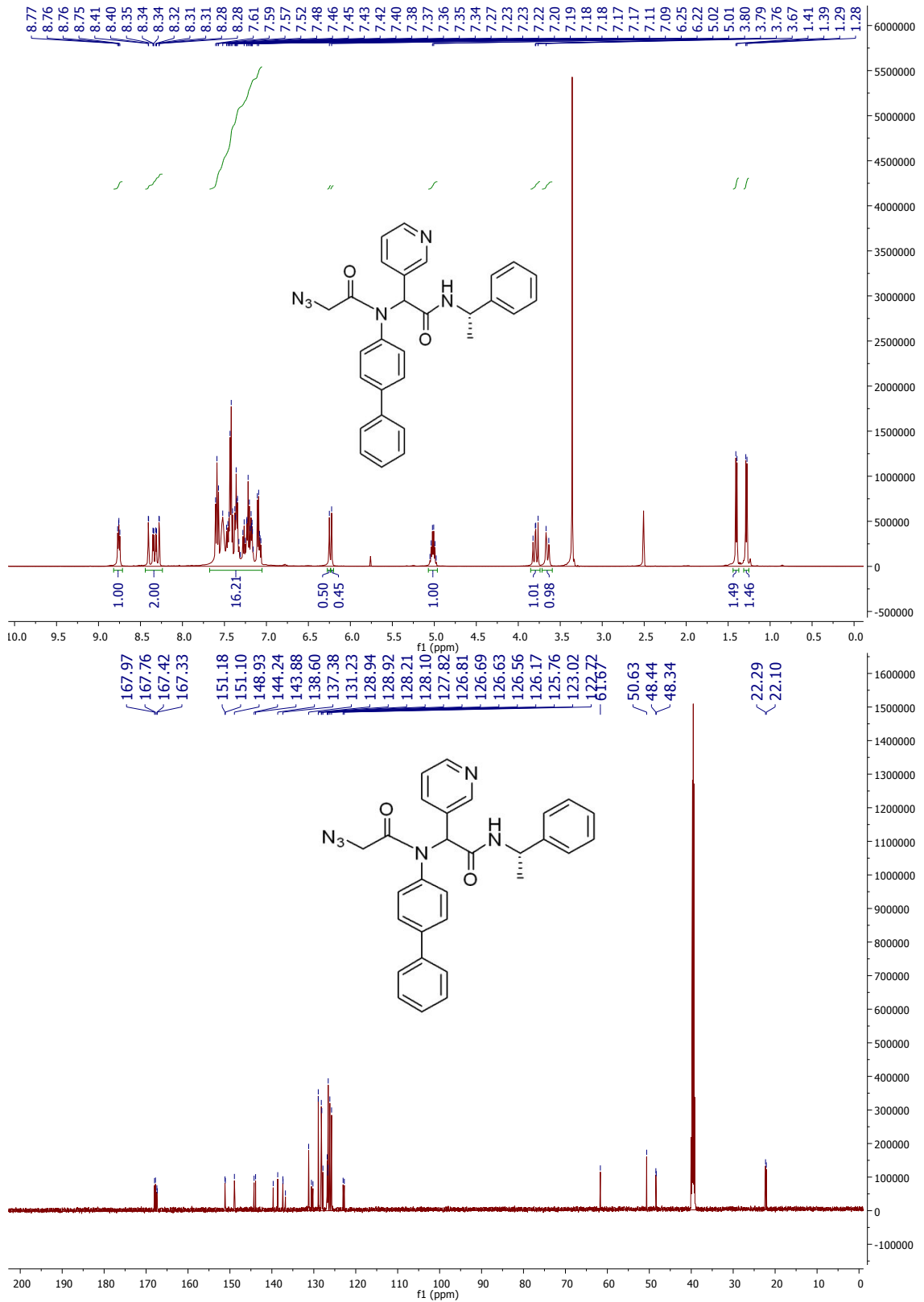


N-([1,1'-biphenyl]-4-yl)-2,2,2-tribromo-N-((R)-2-oxo-2-(((S)-1-phenylethyl)amino)-1-(pyridin-3-yl)ethyl)acetamide (**Jun9-88-6R**). White solid, 35% yield. ^1H NMR (500 MHz, DMSO-d6) δ 8.65 (d, J = 8.0 Hz, 1H), 8.40 (d, J = 1.5 Hz, 1H), 8.33 (dd, J = 4.5, 1.5 Hz, 1H), 8.13-6.86 (m, 16H), 6.18 (s, 1H), 5.03 (p, J = 7.0 Hz, 1H), 1.23 (d, J = 7.0 Hz, 3H). ^{13}C NMR (125 MHz, DMSO-d6) δ 167.4, 159.4, 151.5, 149.1, 143.7, 139.6, 138.6, 137.6, 133.8, 130.2, 128.9, 128.2, 127.8, 126.8, 126.5, 126.2, 125.2, 122.9, 114.5, 66.1, 48.2, 34.6, 22.1. $\text{C}_{29}\text{H}_{24}\text{Br}_3\text{N}_3\text{O}_2$, HRMS calculated for m/z [M+H] $^+$: 683.949685 (calculated), 683.94919 (found).

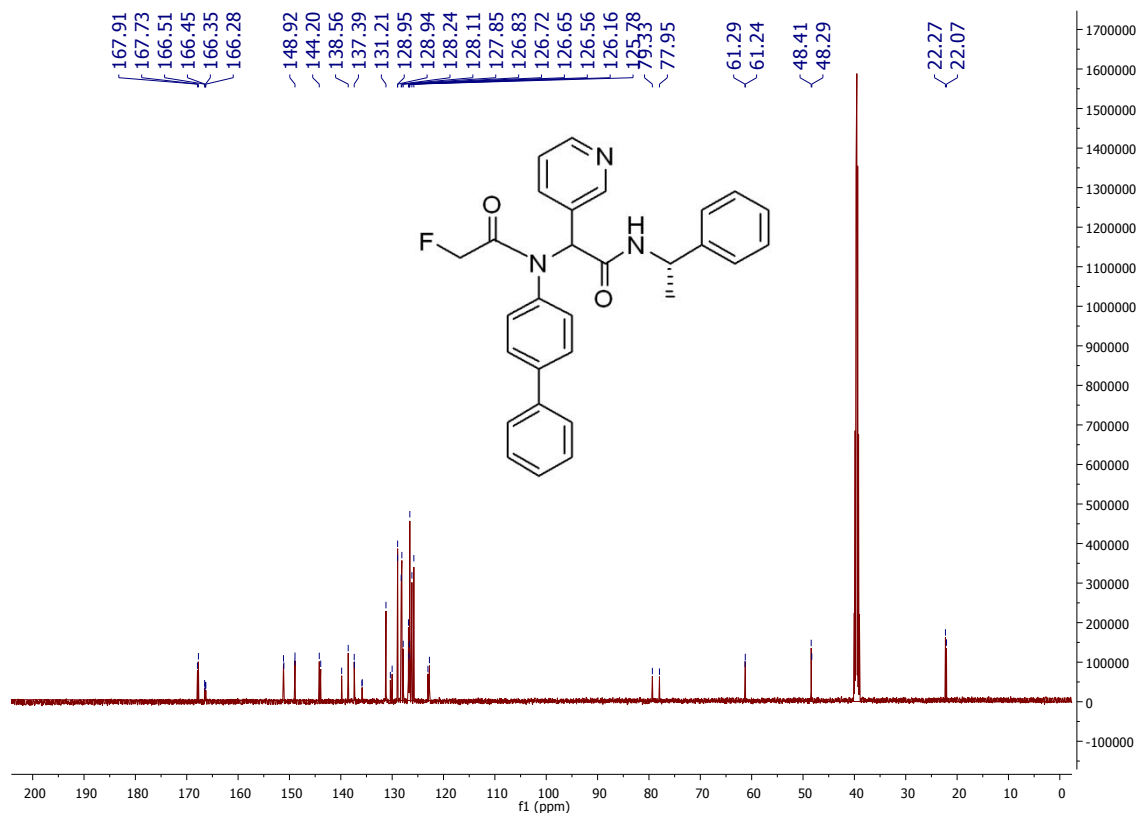
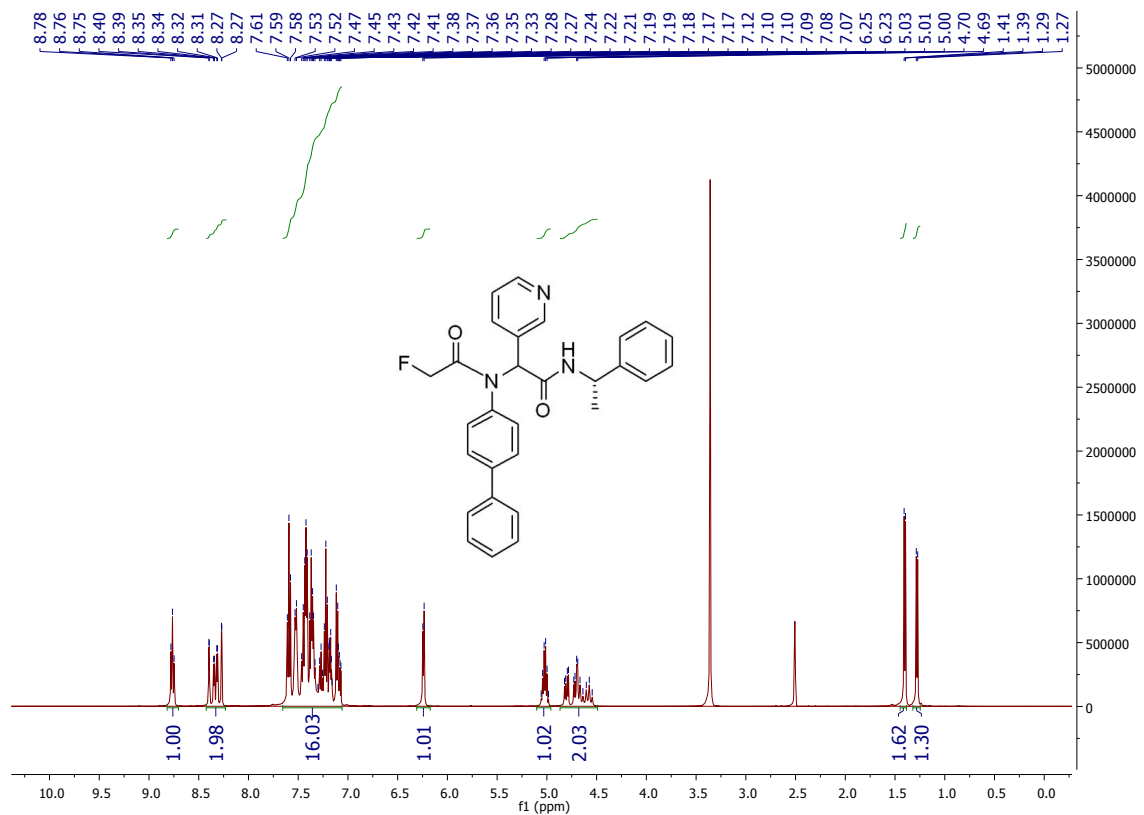


N-([1,1'-biphenyl]-4-yl)-2,2,2-tribromo-N-((S)-2-oxo-2-(((S)-1-phenylethyl)amino)-1-(pyridin-3-yl)ethyl)acetamide (**Jun9-88-6S**). White solid, 35% yield. ^1H NMR (500 MHz, DMSO-d6) δ 8.63 (d, J = 7.5 Hz, 1H), 8.29-8.18 (m, 2H), 7.99-6.77 (m, 16H), 6.08 (s, 1H), 4.92 (p, J = 7.0 Hz, 1H), 1.31 (d, J = 7.0 Hz, 3H). ^{13}C NMR (125 MHz, DMSO-d6) δ 167.3, 159.4, 151.5, 148.9, 144.3, 139.6, 138.5, 137.8, 137.3, 133.8, 129.8, 128.9, 128.1, 127.8, 126.6, 126.5, 125.7, 125.1, 122.6, 66.0, 48.4, 34.5, 22.3. $\text{C}_{29}\text{H}_{24}\text{Br}_3\text{N}_3\text{O}_2$, HRMS calculated for m/z [M+H] $^+$: 683.949685 (calculated), 683.94919 (found).

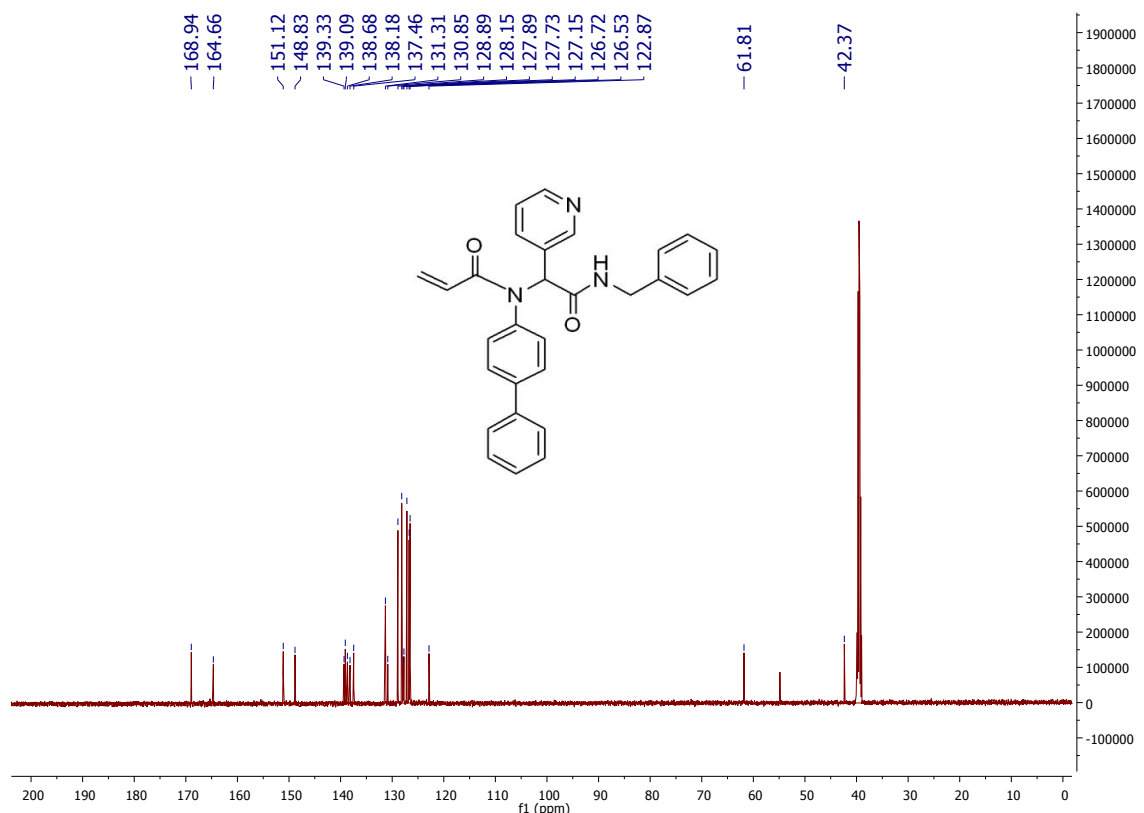
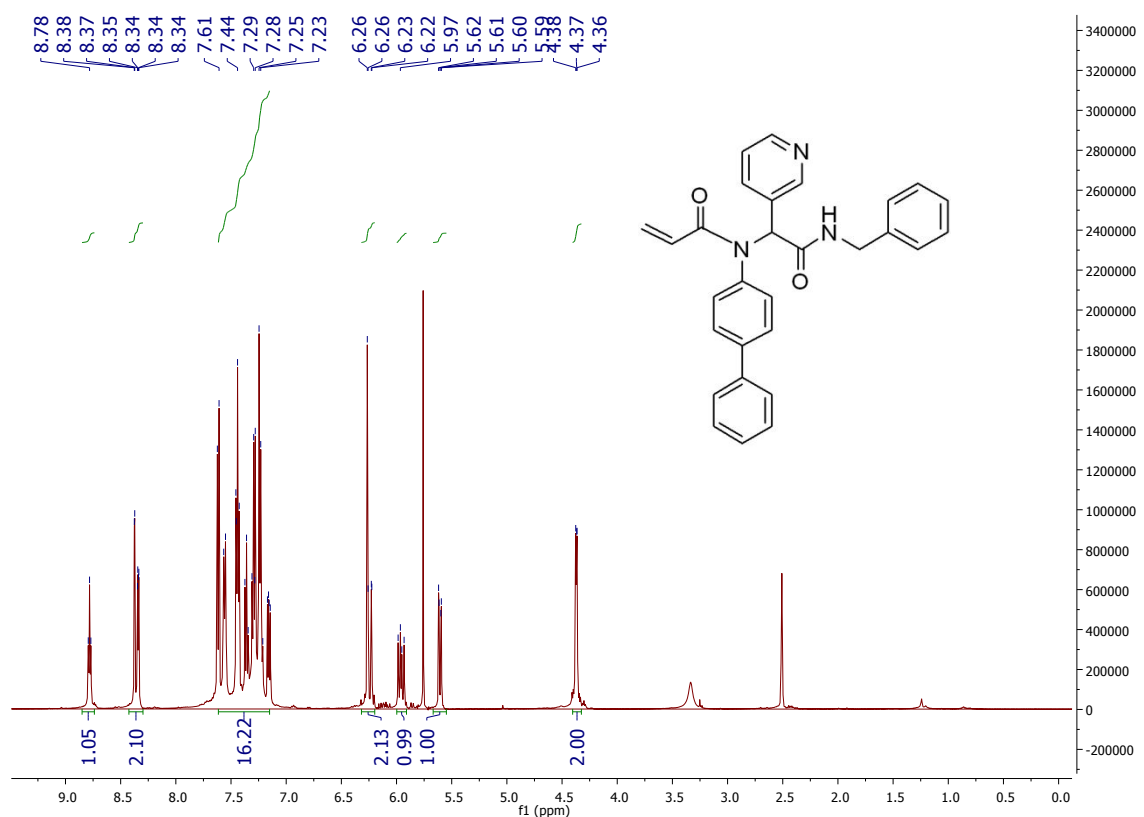
HNMR and CNMR spectra of Jun9-61-1



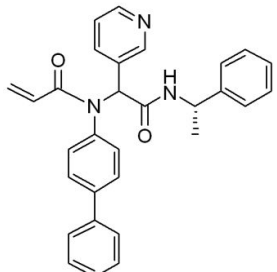
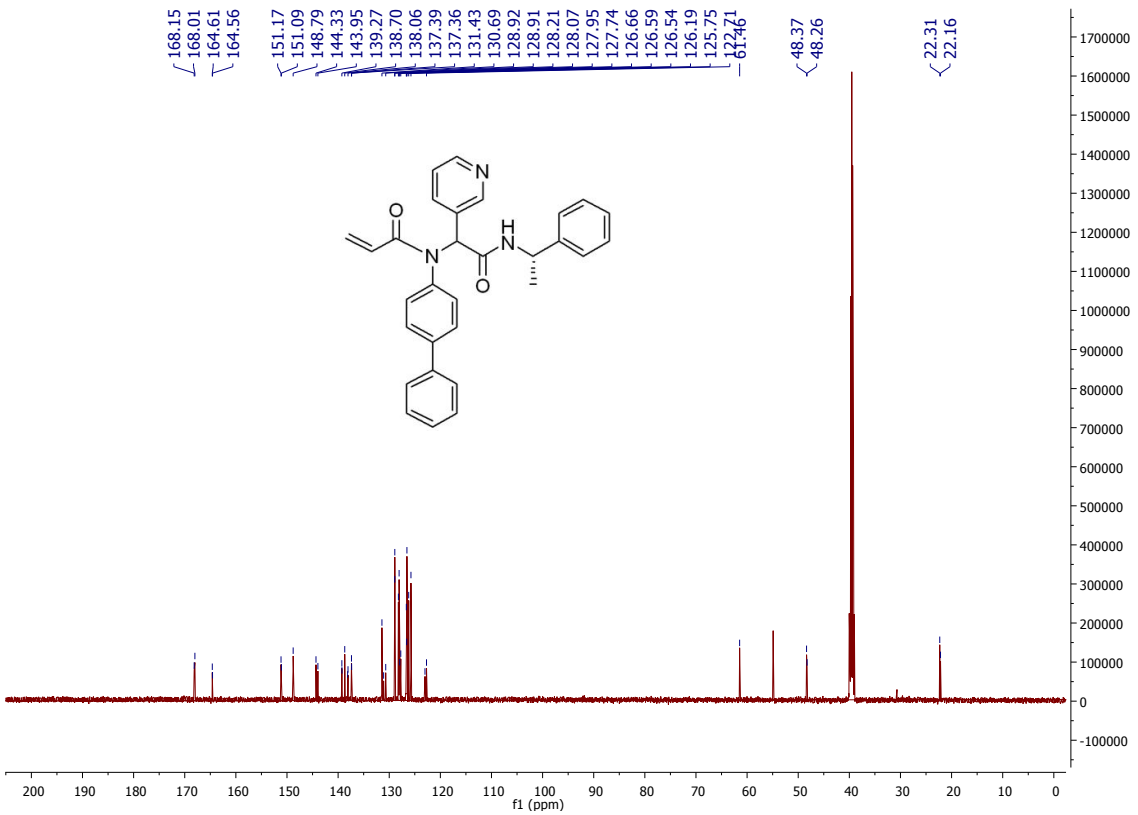
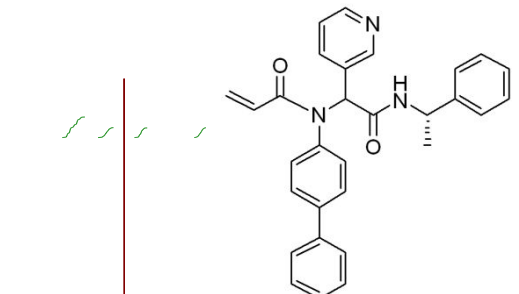
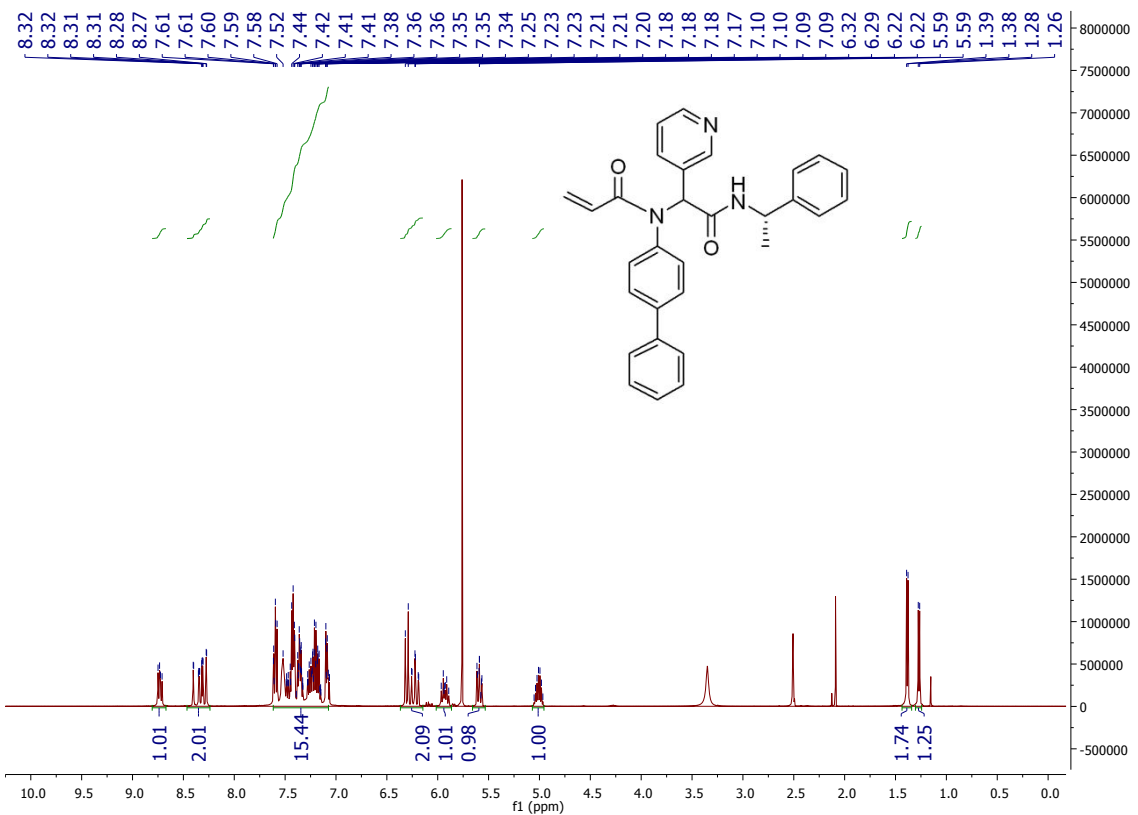
HNMR and CNMR spectra of Jun9-61-4



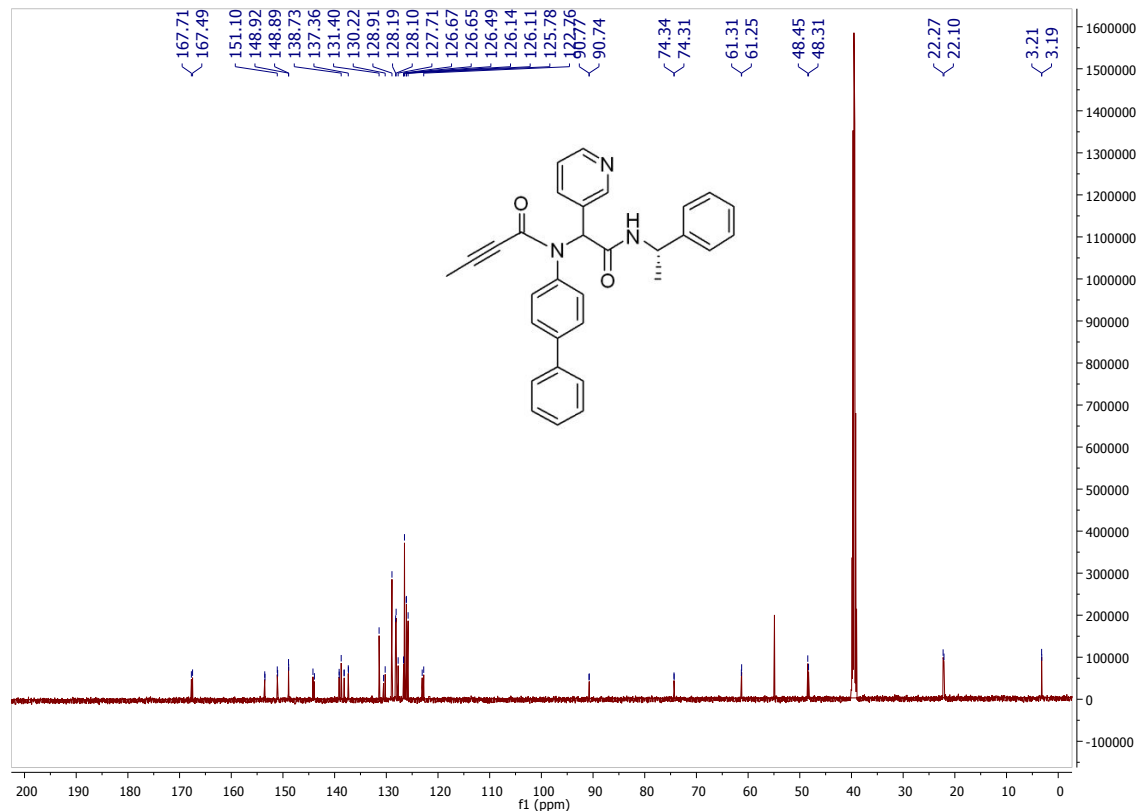
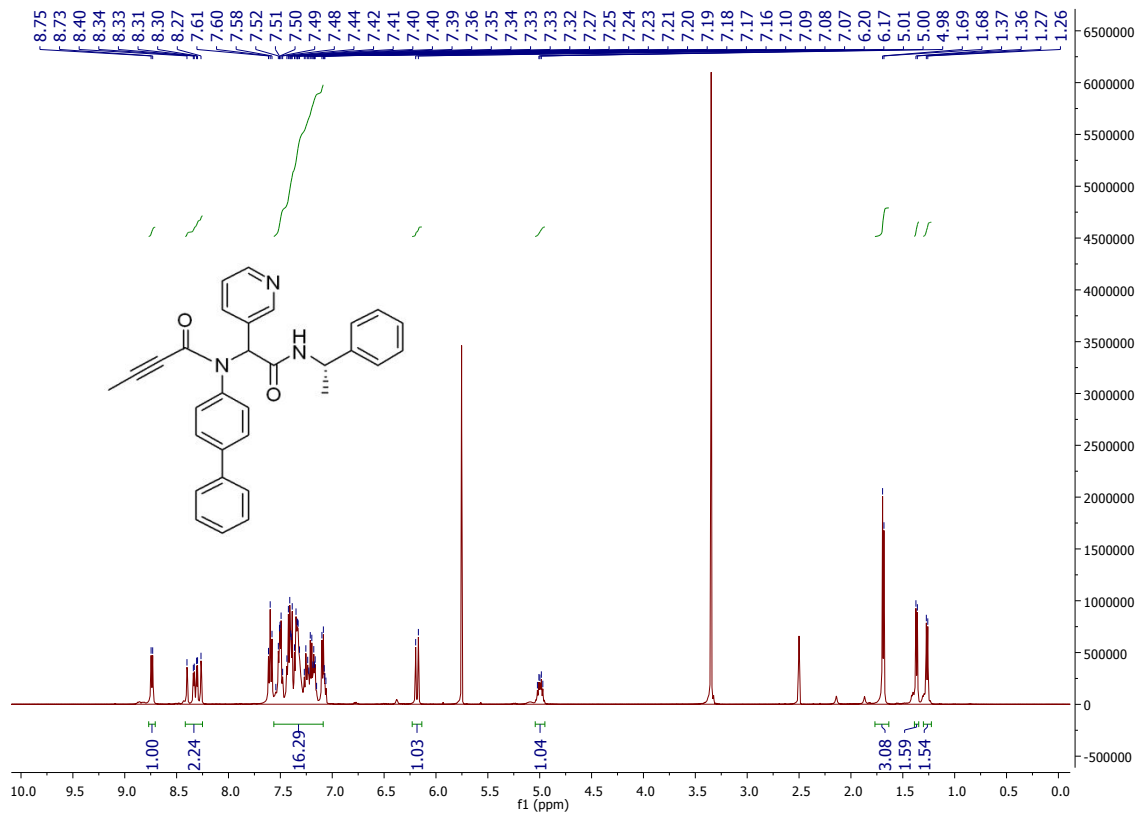
HNMR and CNMR spectra of Jun10-15-2



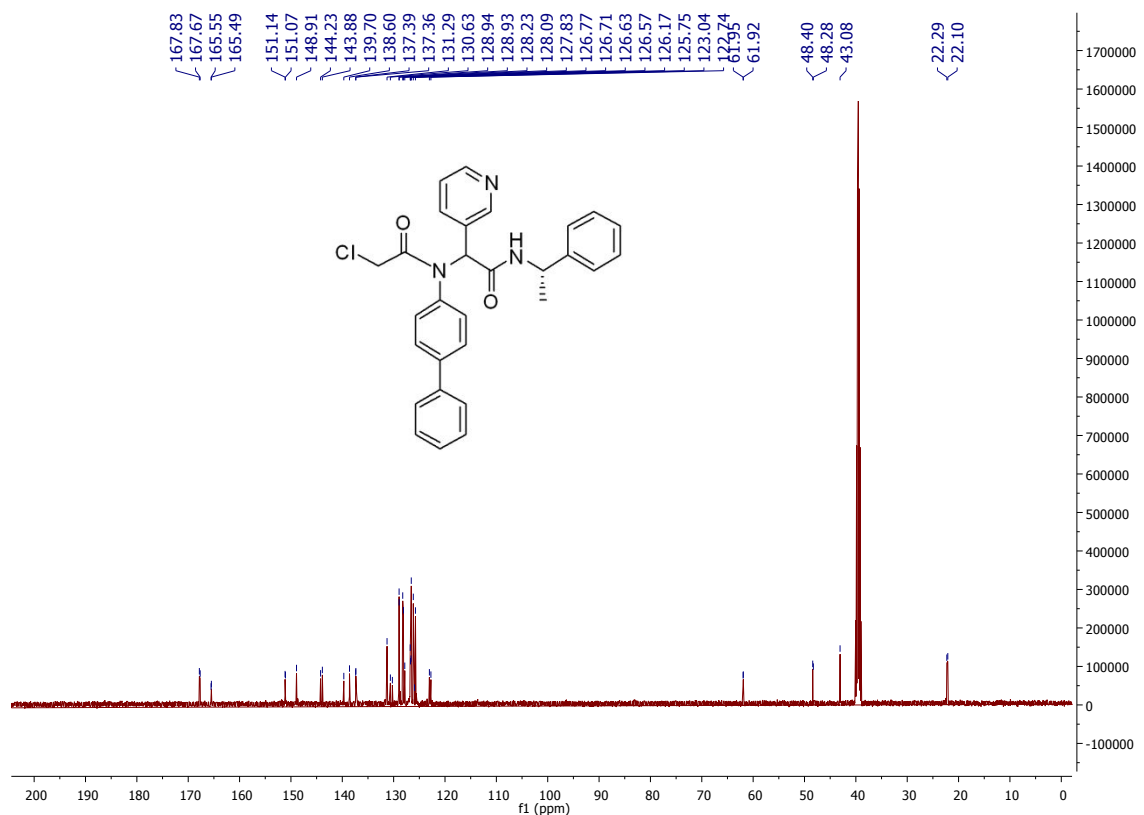
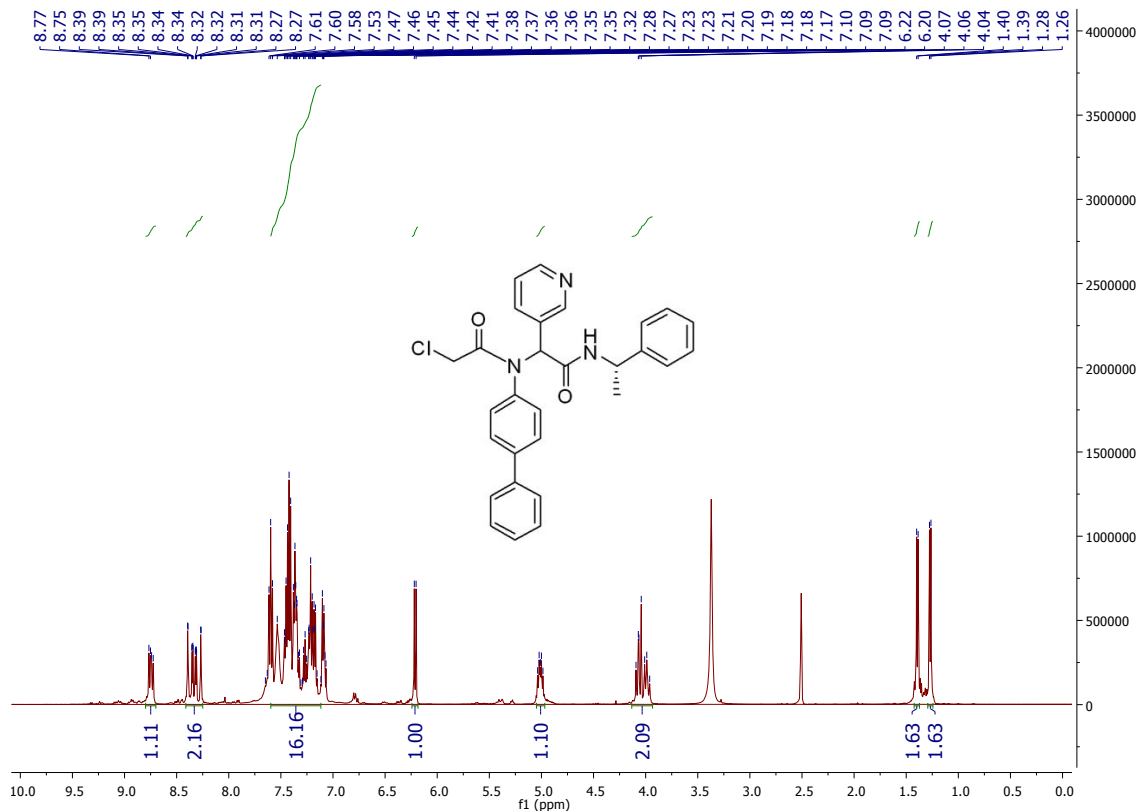
HNMR and CNMR spectra of Jun9-51-3



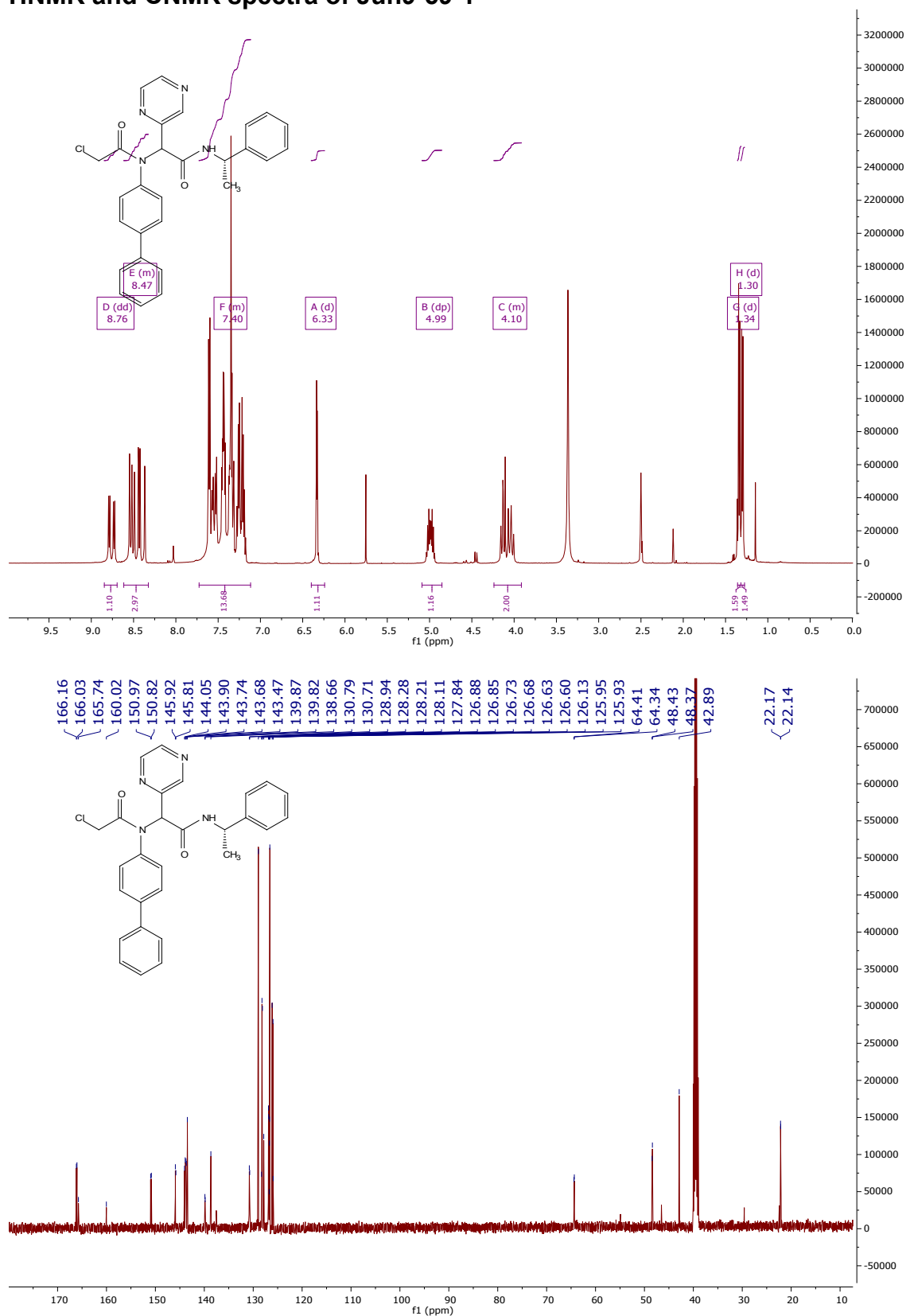
HNMR and CNMR spectra of Jun9-62-1



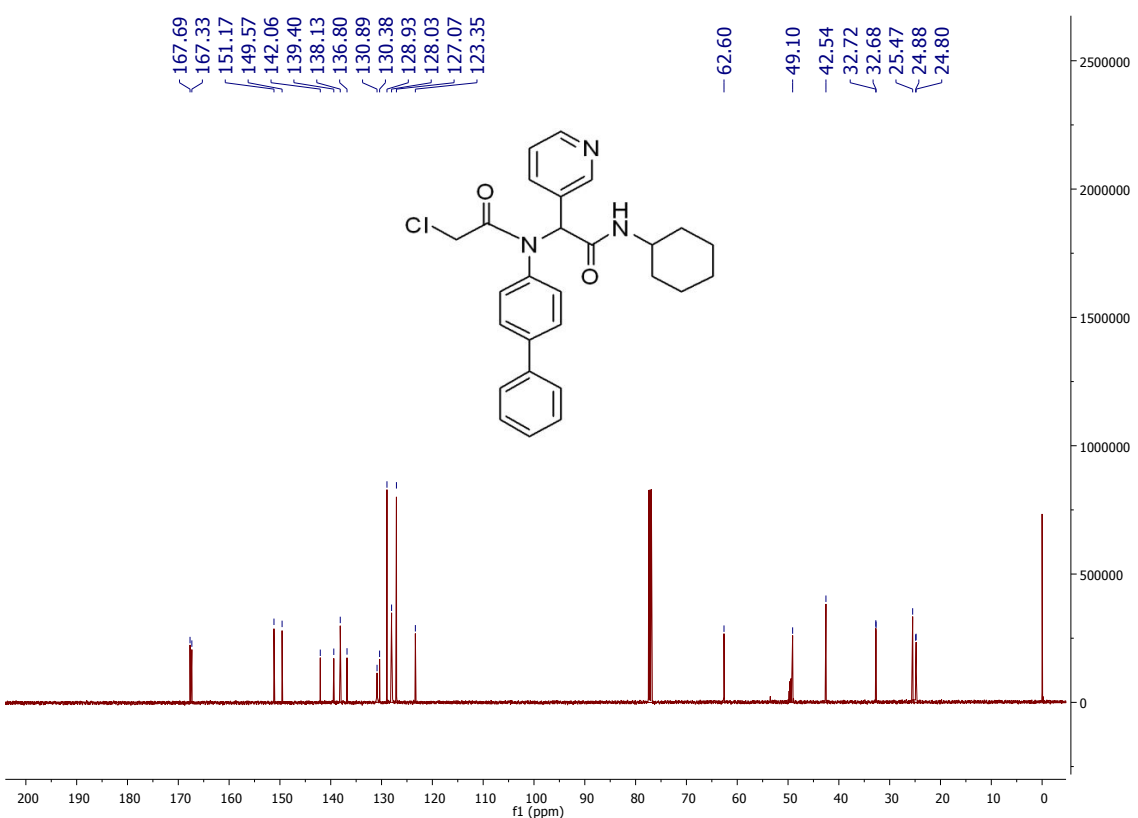
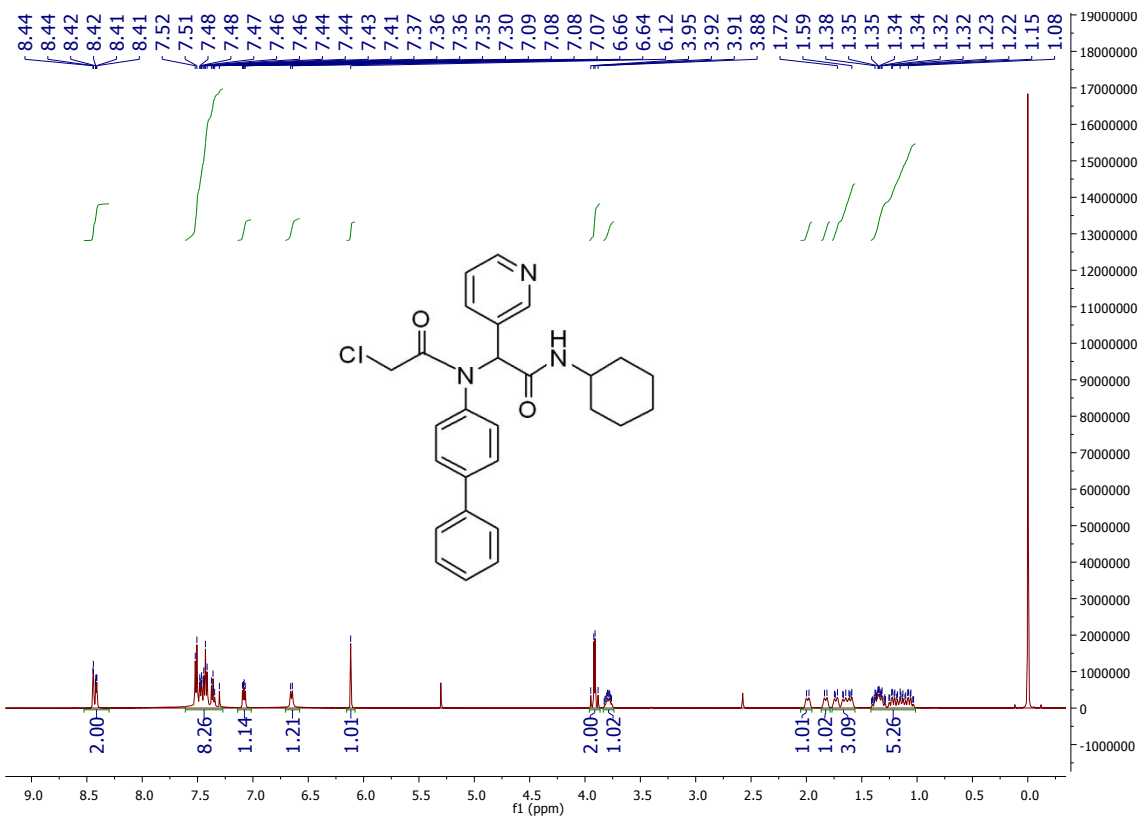
HNMR and CNMR spectra of Jun9-54-1



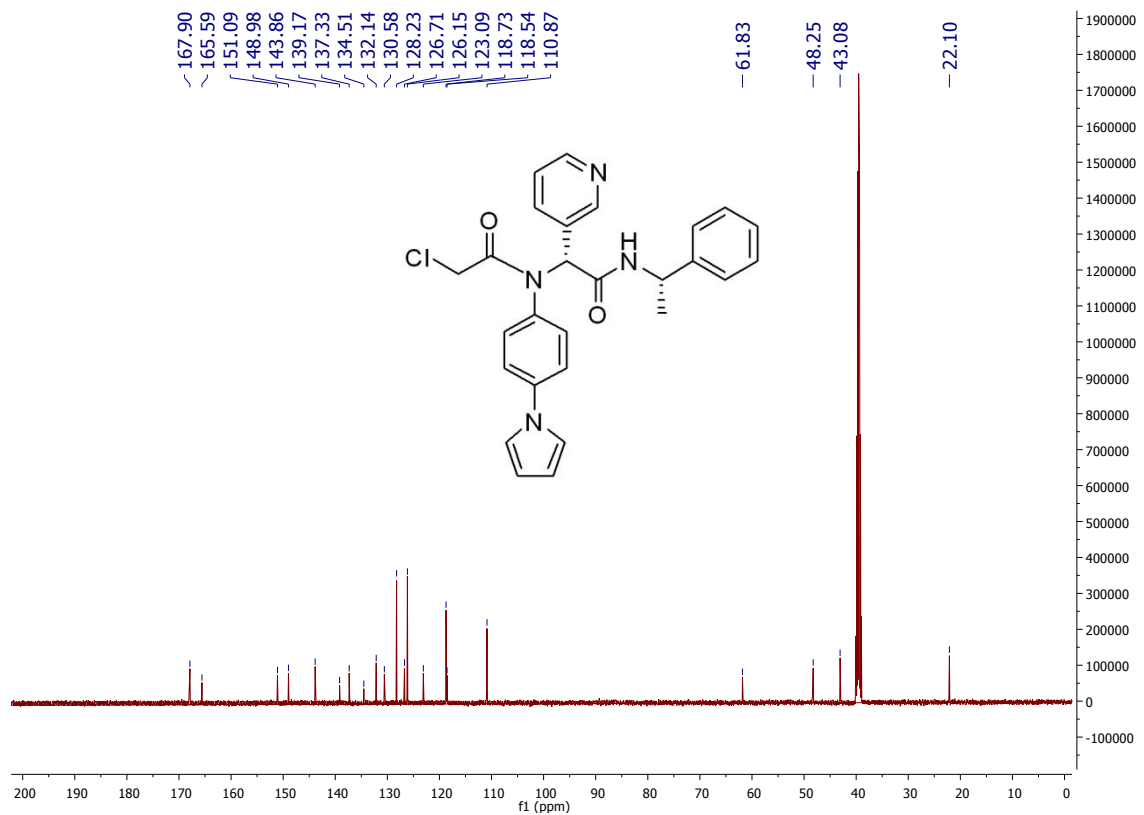
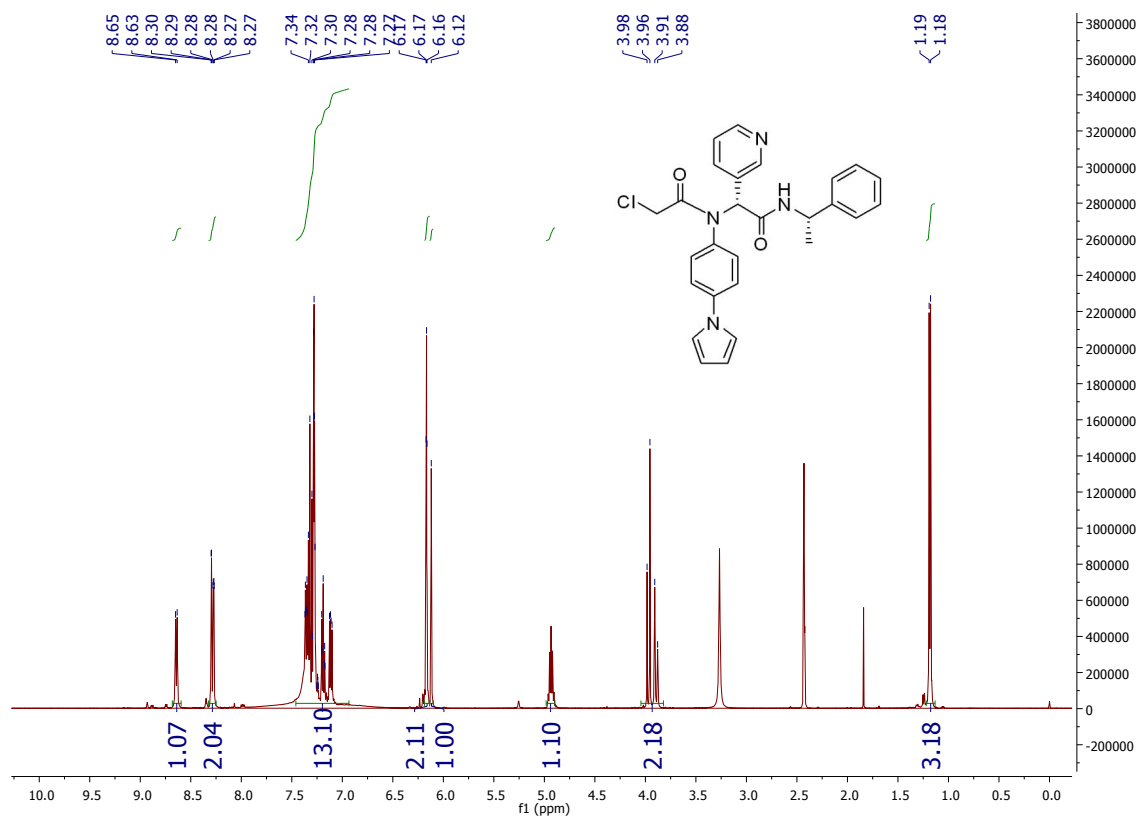
HNMR and CNMR spectra of Jun9-59-1



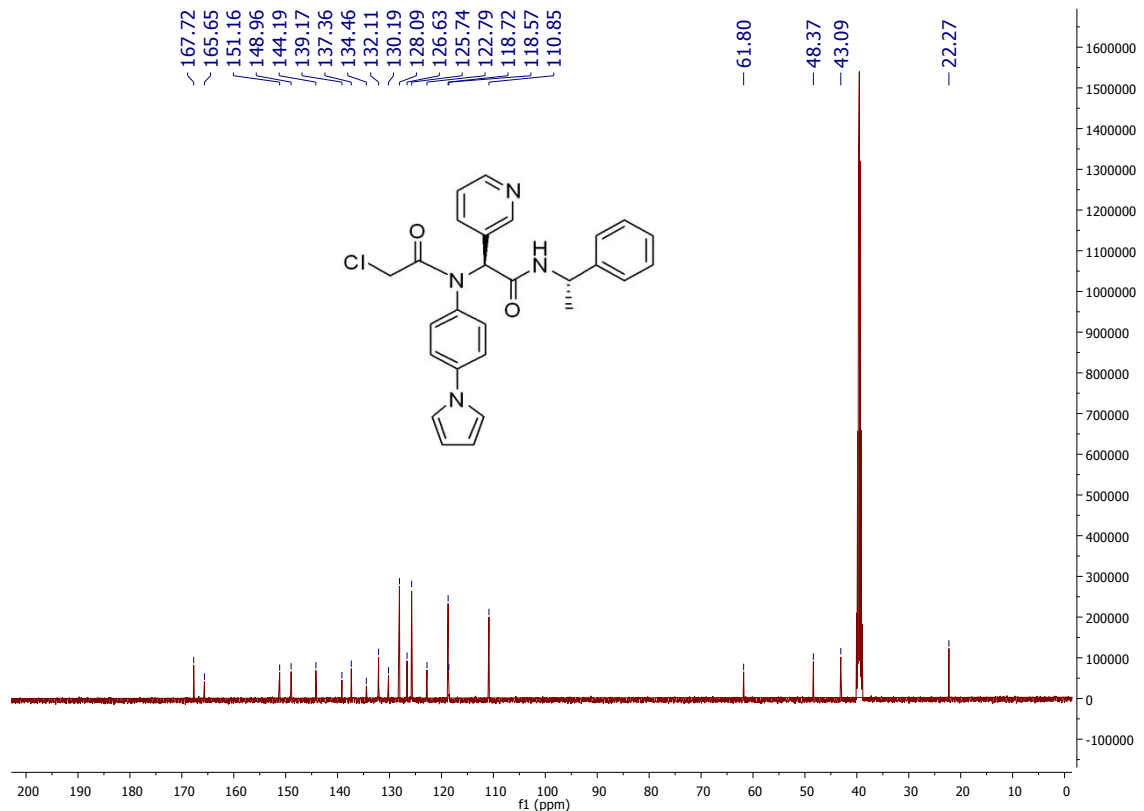
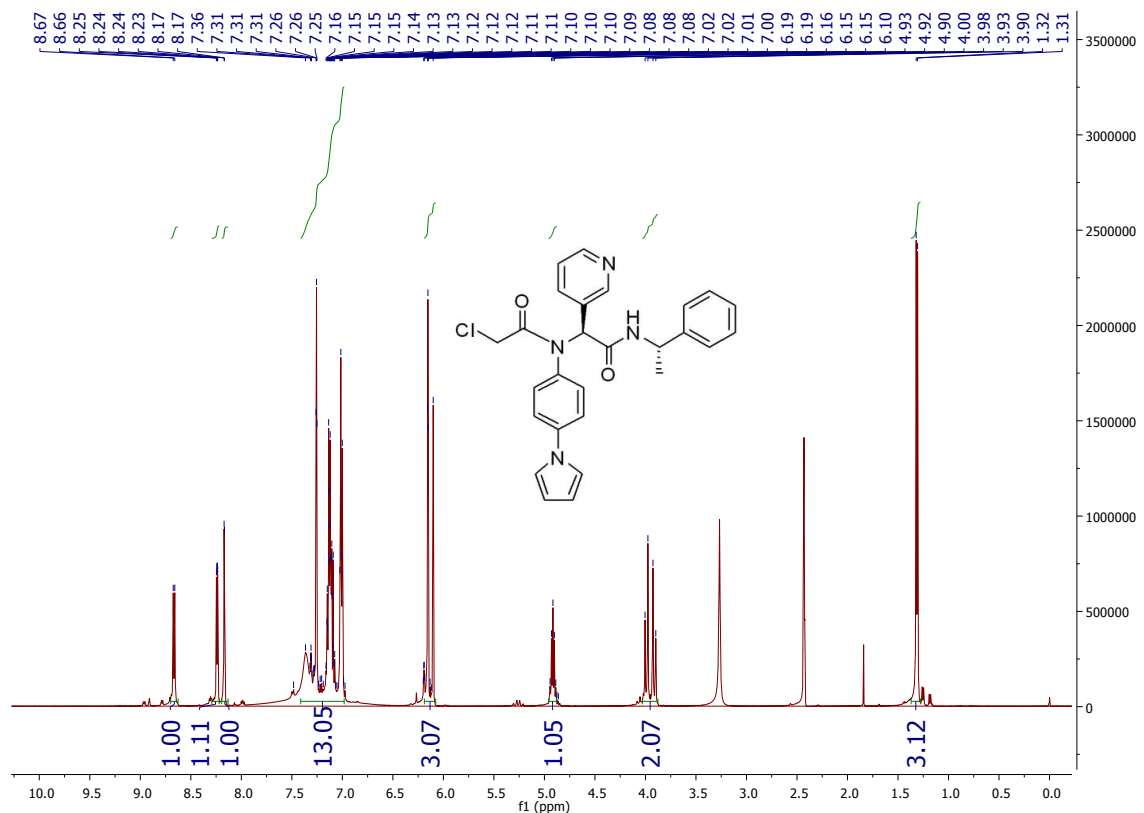
HNMR and CNMR spectra of Jun9-55-2



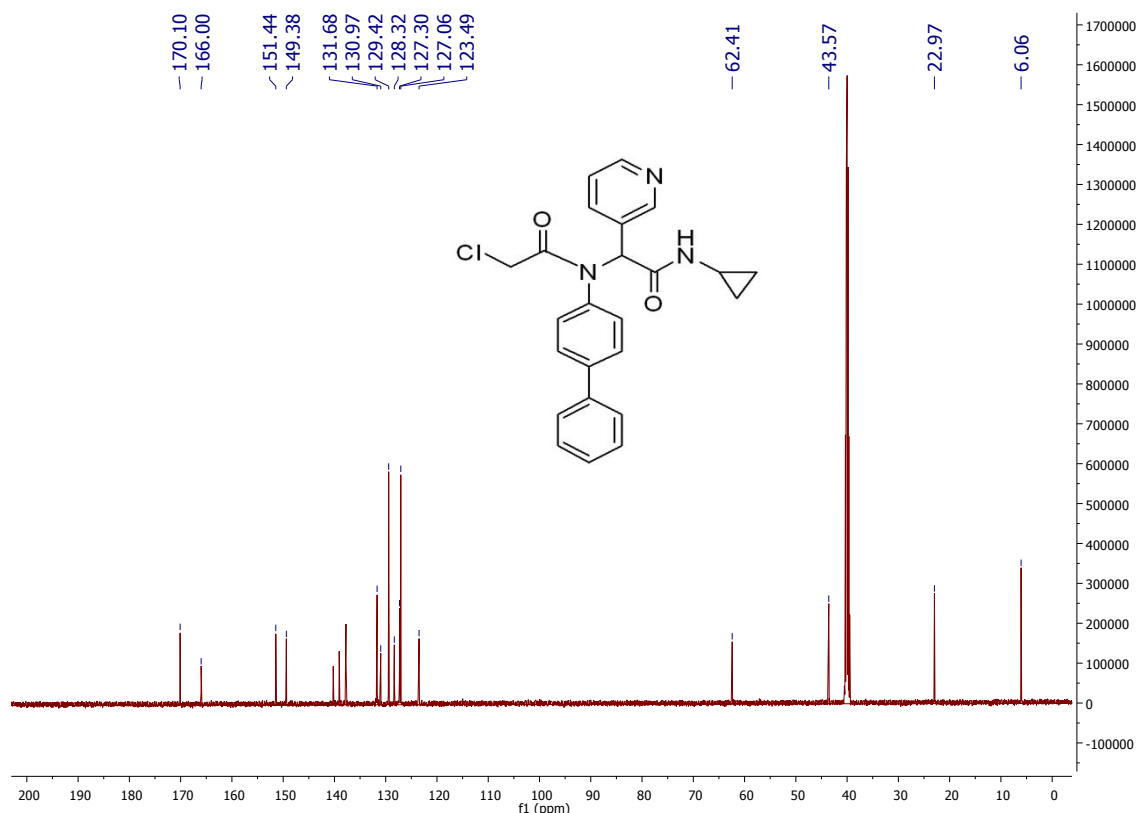
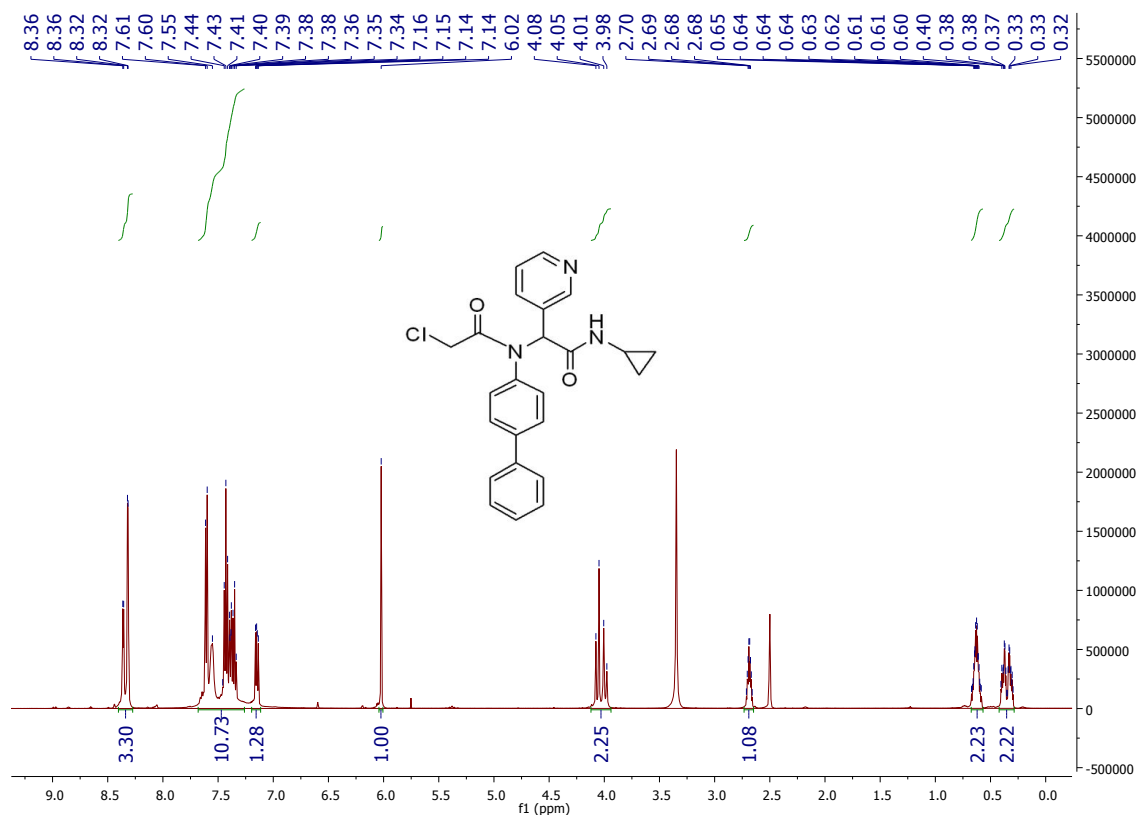
HNMR and CNMR spectra of Jun9-57-3R



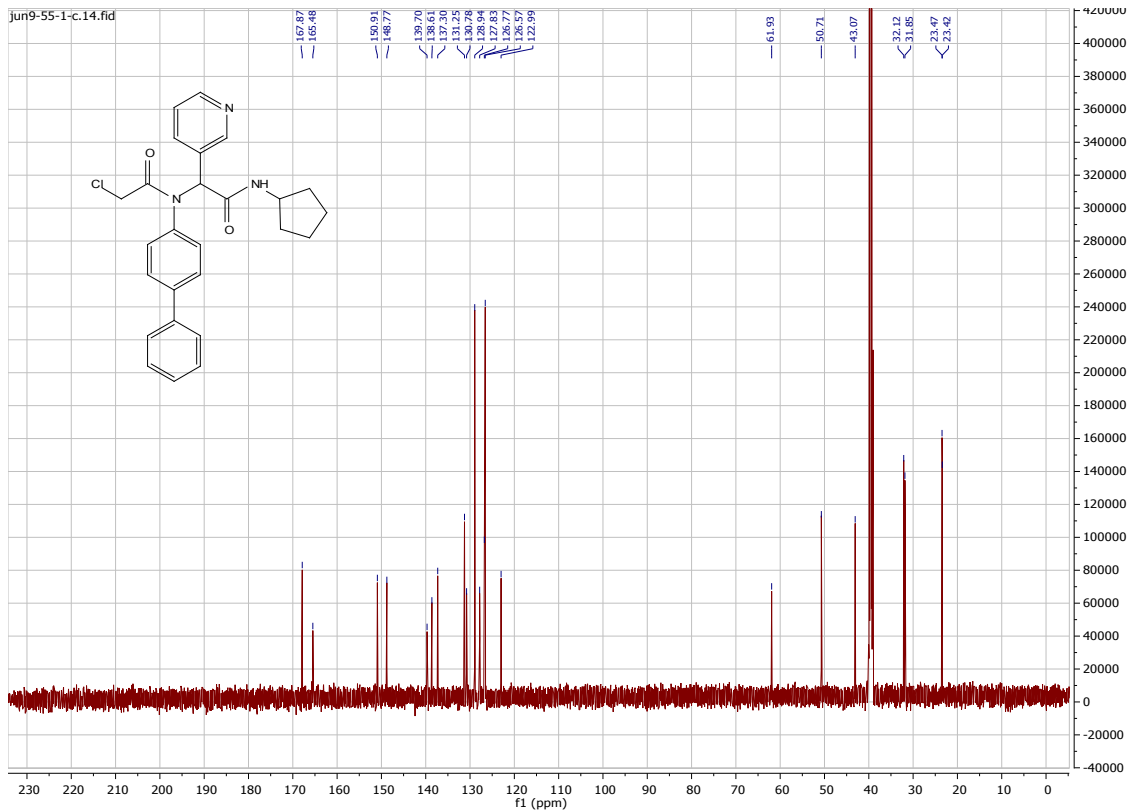
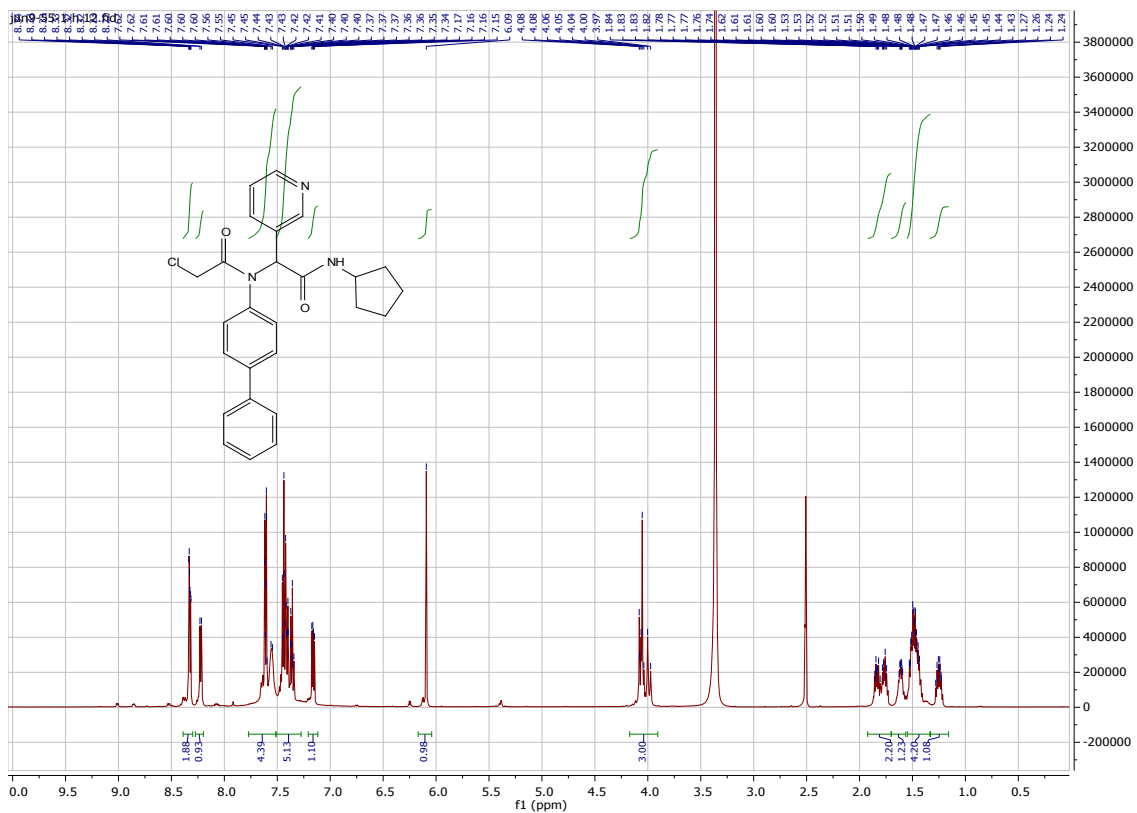
HNMR and CNMR spectra of Jun9-57-3S



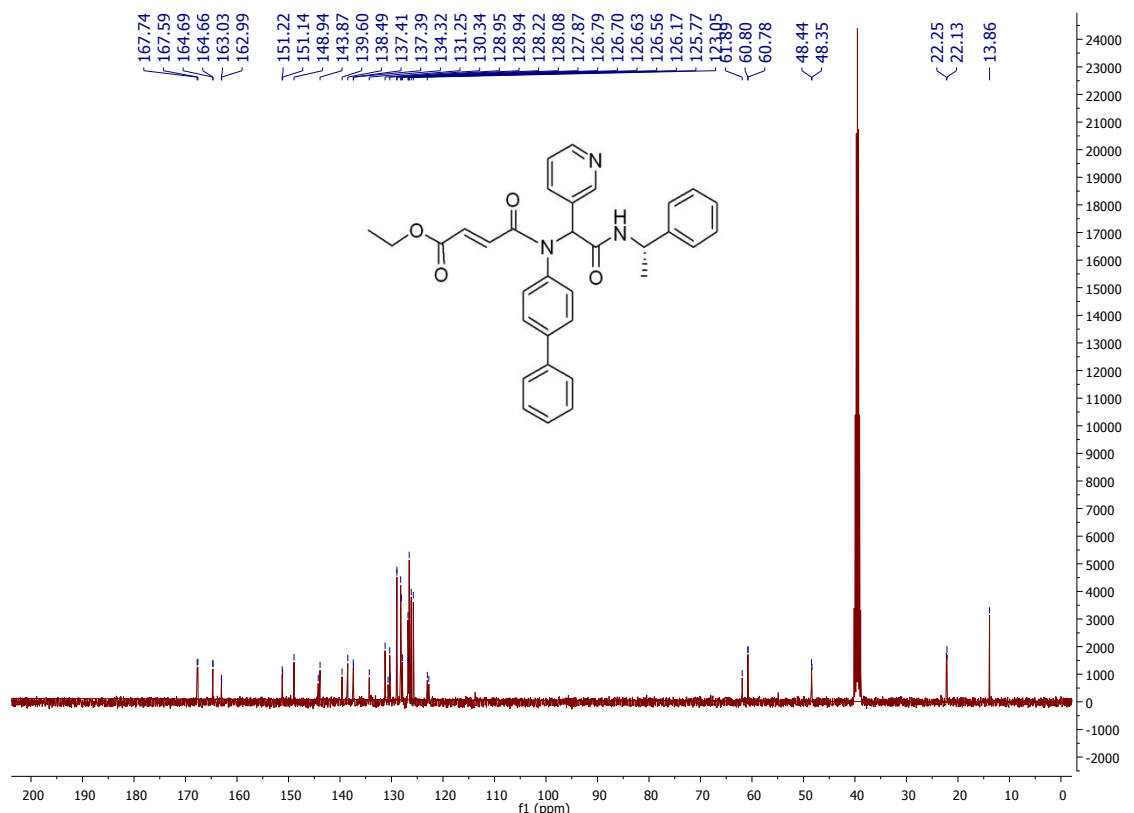
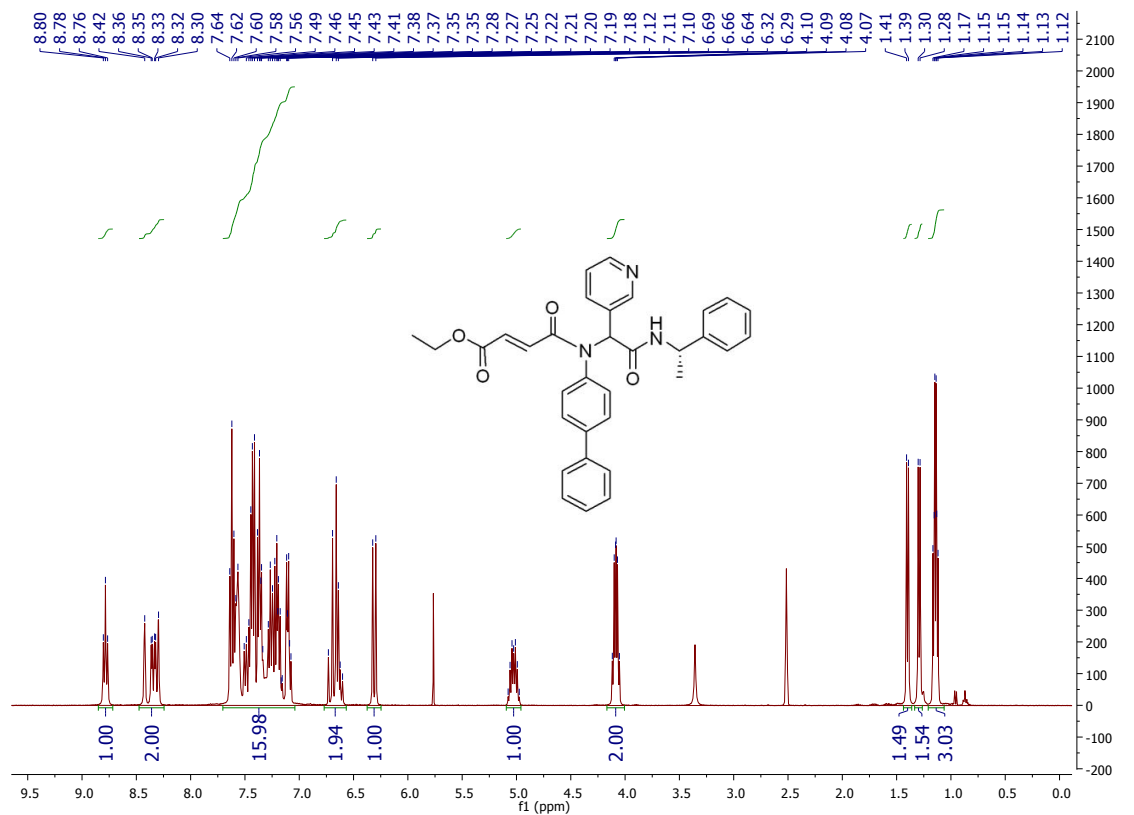
HNMR and CNMR spectra of Jun9-57-2



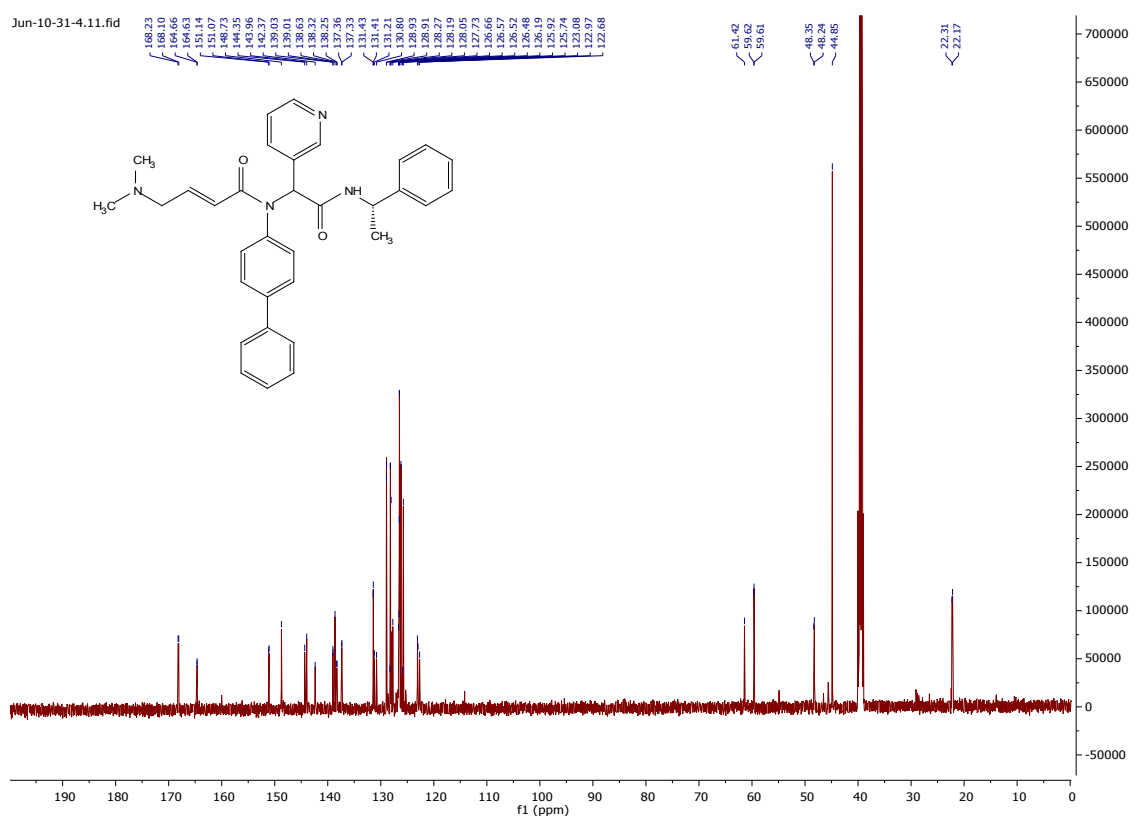
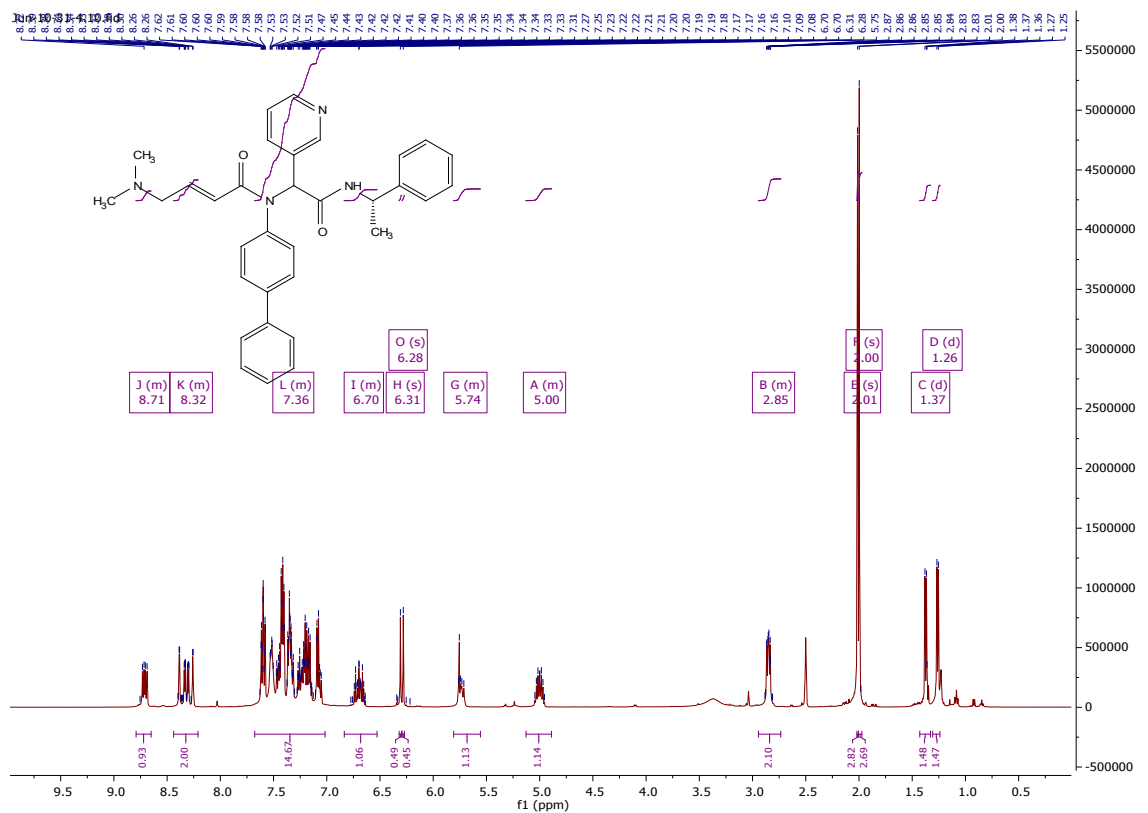
HNMR and CNMR spectra of Jun9-55-1



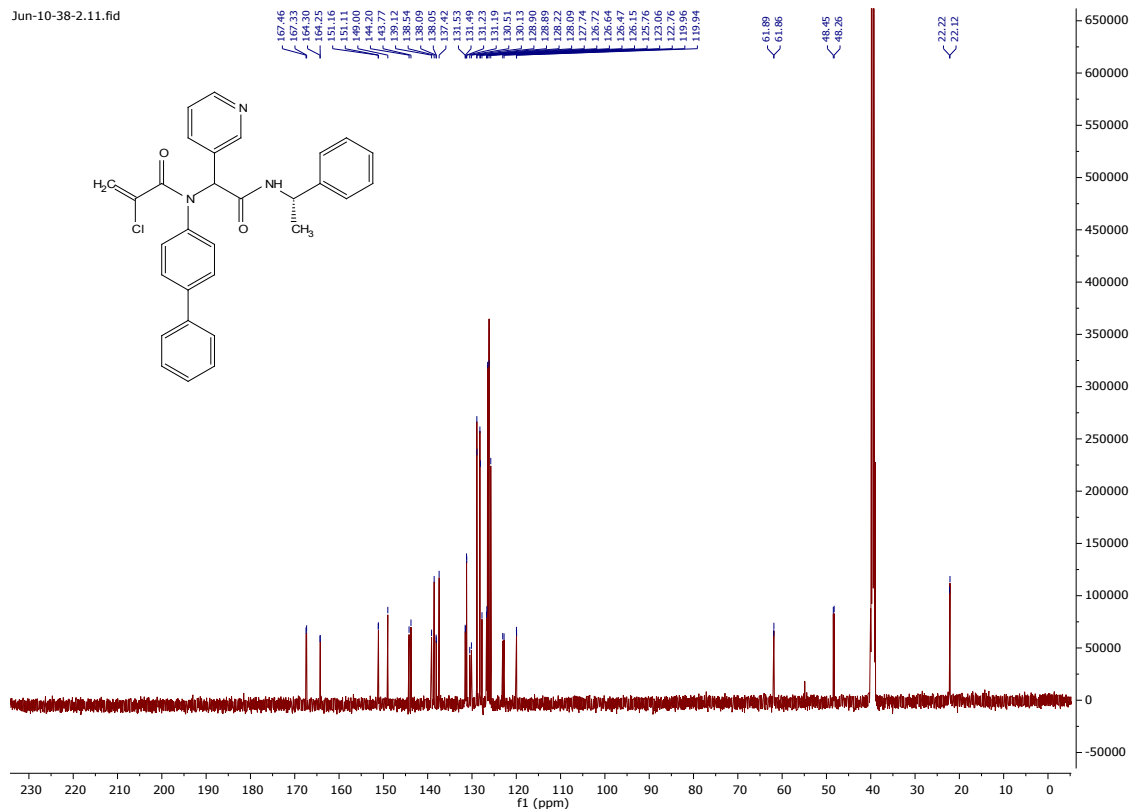
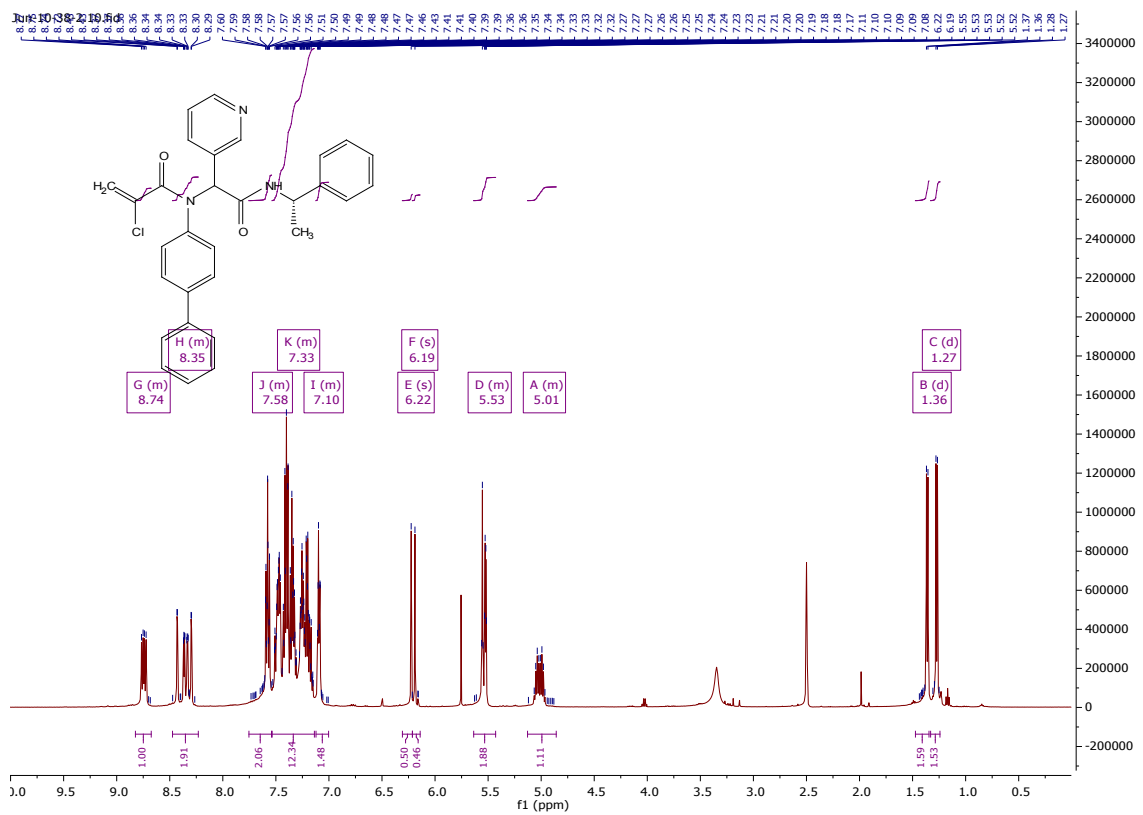
HNMR and CNMR spectra of Jun9-72-3



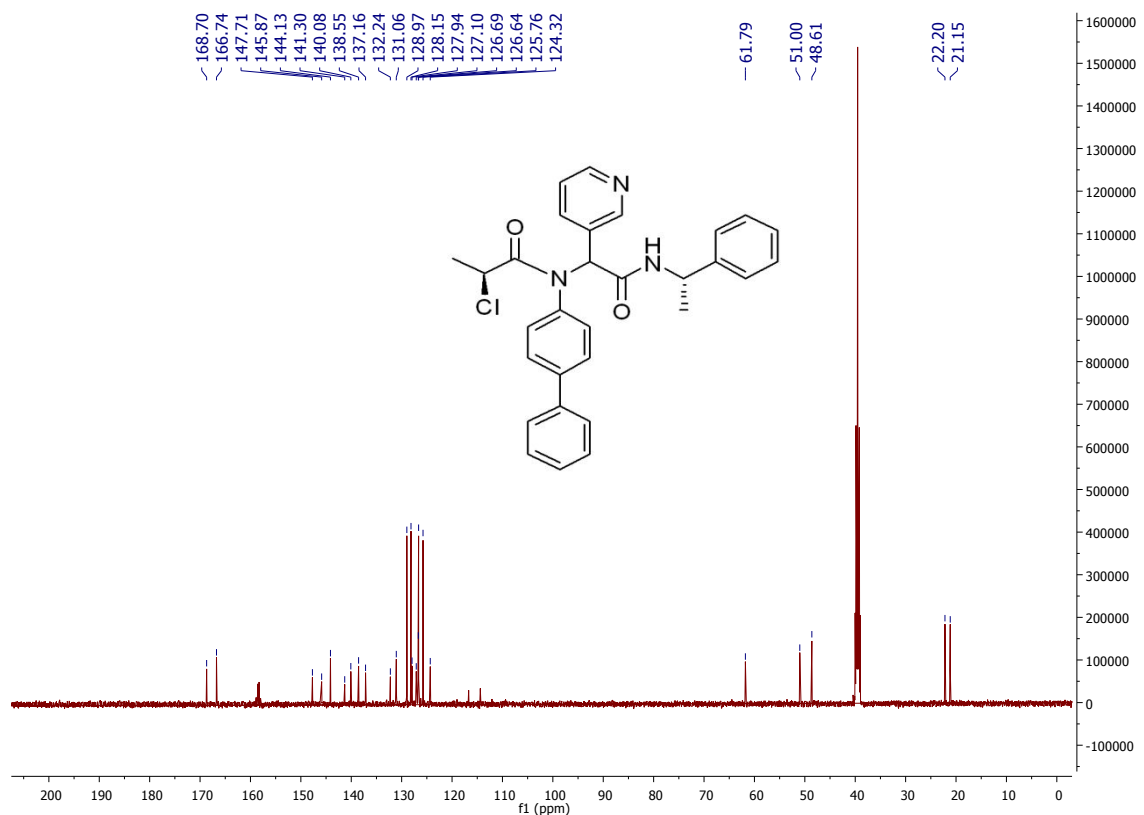
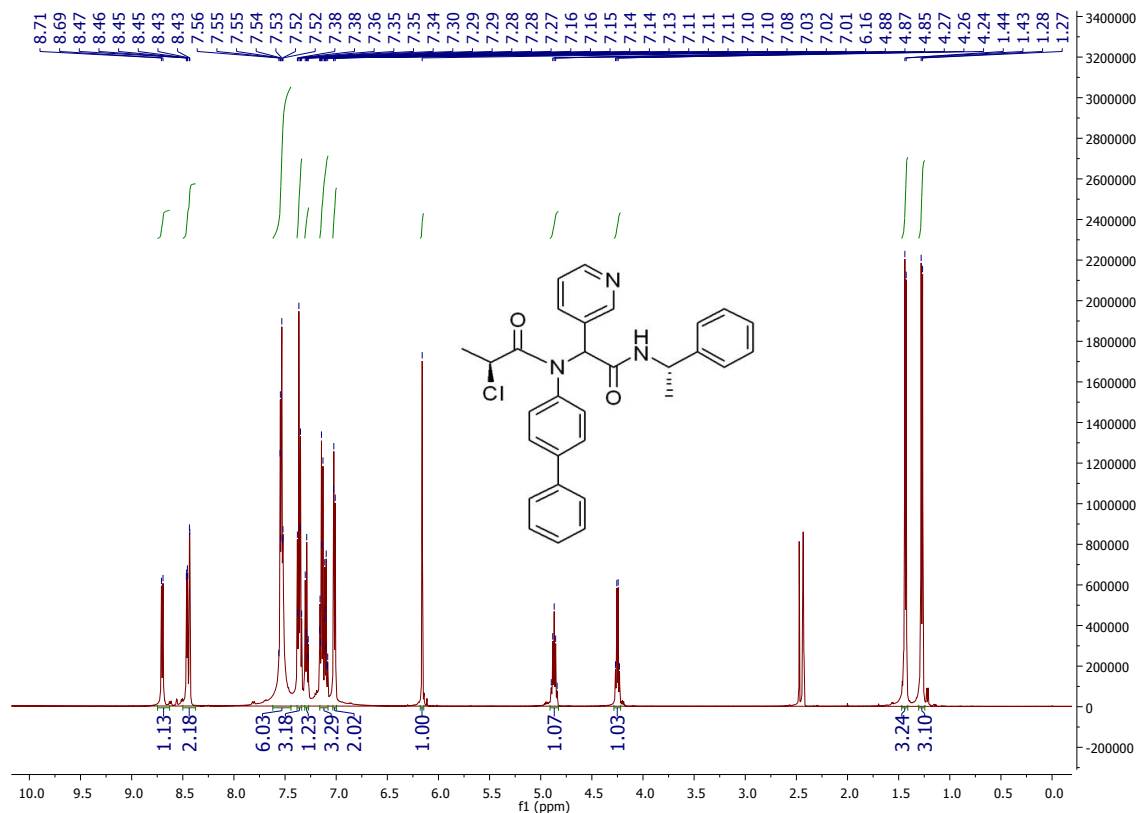
HNMR and CNMR spectra of Jun10-31-4



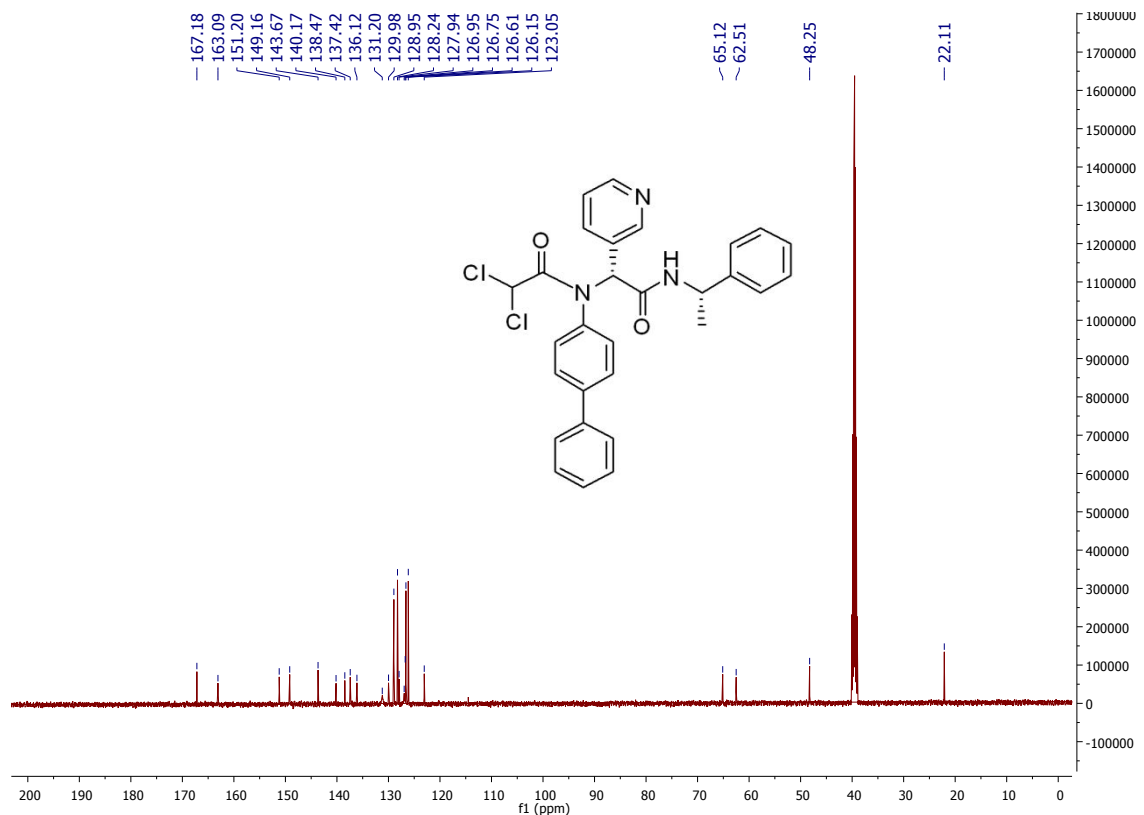
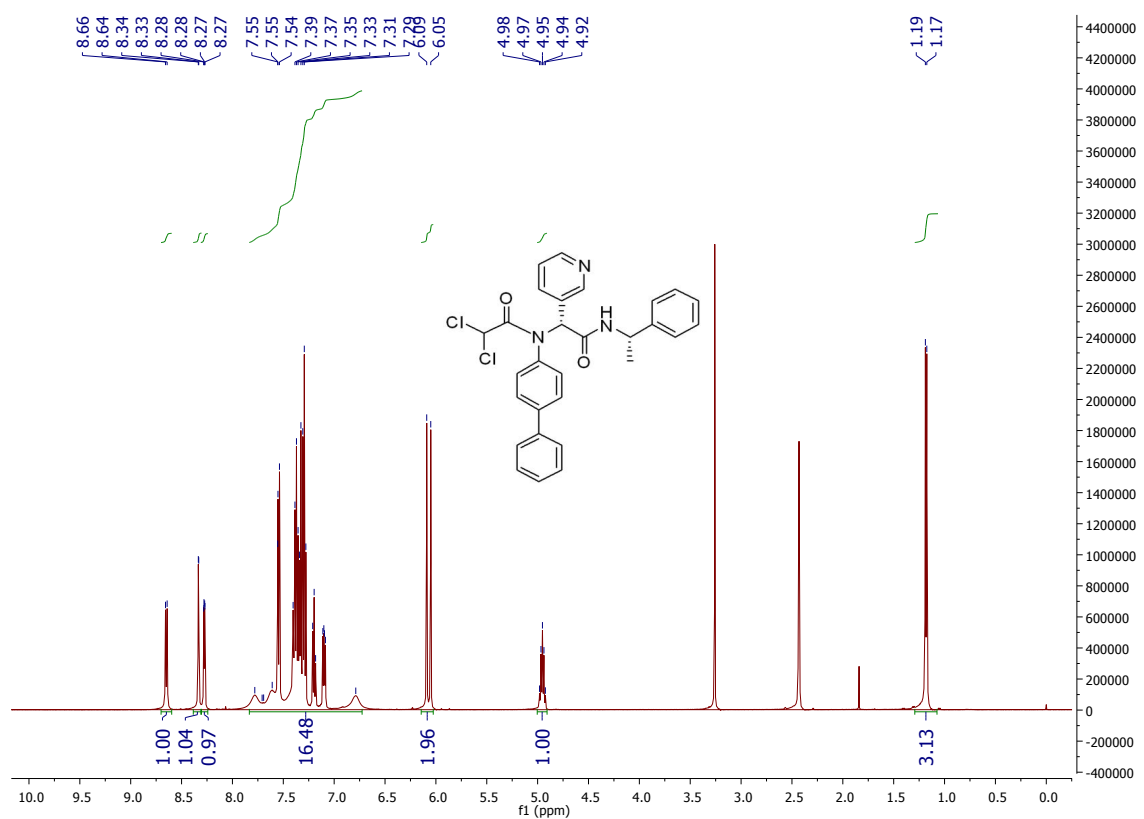
HNMR and CNMR spectra of Jun10-38-2



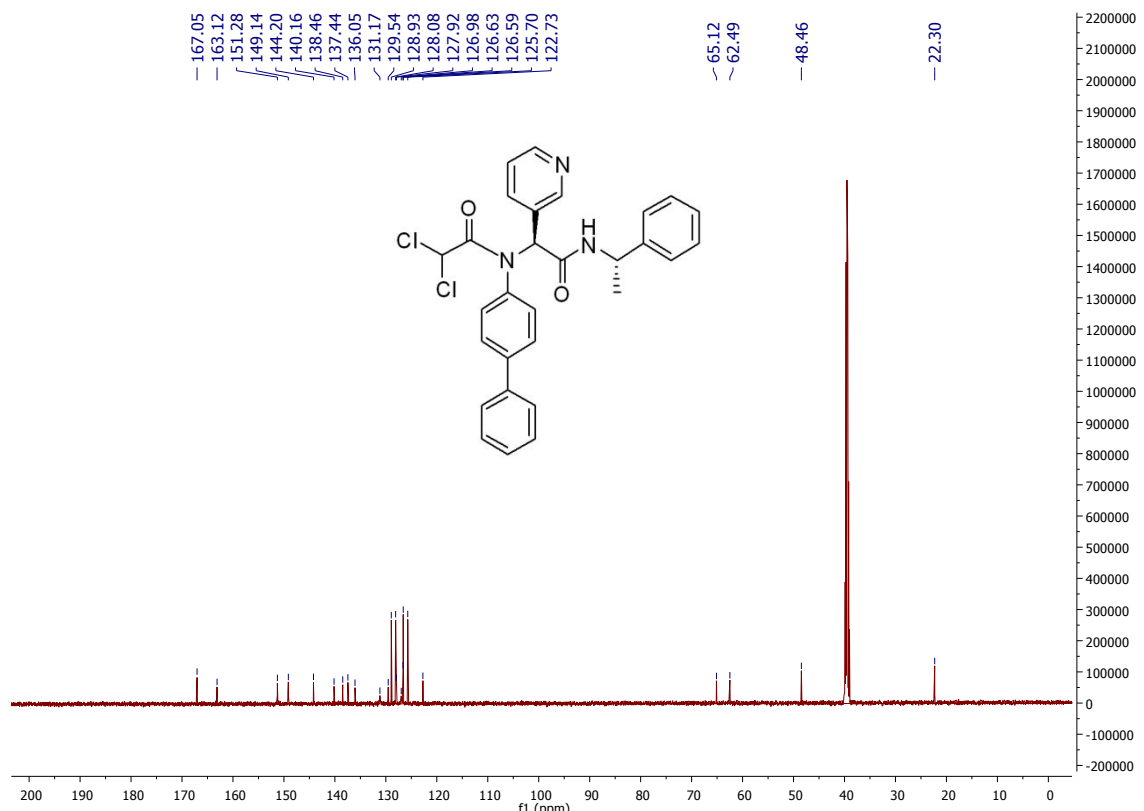
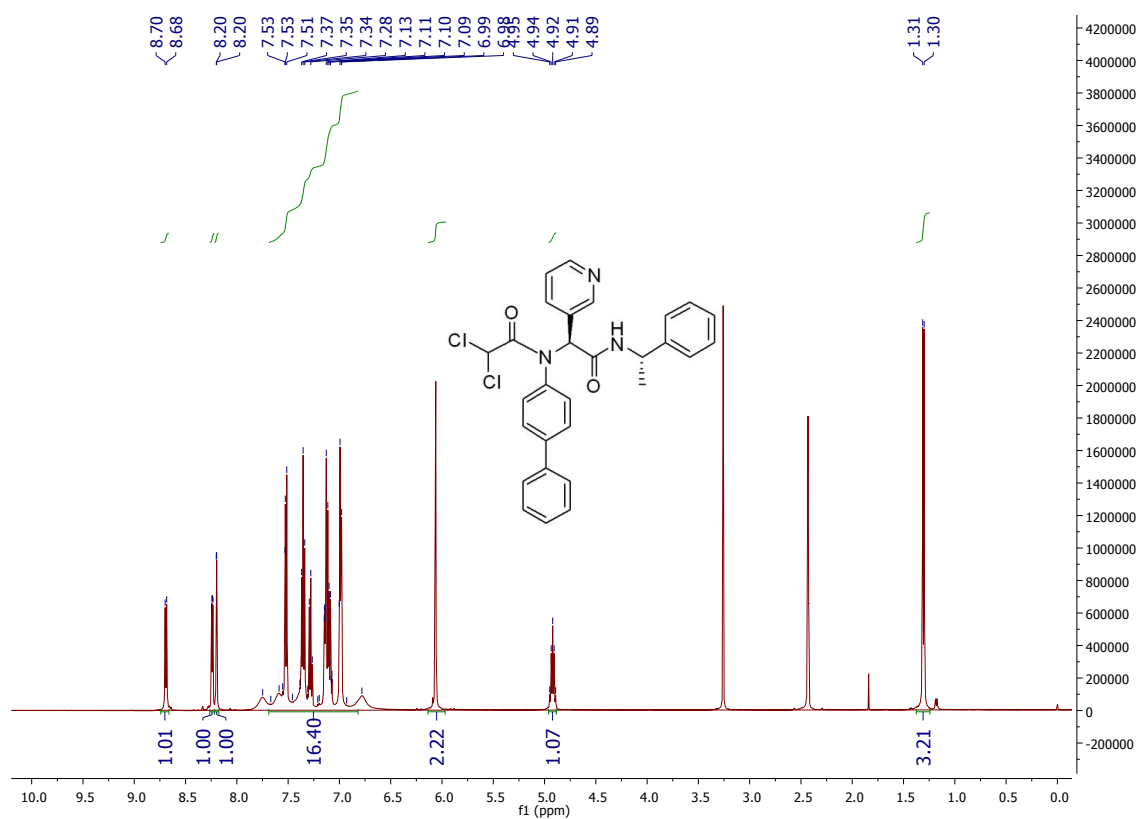
HNMR and CNMR spectra of Jun9-77-1



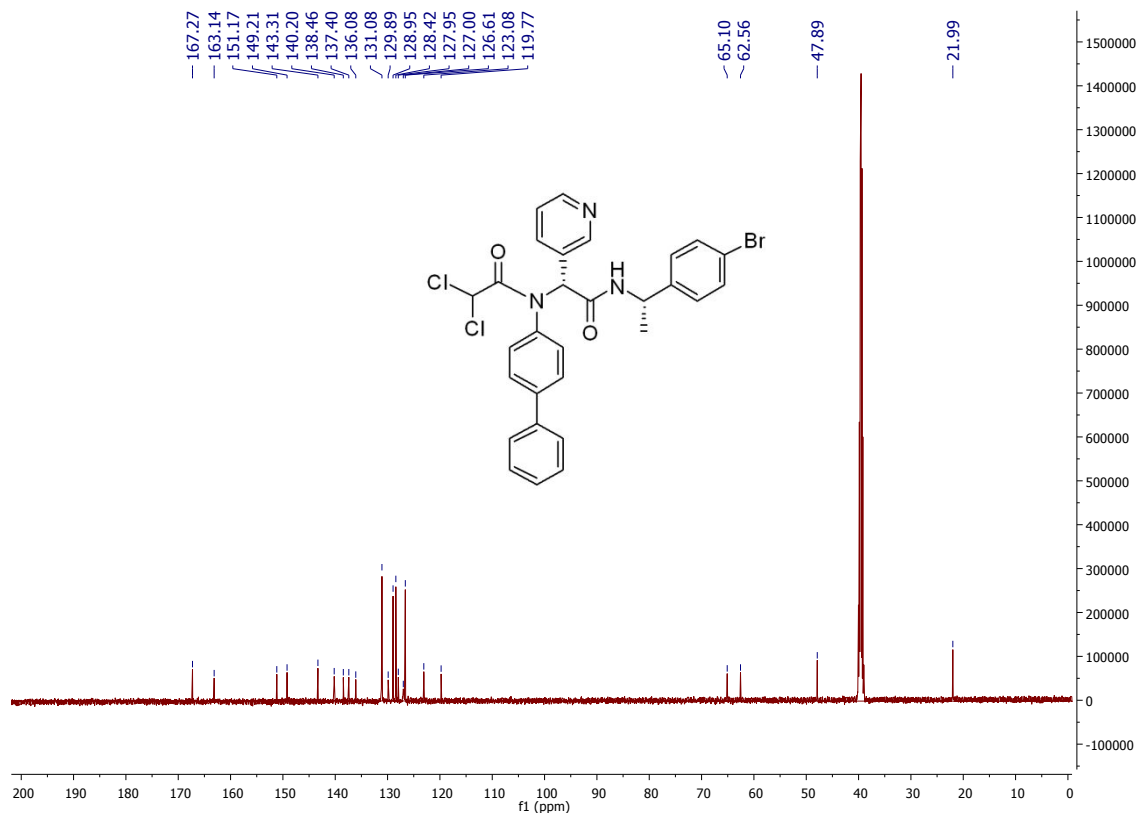
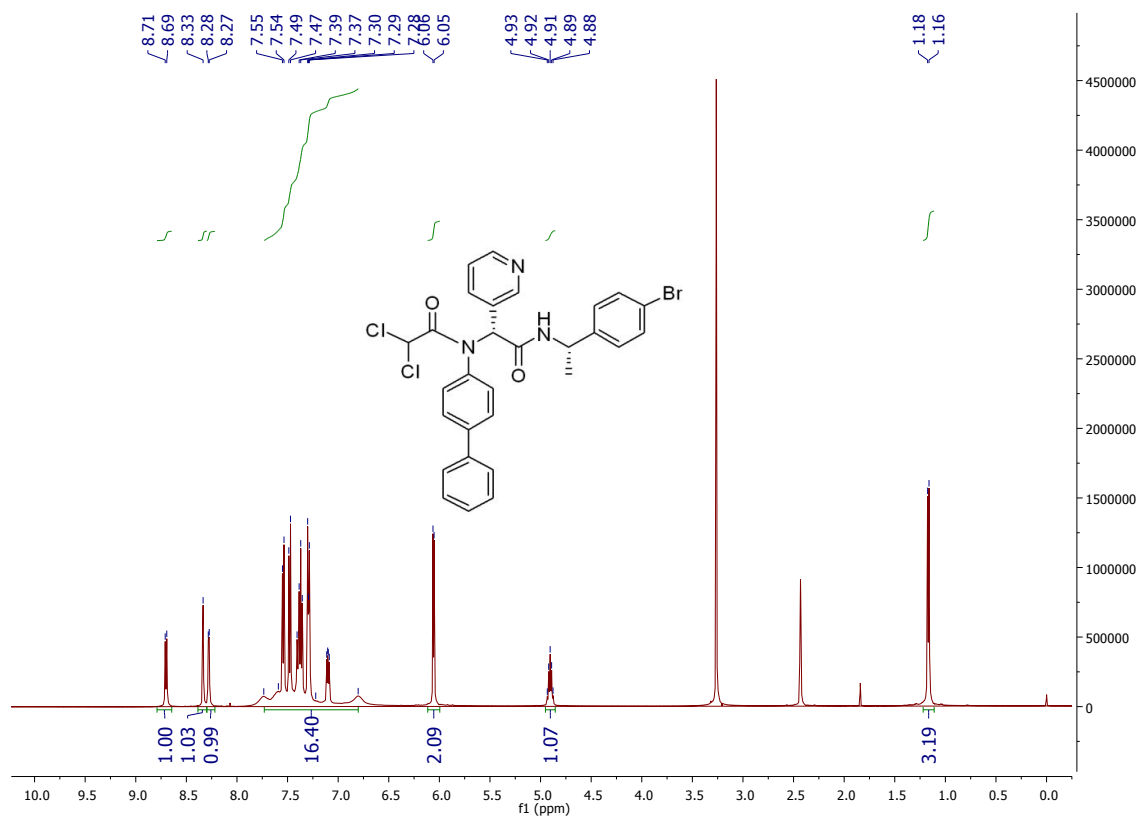
HNMR and CNMR spectra of Jun9-62-2R



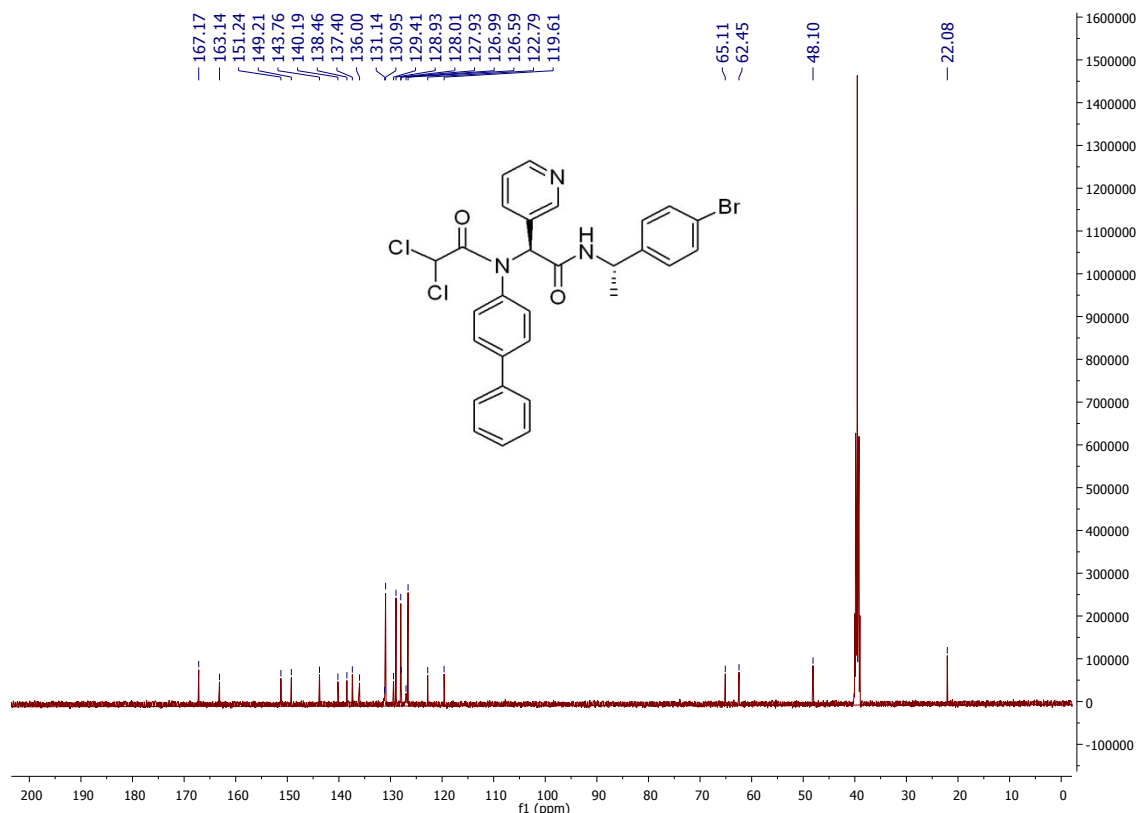
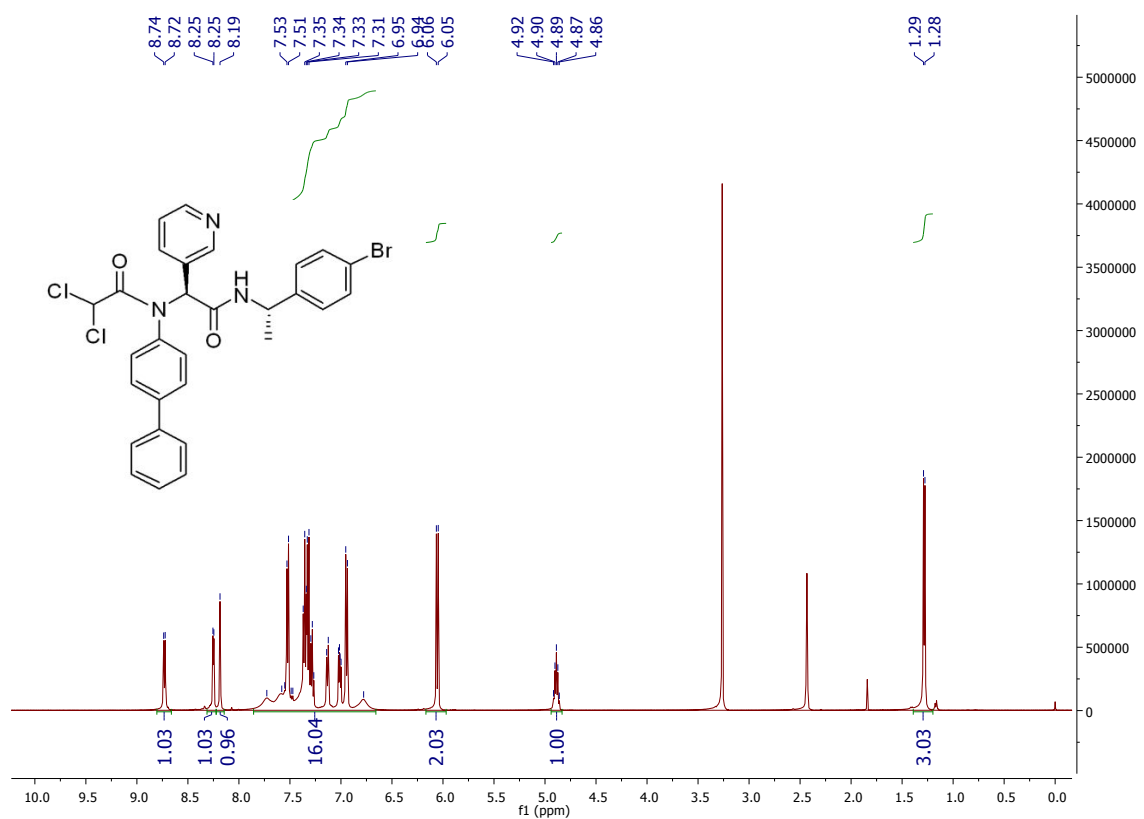
HNMR and CNMR spectra of Jun9-62-2S



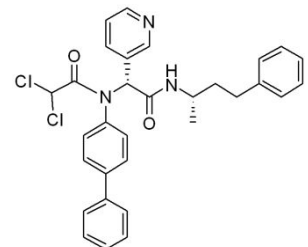
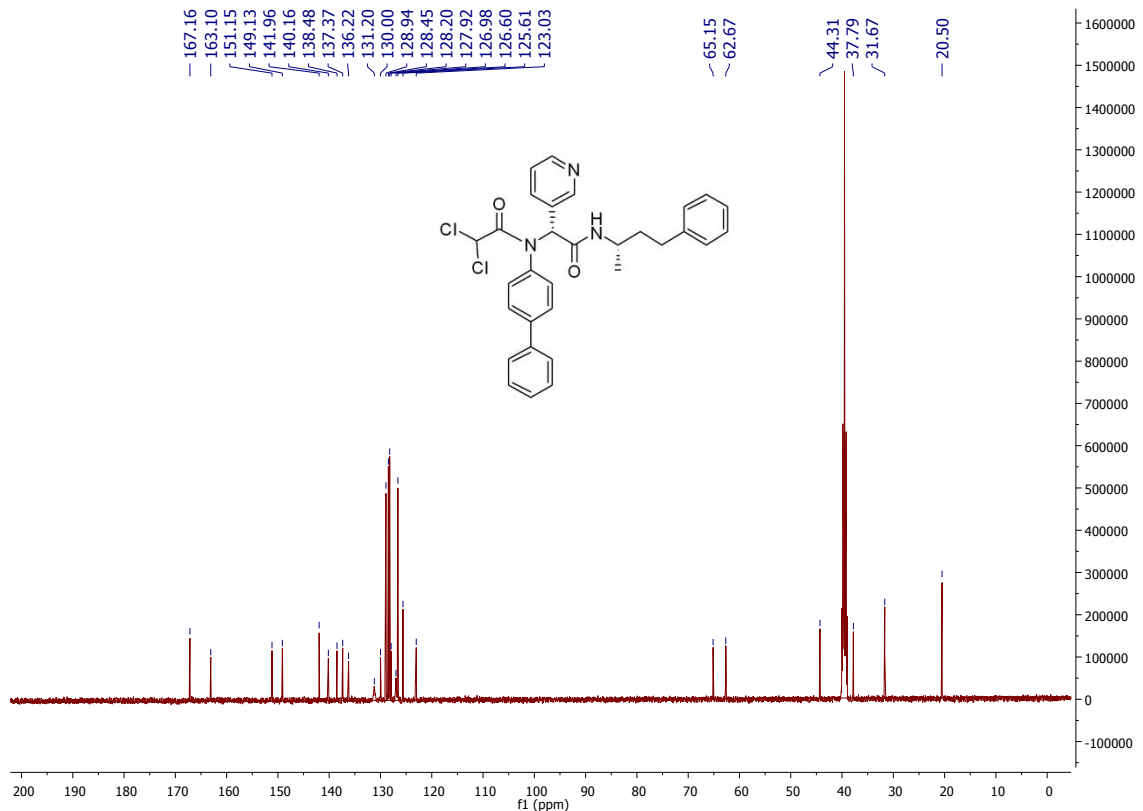
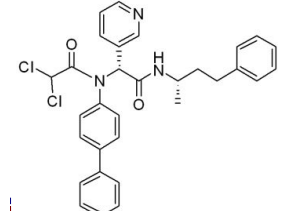
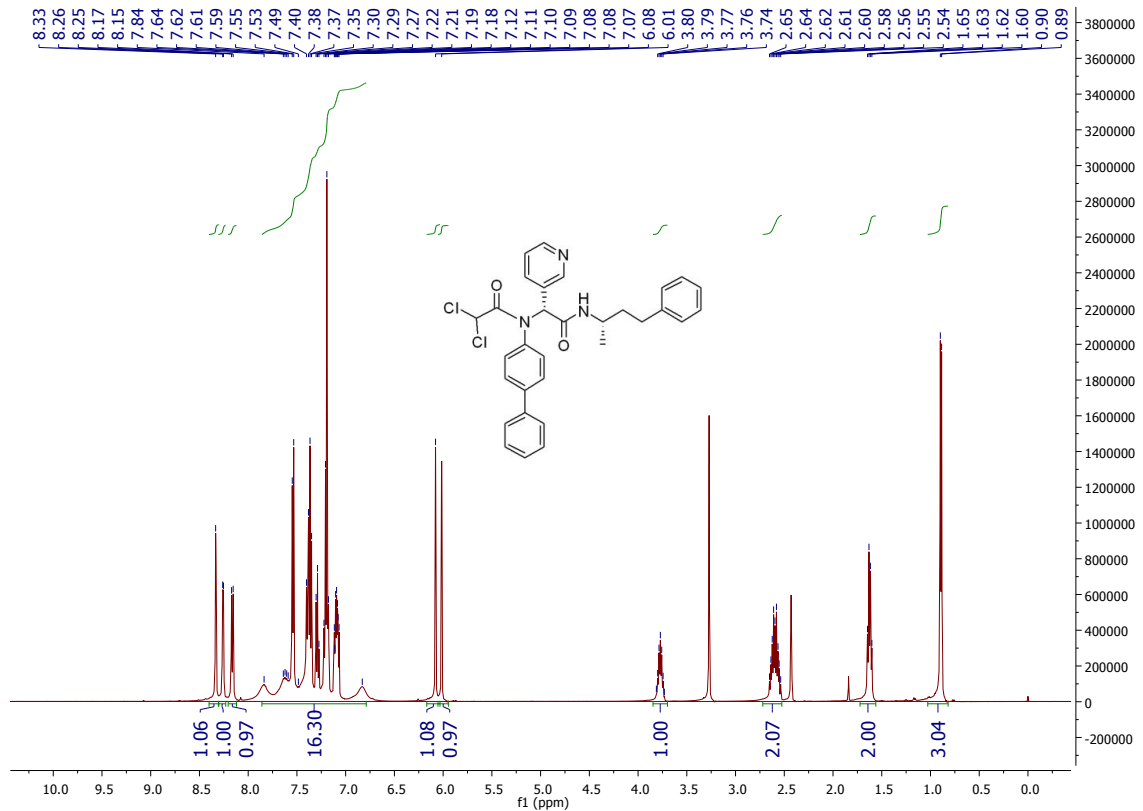
HNMR and CNMR spectra of Jun9-90-3R



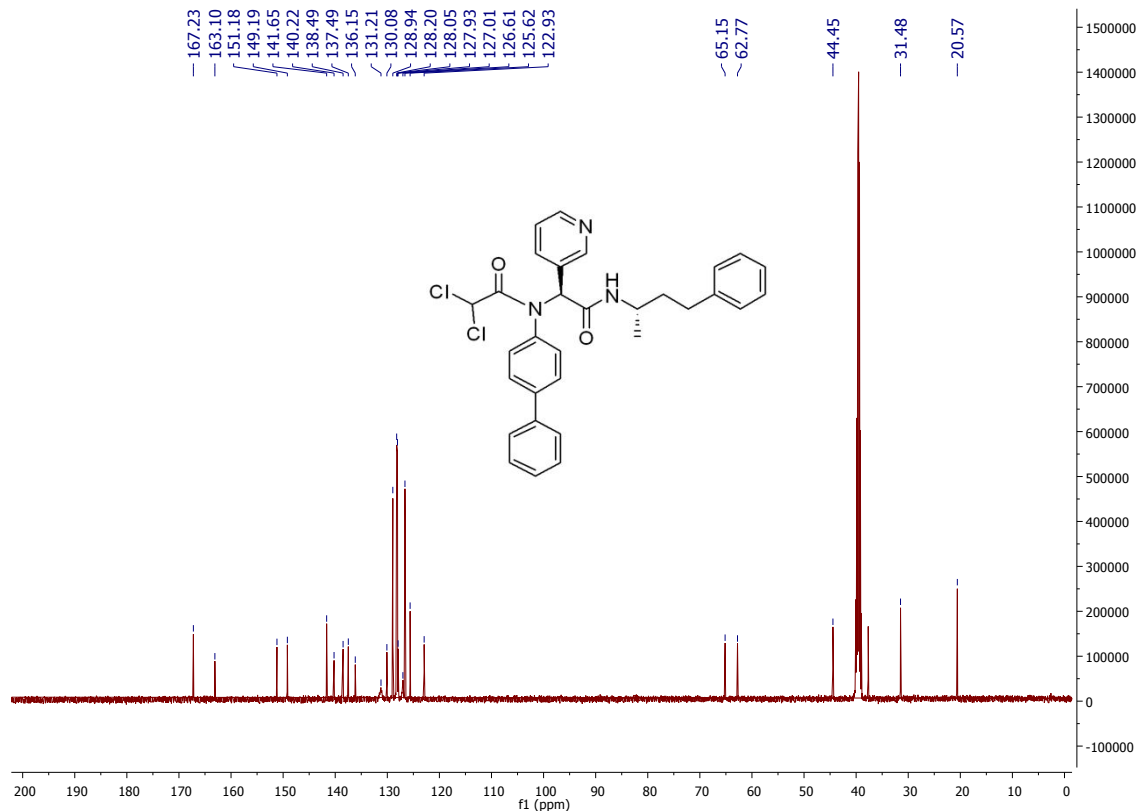
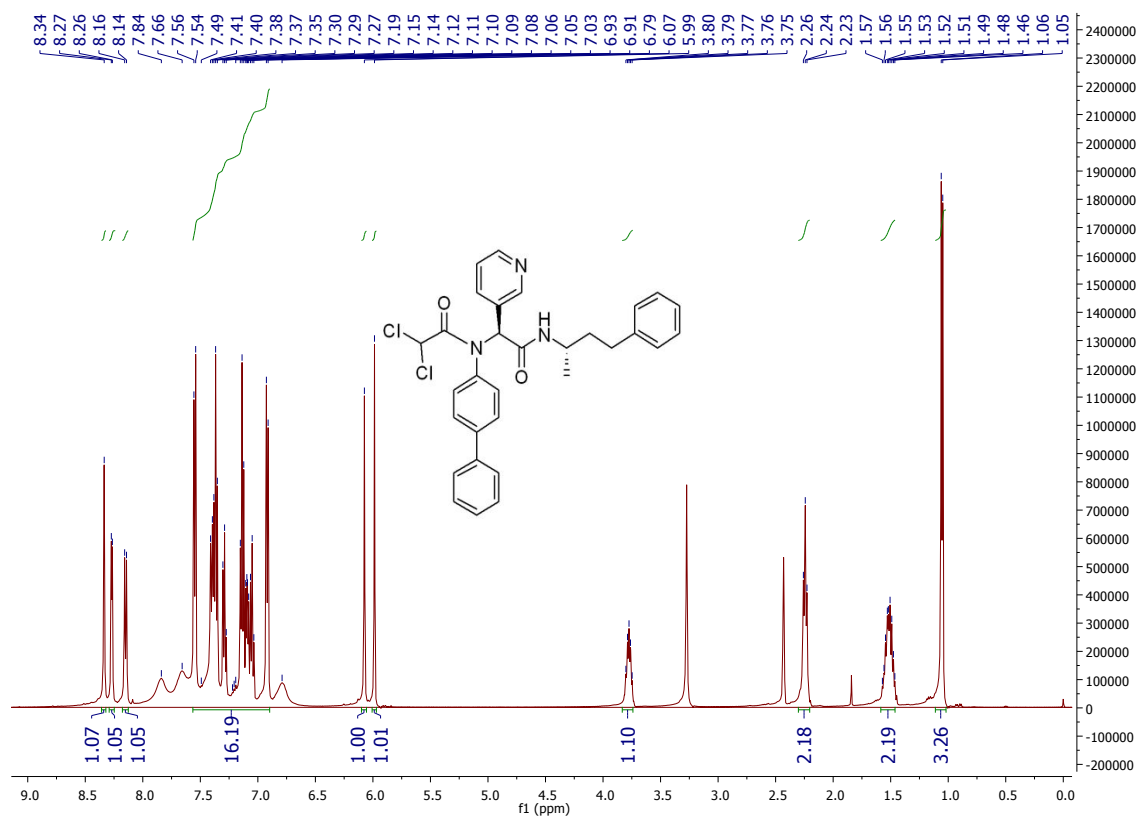
HNMR and CNMR spectra of Jun9-90-3S



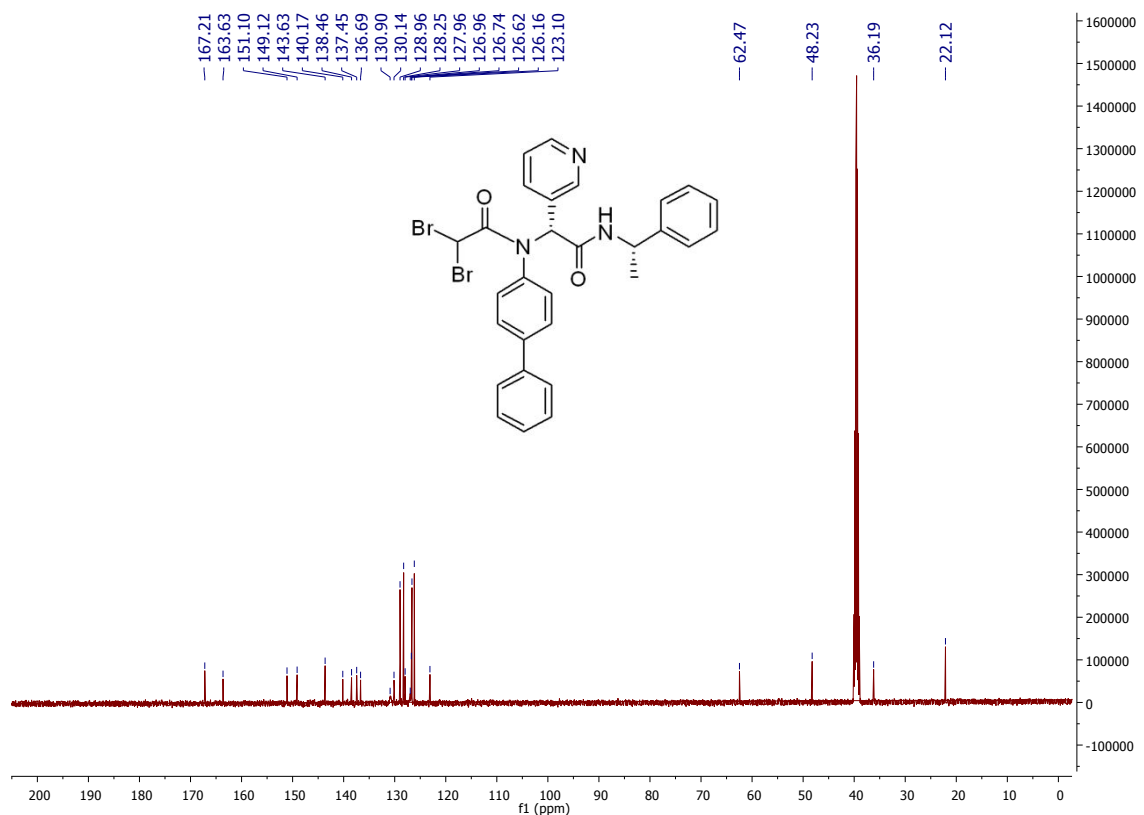
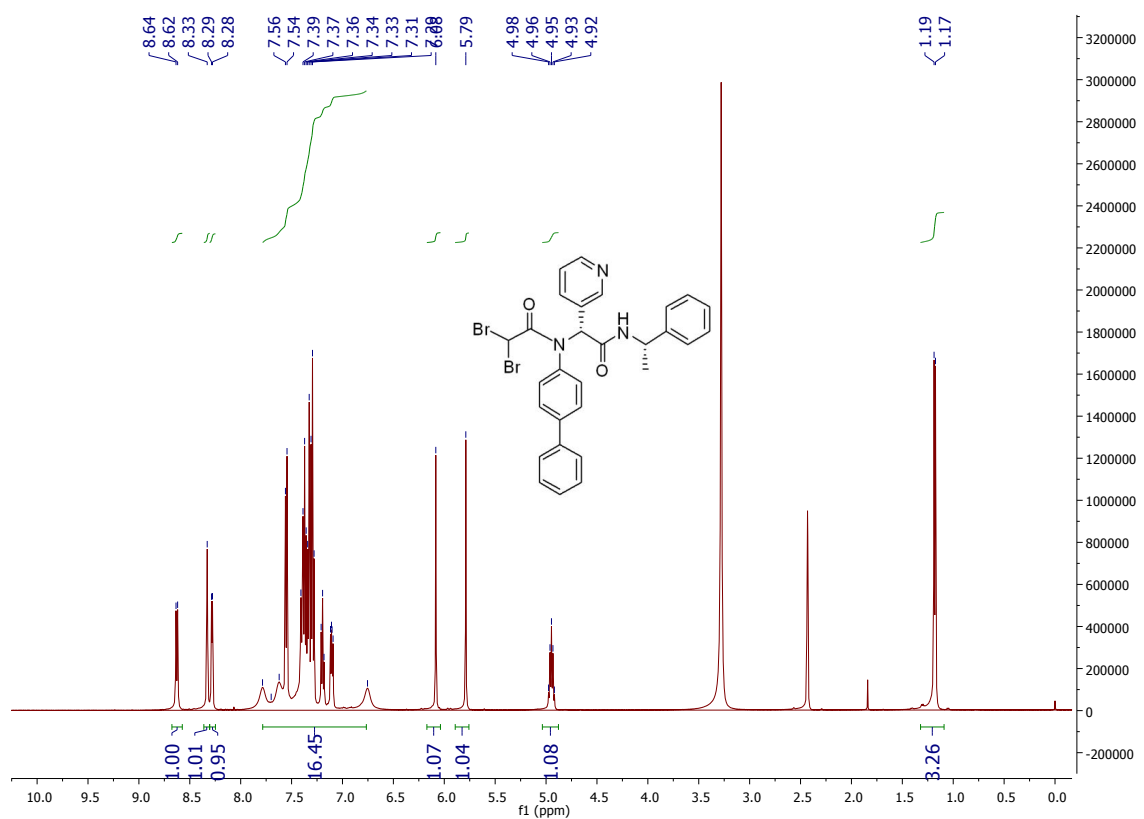
HNMR and CNMR spectra of Jun9-90-4R



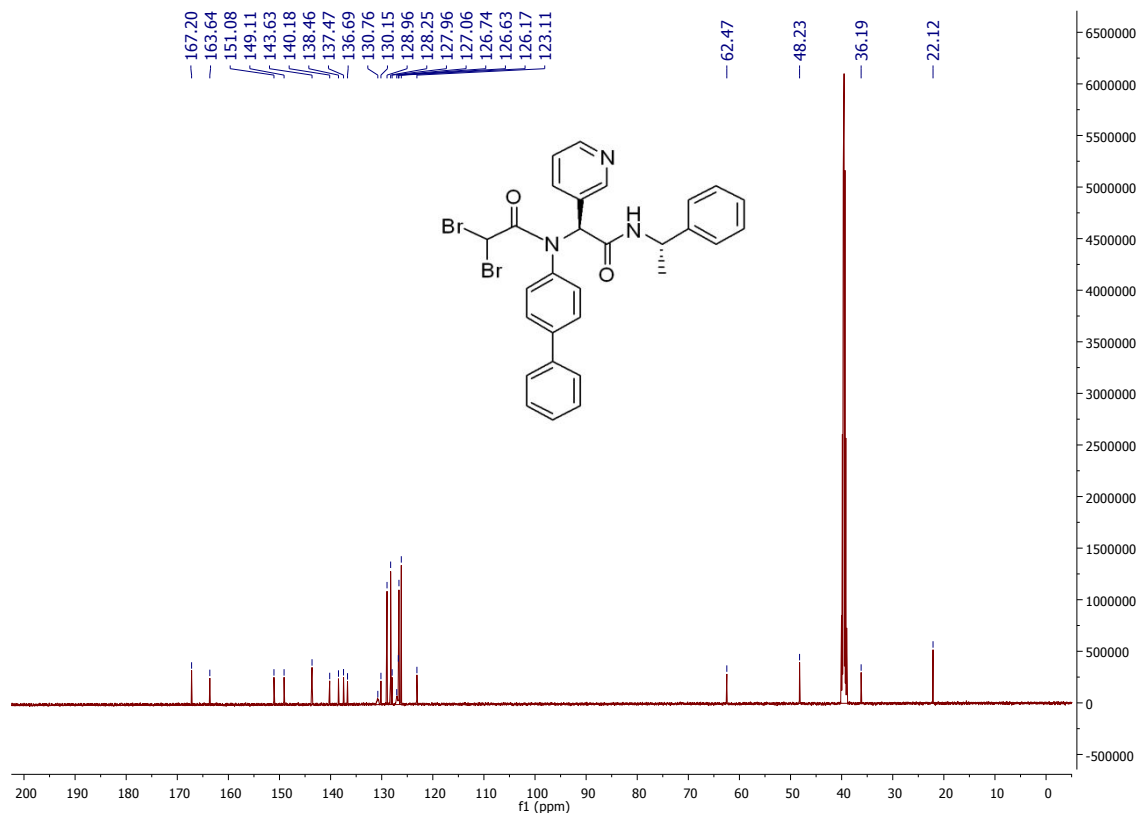
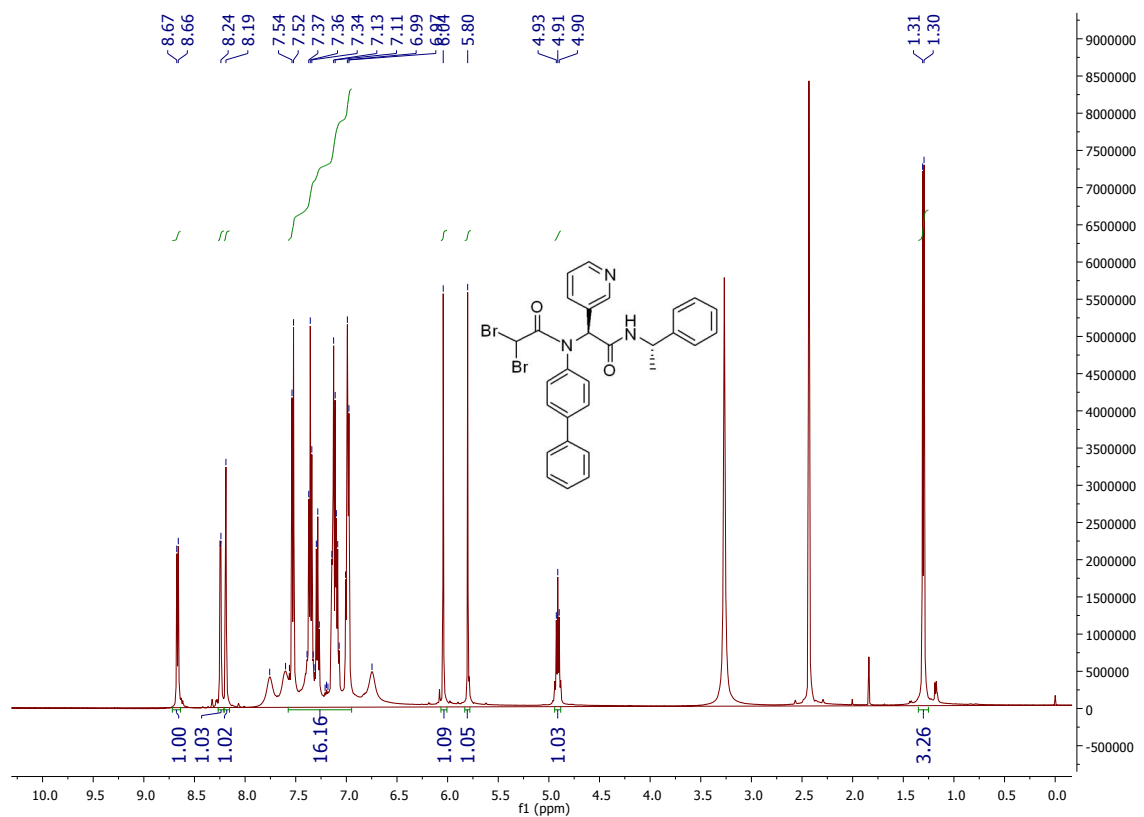
HNMR and CNMR spectra of Jun9-90-4S



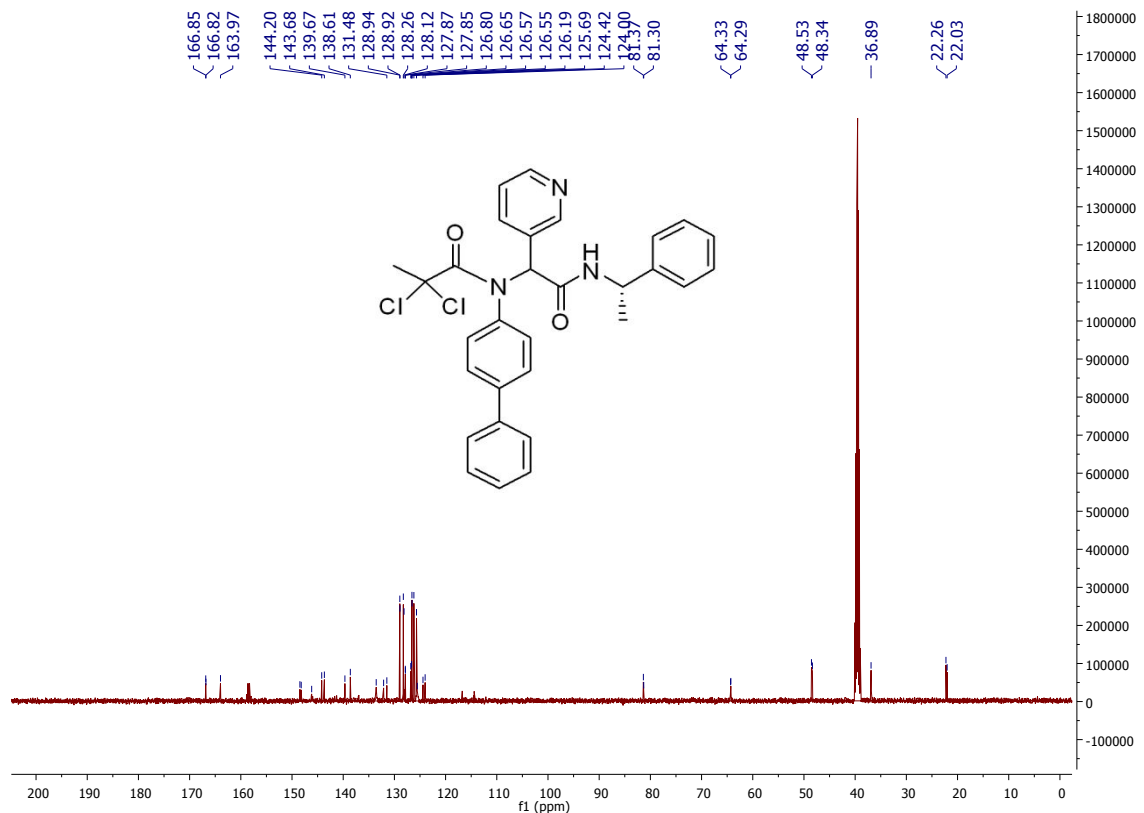
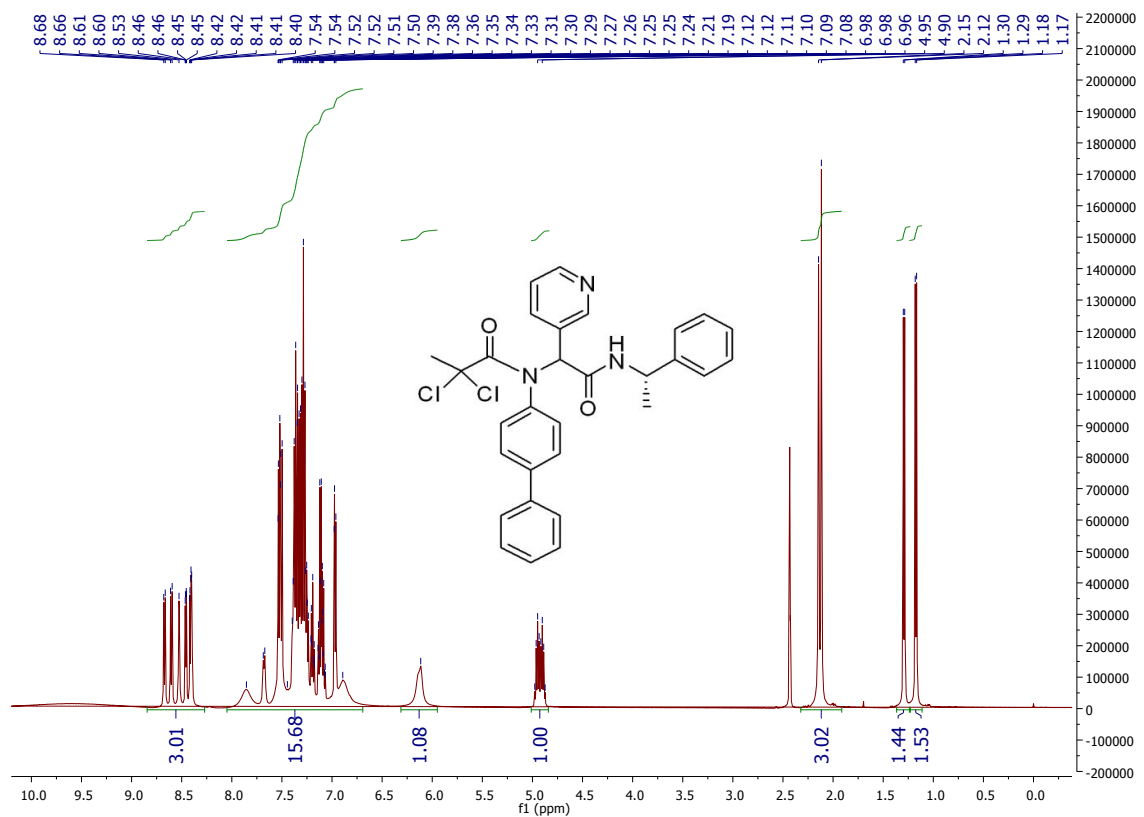
HNMR and CNMR spectra of Jun9-89-2R



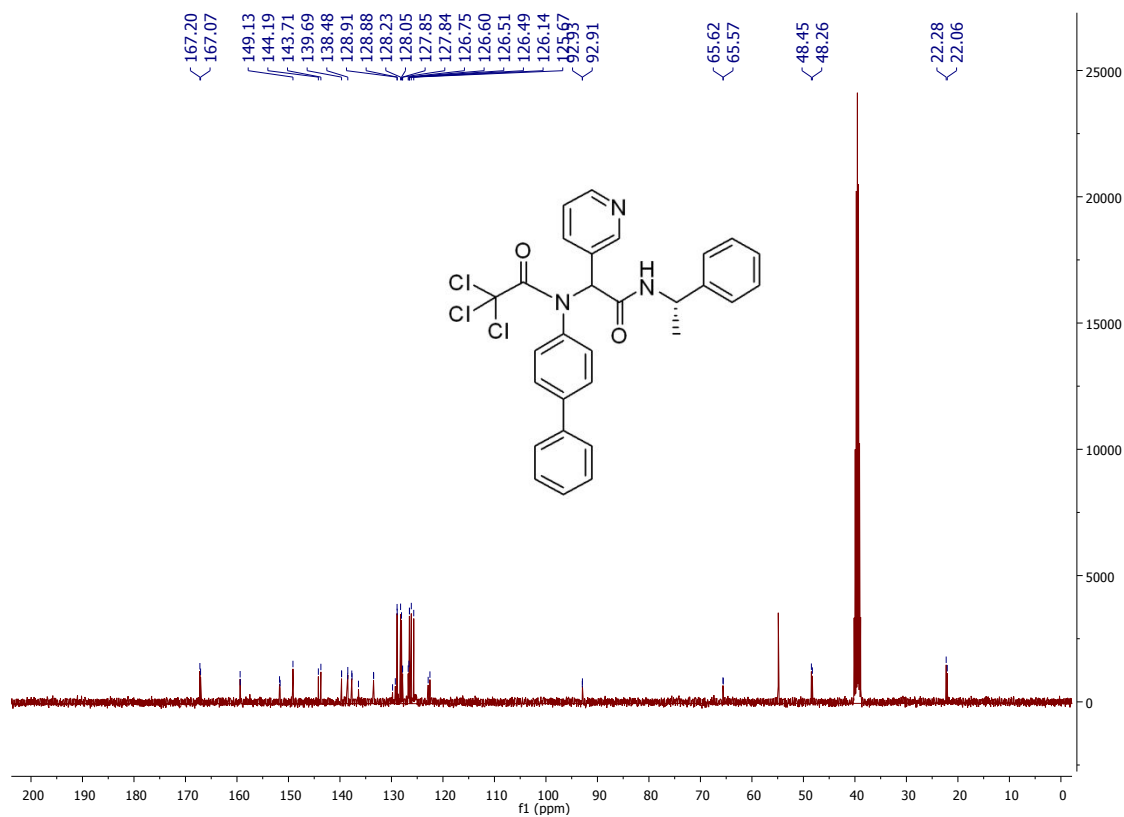
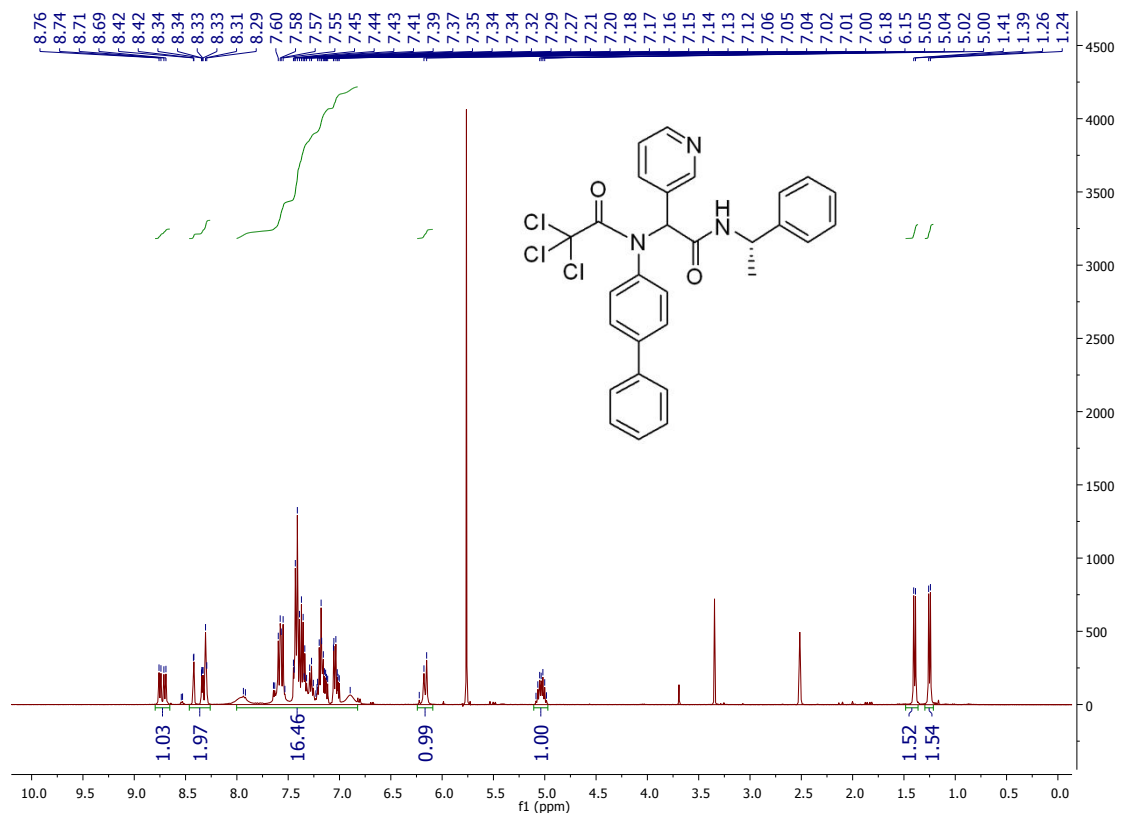
HNMR and CNMR spectra of Jun9-89-2S



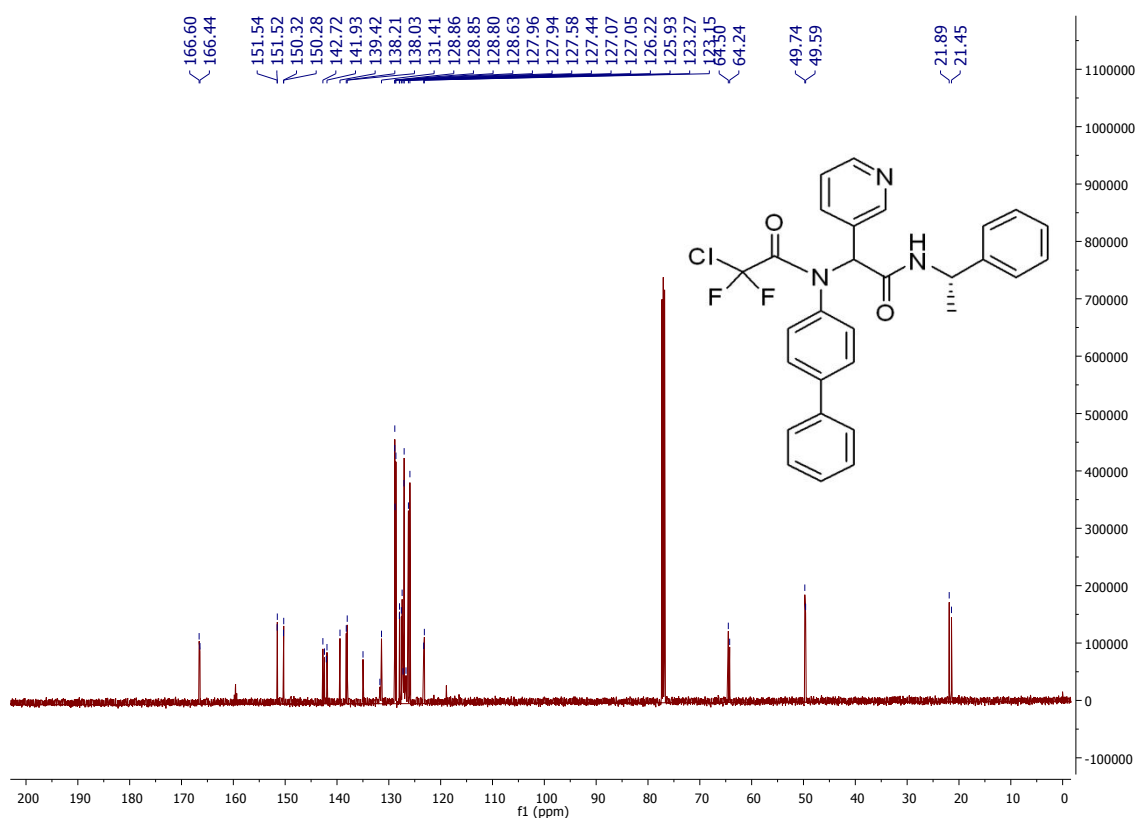
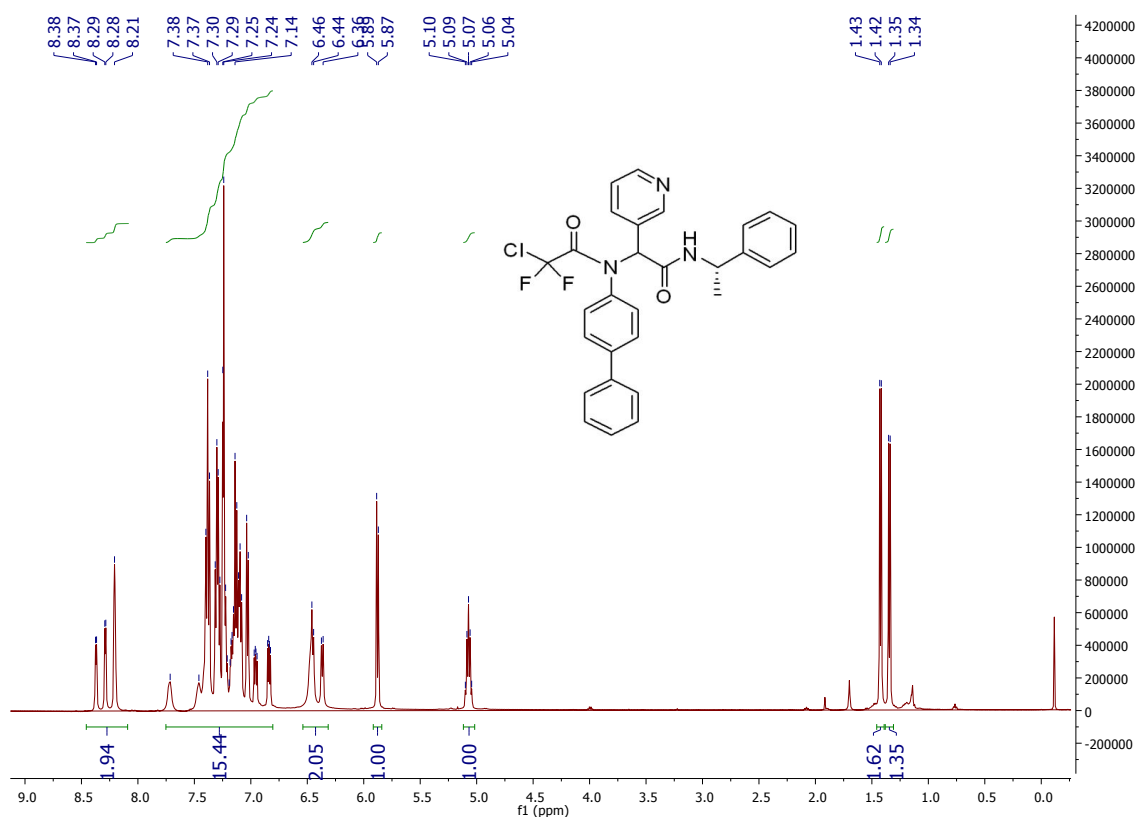
HNMR and CNMR spectra of Jun9-76-4



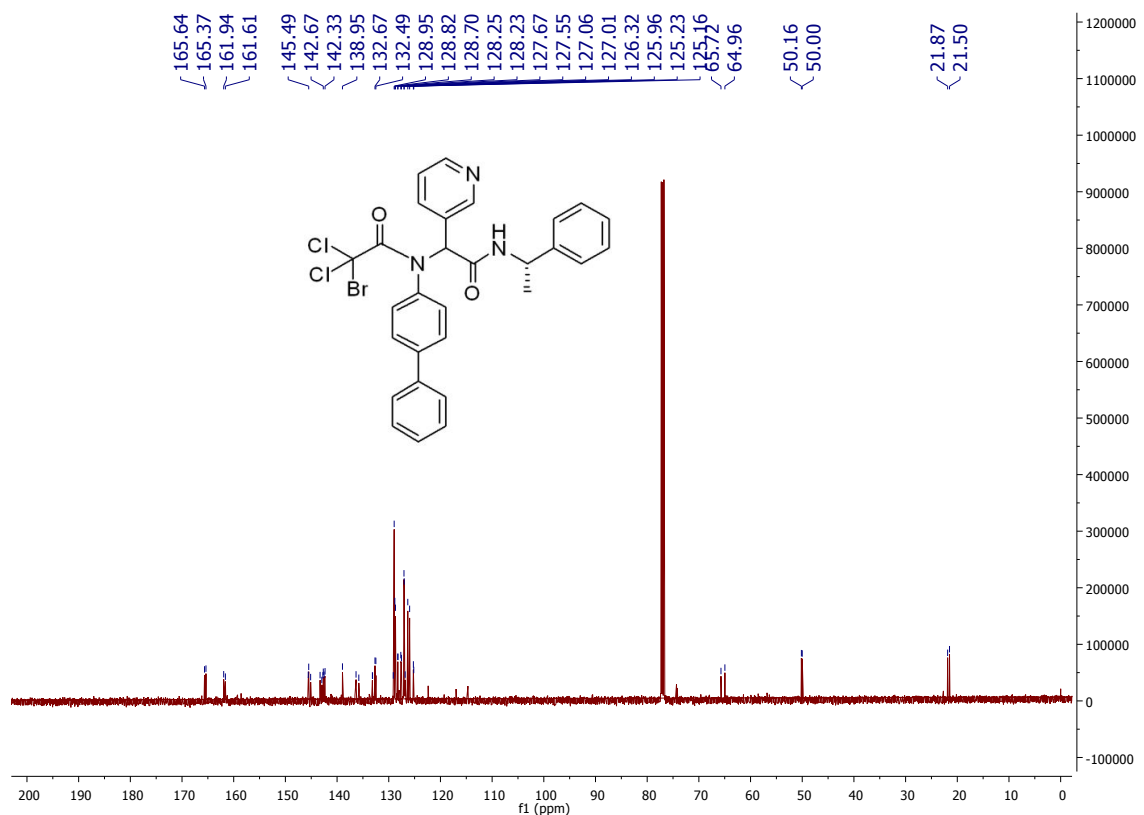
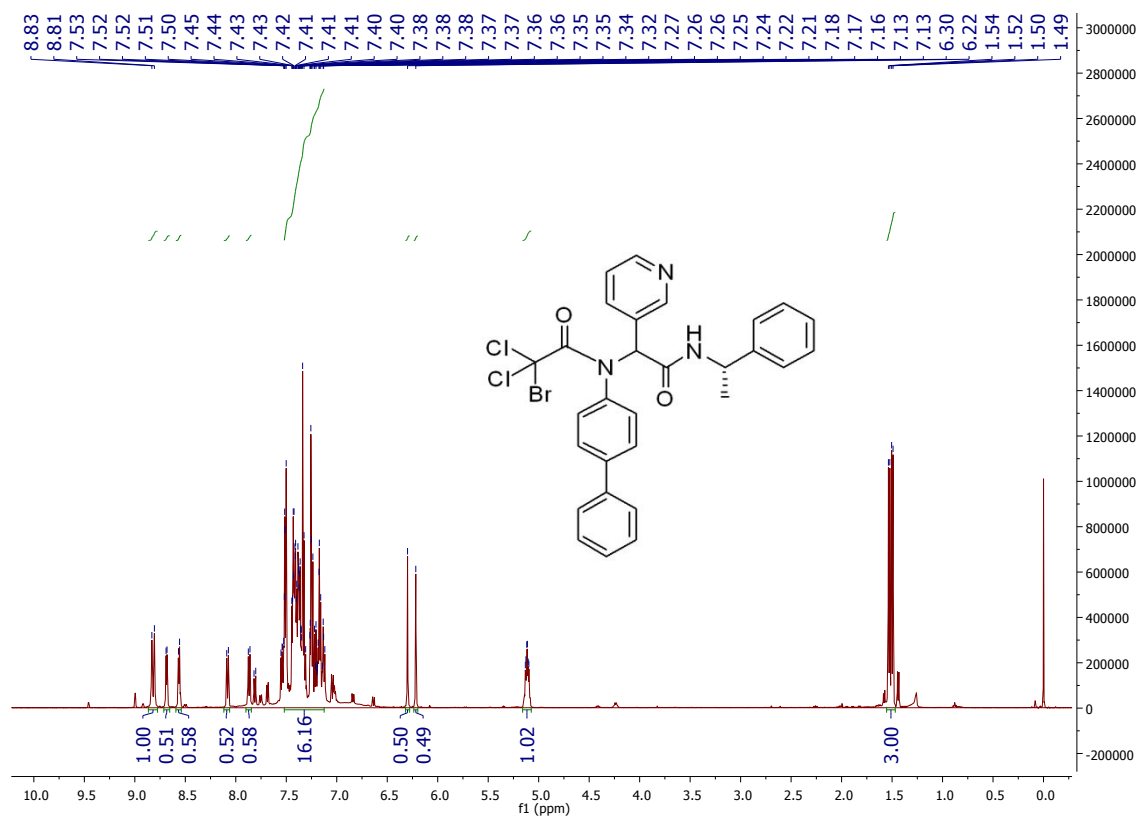
HNMR and CNMR spectra of Jun9-72-4



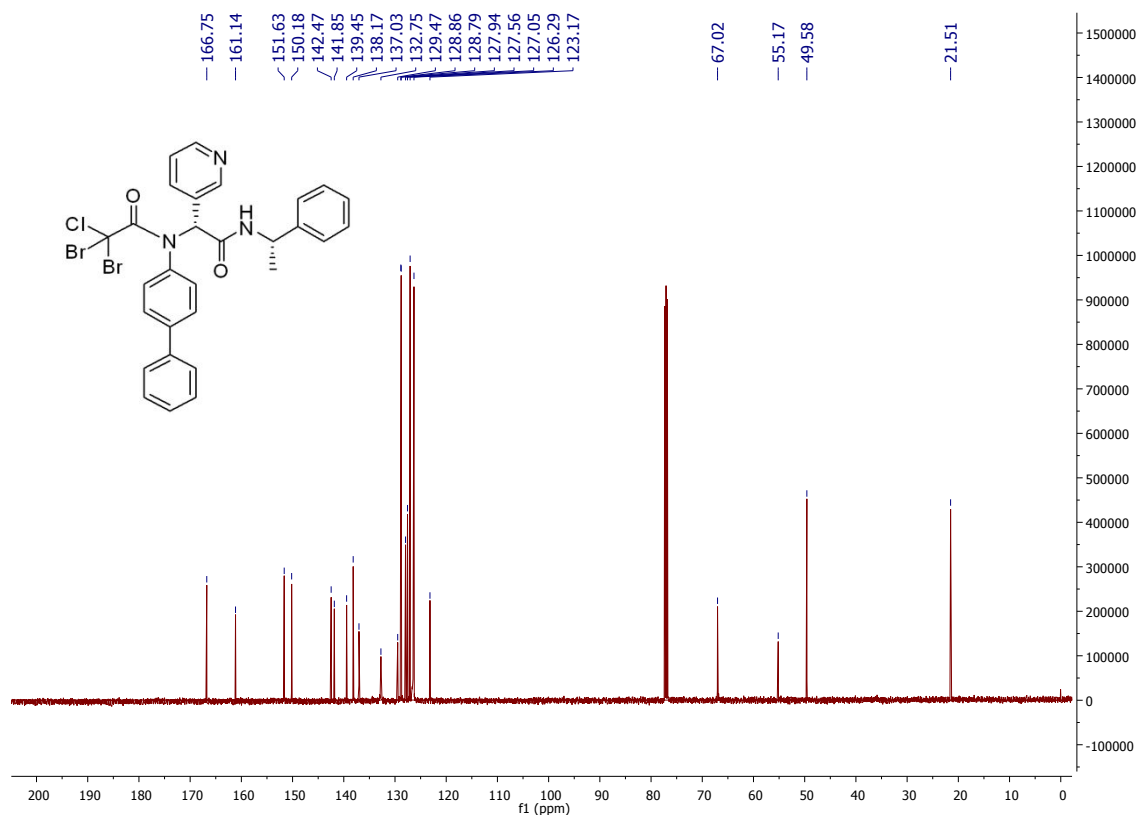
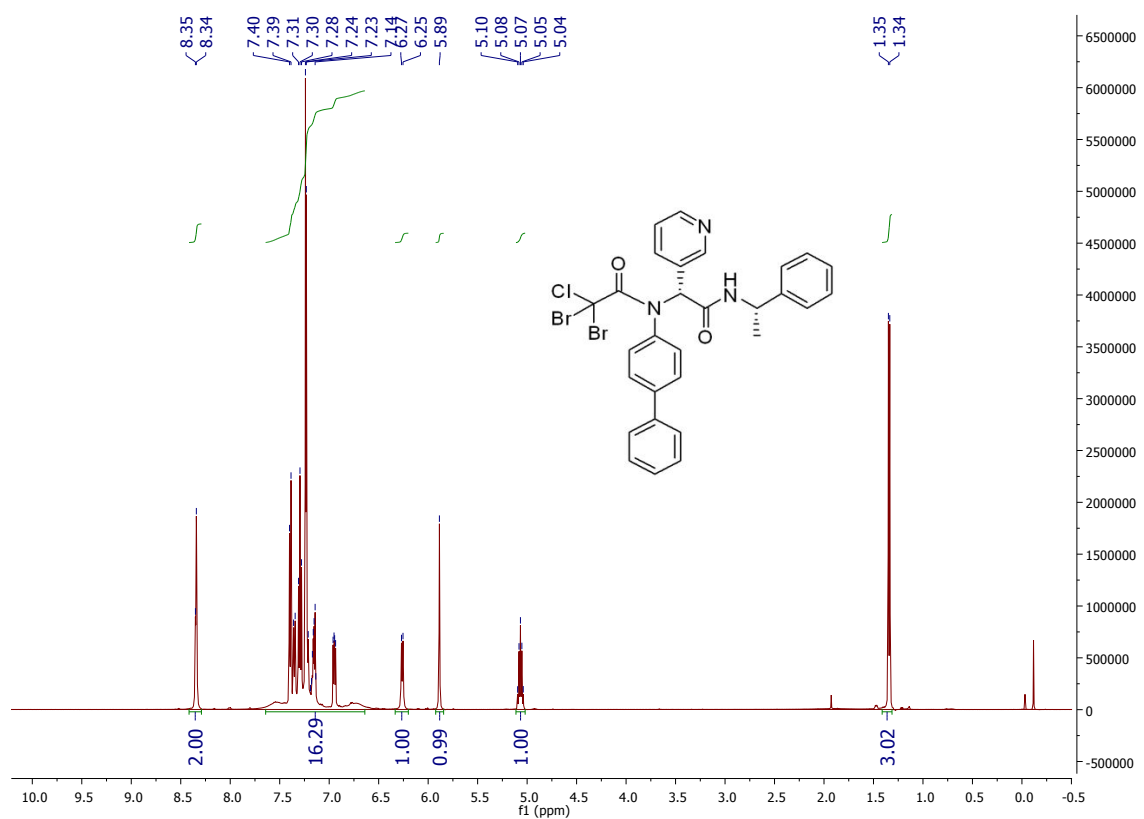
HNMR and CNMR spectra of Jun9-77-2



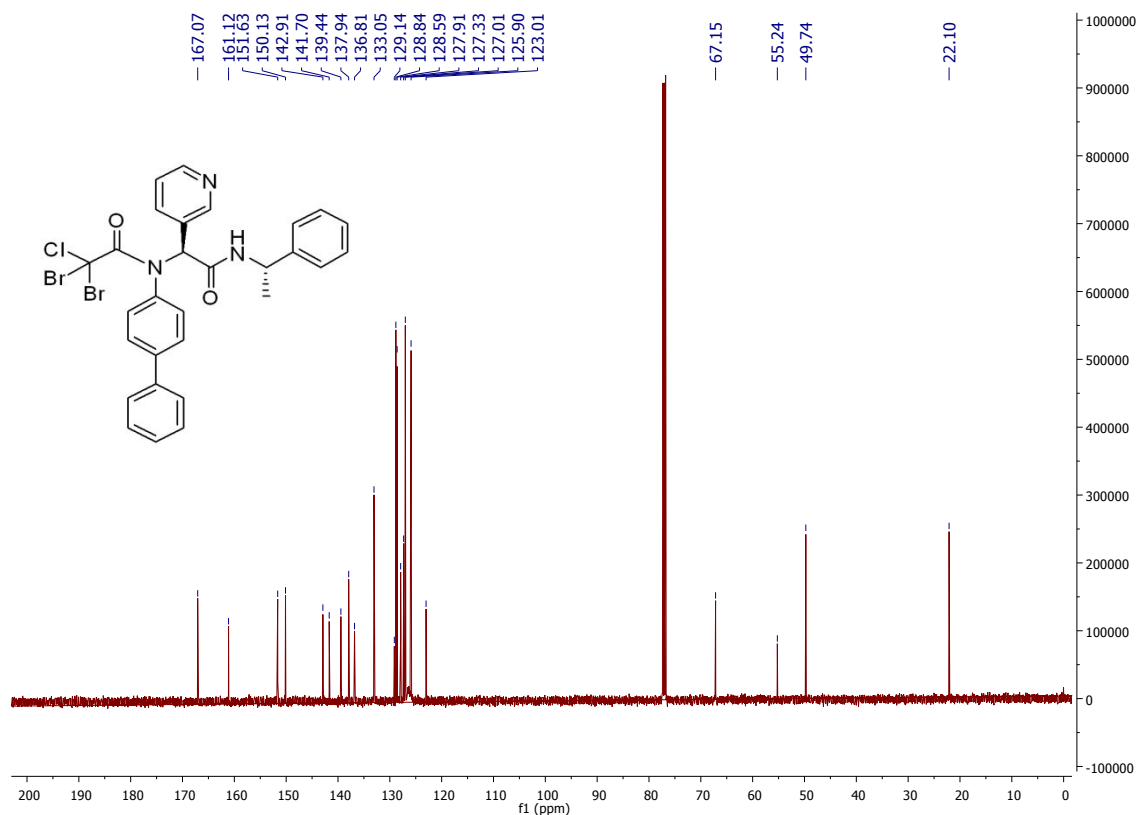
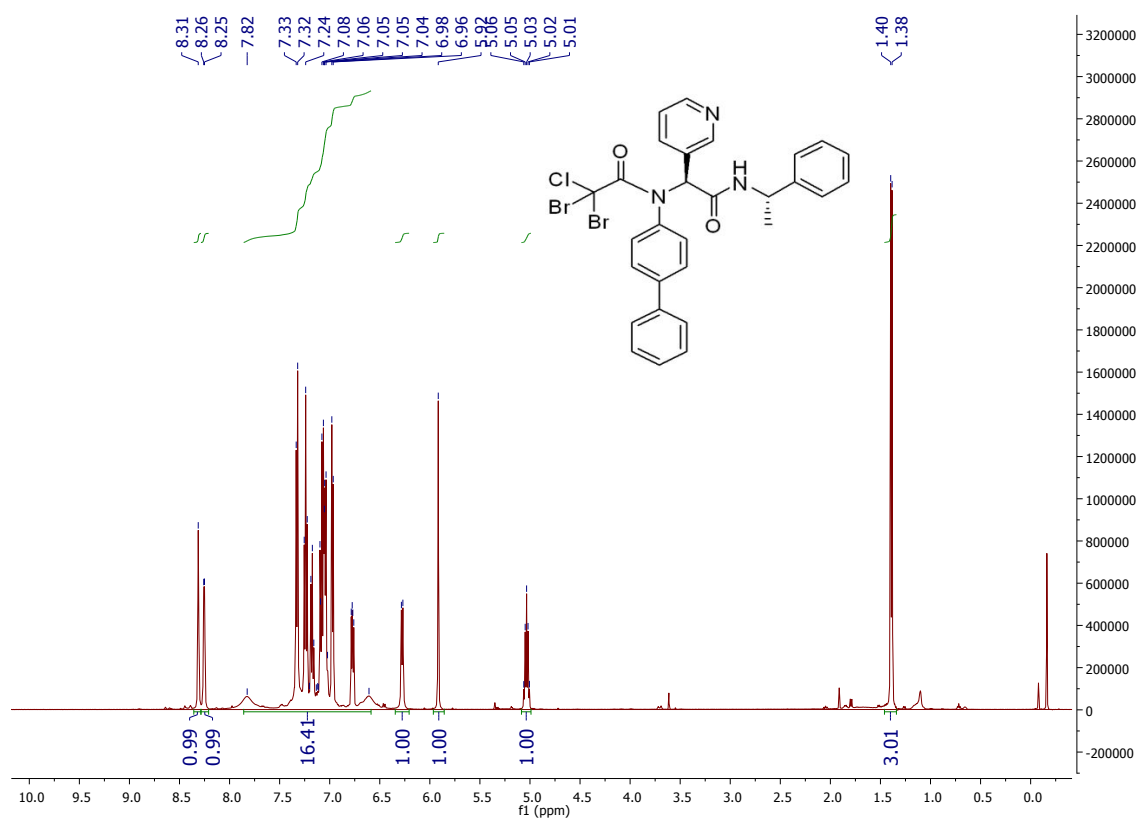
HNMR and CNMR spectra of Jun9-89-3



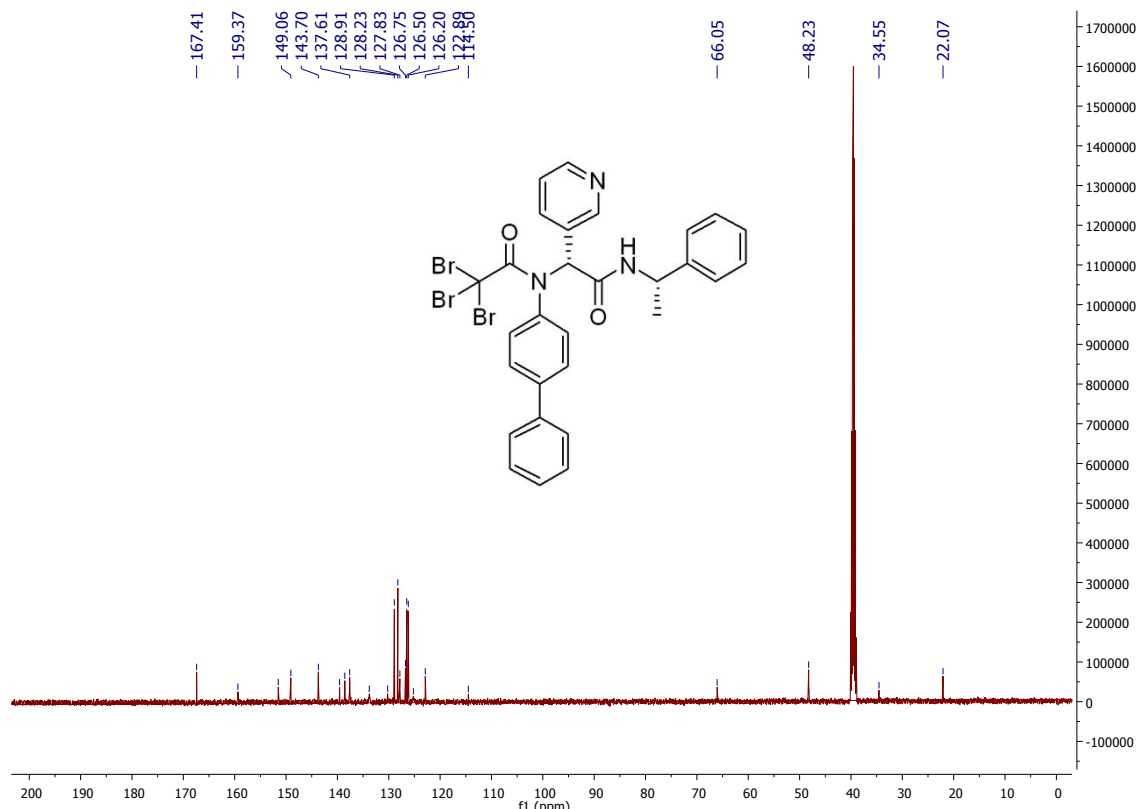
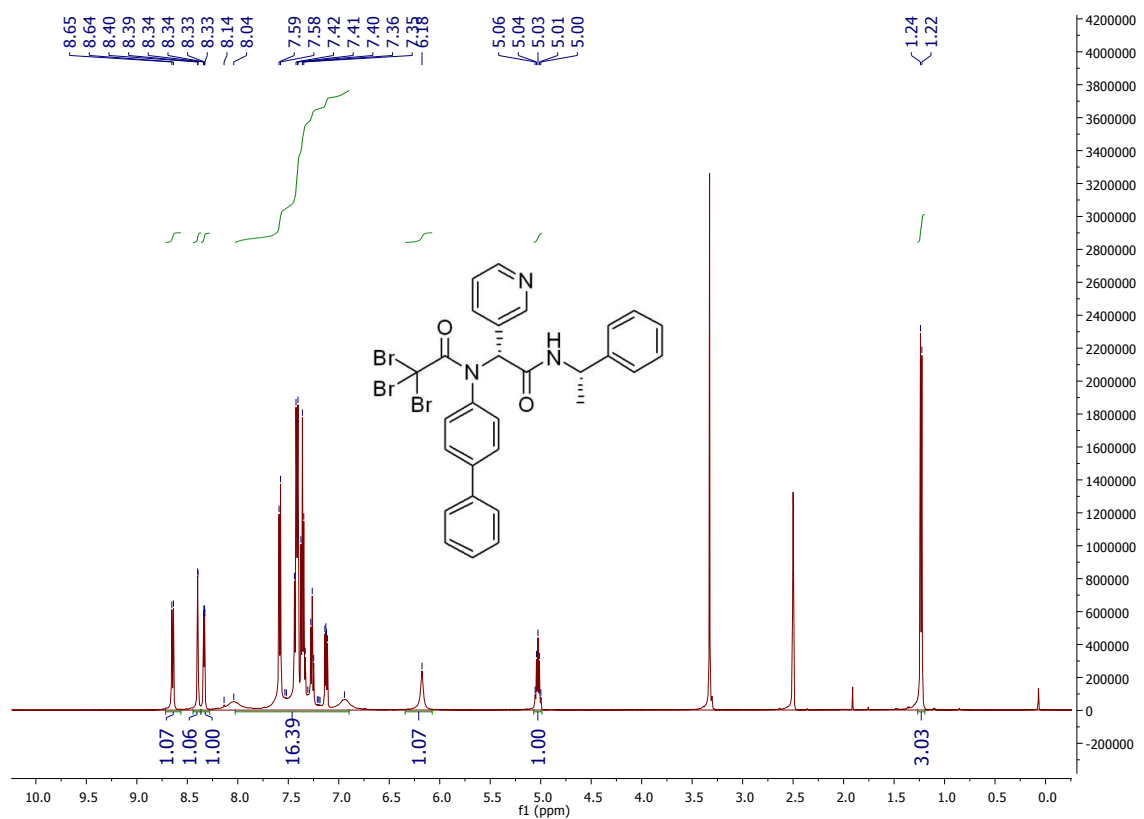
HNMR and CNMR spectra of Jun9-89-4R



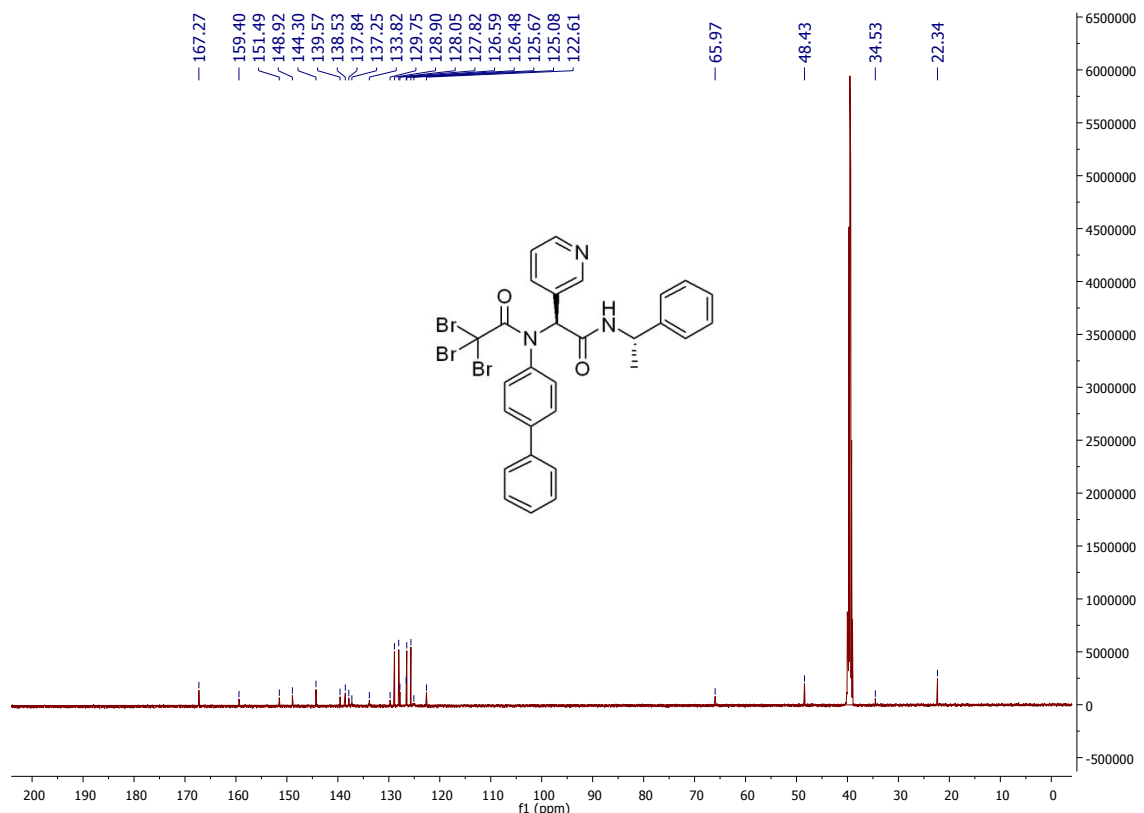
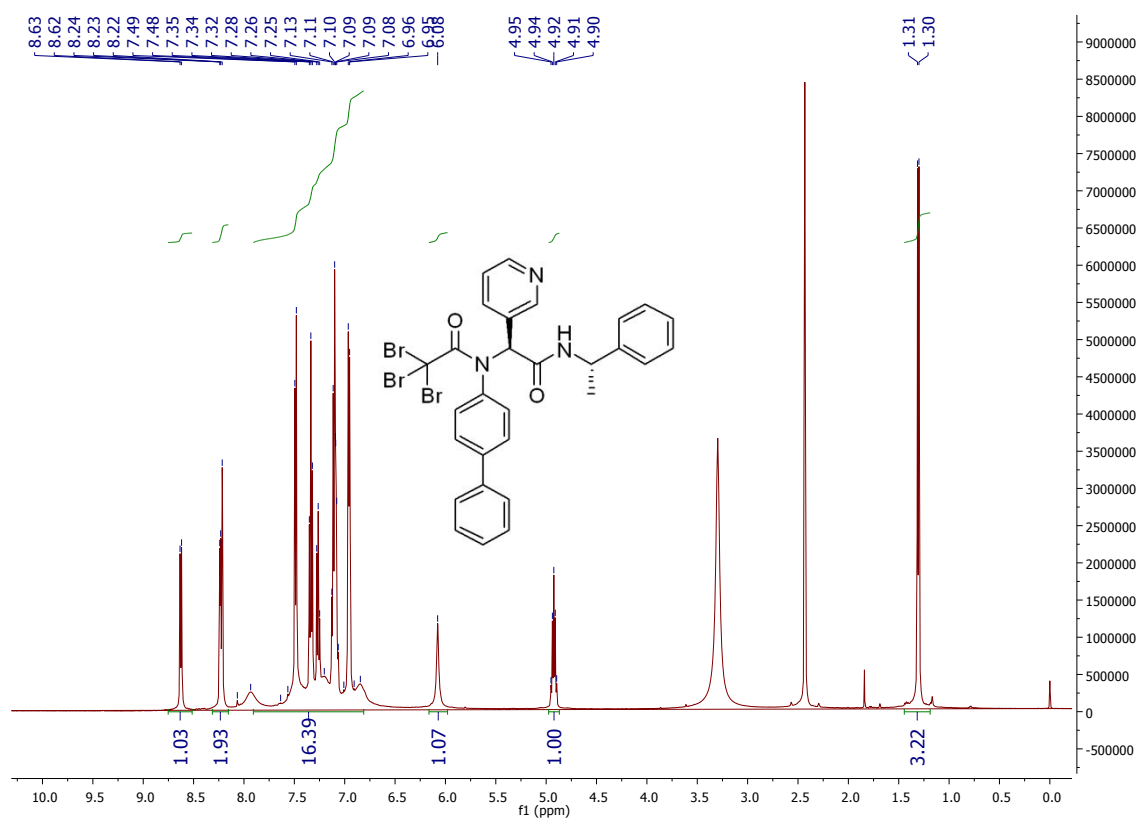
HNMR and CNMR spectra of Jun9-89-4S



HNMR and CNMR spectra of Jun9-88-6R



HNMR and CNMR spectra of Jun9-88-6S



References

1. Sacco, M. D.; Ma, C.; Lagarias, P.; Gao, A.; Townsend, J. A.; Meng, X.; Dube, P.; Zhang, X.; Hu, Y.; Kitamura, N.; Hurst, B.; Tarbet, B.; Marty, M. T.; Kolocouris, A.; Xiang, Y.; Chen, Y.; Wang, J., Structure and inhibition of the SARS-CoV-2 main protease reveal strategy for developing dual inhibitors against M(pro) and cathepsin L. *Sci. Adv.* **2020**, 6 (50), eabe0751.
2. Xia, Z.; Sacco, M.; Hu, Y.; Ma, C.; Meng, X.; Zhang, F.; Szeto, T.; Xiang, Y.; Chen, Y.; Wang, J., Rational Design of Hybrid SARS-CoV-2 Main Protease Inhibitors Guided by the Superimposed Cocrystal Structures with the Peptidomimetic Inhibitors GC-376, Telaprevir, and Boceprevir. *ACS Pharmacol. Transl. Sci.* **2021**, 4 (4), 1408-1421.
3. Ma, C.; Sacco, M. D.; Hurst, B.; Townsend, J. A.; Hu, Y.; Szeto, T.; Zhang, X.; Tarbet, B.; Marty, M. T.; Chen, Y.; Wang, J., Boceprevir, GC-376, and calpain inhibitors II, XII inhibit SARS-CoV-2 viral replication by targeting the viral main protease. *Cell Res.* **2020**, 30 (8), 678-692.
4. Strelow, J. M., A Perspective on the Kinetics of Covalent and Irreversible Inhibition. *SLAS Discov* **2017**, 22 (1), 3-20.
5. Marty, M. T.; Baldwin, A. J.; Marklund, E. G.; Hochberg, G. K. A.; Benesch, J. L. P.; Robinson, C. V., Bayesian Deconvolution of Mass and Ion Mobility Spectra: From Binary Interactions to Polydisperse Ensembles. *Anal. Chem.* **2015**, 87 (8), 4370-4376.
6. Otwinowski, Z.; Minor, W., Processing of X-ray diffraction data collected in oscillation mode. *Methods Enzymol.* **1997**, 276, 307-326.

7. Vagin, A.; Teplyakov, A., Molecular replacement with MOLREP. *Acta Crystallogr D Biol Crystallogr* **2010**, *66* (Pt 1), 22-25.
8. Murshudov, G. N.; Skubák, P.; Lebedev, A. A.; Pannu, N. S.; Steiner, R. A.; Nicholls, R. A.; Winn, M. D.; Long, F.; Vagin, A. A., REFMAC5 for the refinement of macromolecular crystal structures. *Acta Crystallogr D Biol Crystallogr* **2011**, *67* (Pt 4), 355-367.
9. Emsley, P.; Cowtan, K., Coot: model-building tools for molecular graphics. *Acta Crystallogr D Biol Crystallogr* **2004**, *60* (Pt 12 Pt 1), 2126-2132.
10. Kitamura, N.; Sacco, M. D.; Ma, C.; Hu, Y.; Townsend, J. A.; Meng, X.; Zhang, F.; Zhang, X.; Ba, M.; Szeto, T.; Kukuljac, A.; Marty, M. T.; Schultz, D.; Cherry, S.; Xiang, Y.; Chen, Y.; Wang, J., Expedited Approach toward the Rational Design of Noncovalent SARS-CoV-2 Main Protease Inhibitors. *J Med Chem* **2021**, doi: 10.1021/acs.jmedchem.1c00509.